UNIVERSITY OF HAWAII
MAY 2 '60

This Issue Completes Volume 1

Journal of MOLECULAR BIOLOGY

EDITOR-IN-CHIEF: J. C. KENDREW

Volume I, Number 4-5, December 1959

ACADEMIC PRESS LTD., LONDON
ACADEMIC PRESS INC., NEW YORK

JOURNAL OF MOLECULAR BIOLOGY

EDITOR-IN-CHIEF

J. C. KENDREW, Peterhouse, Cambridge, England

EDITORIAL BOARD

P. DOTY, Department of Chemistry, Harvard University, Cambridge, Mass., U.S.A.
A. F. HUXLEY, Physiological Laboratory, University of Cambridge, England.
R. L. SINSHEIMER, Division of Biology, California Institute of Technology, Pasadena, Cal., U.S.A.
J. D. WATSON, Biological Laboratories, Harvard University, Cambridge, Mass., U.S.A.
M. H. F. WILKINS, Physics Department, King's College, London, England.

ADVISORY BOARD

S. BENZER, Purdue University, U.S.A.
M. CALVIN, University of California, Berkeley, U.S.A.
F. H. C. CRICK, University of Cambridge, England.
J. F. DANIELLI, King's College, London, England.
A. ENGSTRÖM, Karolinska Institutet, Stockholm, Sweden.
A. D. HERSHEY, Carnegie Institute, Cold Spring Harbor, U.S.A.
F. JACOB, Pasteur Institute, Paris, France.
A. KORNBERG, Stanford University, Stanford, California, U.S.A.
C. LEVINTHAL, Massachusetts Institute of Technology, Cambridge, Mass., U.S.A.
S. E. LURIA, Massachusetts Institute of Technology, Cambridge, Mass., U.S.A.
D. MAZIA, University of California, Berkeley, U.S.A.
P. B. MEDAWAR, University College, London, England.
L. E. ORGEL, University of Cambridge, England.
M. F. PERUTZ, University of Cambridge, England.
R. D. PRESTON, University of Leeds, England.
G. N. RAMACHANDRAN, University of Madras, India.
A. RICH, Massachusetts Institute of Technology, Cambridge, Mass., U.S.A.
G. SCHRAMM, Max-Planck Institut, Tübingen, Germany.
F. S. SJØSTRAND, Karolinska Institutet, Stockholm, Sweden.
I. WATANABE, University of Tokyo, Japan.
R. C. WILLIAMS, University of California, Berkeley, U.S.A.

Published by Academic Press Inc. (London) Limited

Volume I, 1959: 100*s*. ($14.00)

Subscription orders should be sent to Academic Press Inc. (London) Limited, 17 Old Queen Street, London, S.W.1, with the exception of those originating in the U.S.A., Canada, Central America, and South America; these should be sent to Academic Press Inc., 111 Fifth Avenue, New York 3, N.Y.

Copyright © 1959, by Academic Press Inc. (London) Limited

J. Mol. Biol. (1959) **1**, 301-320

A Metabolic Study of the RNA-Amino Acid Complexes in *Escherichia Coli*†

SANDFORD LACKS‡ AND FRANCOIS GROS

Service de Biochimie cellulaire, Institut Pasteur, Paris, France

(*Received 19 May 1959*)

Incorporation of radioactive amino acids into *Escherichia coli* results in the formation of a pool which consists of amino acids covalently linked to the non-centrifugable fraction of RNA. The size of this pool corresponds approximately to 1/20 of the native pool of "free" amino acids. Amino acids are fixed on specific loci of the RNA, as there is no observable competition between various amino acids.

The amino acids bound to RNA undergo an extremely rapid renewal. This renewal is considerably reduced when protein synthesis is inhibited either by chloramphenicol or by starvation for an amino acid. The slow residual renewal in the presence of chloramphenicol seems to be due to an exchange reaction independent of protein synthesis. Direct fixation of the radioactive amino acid into free loci is not inhibited by chloramphenicol.

Labeling of the RNA pool followed by dilution with unlabeled amino acid is accompanied by a complete loss of radioactivity from the pool and by an almost equivalent gain of radioactivity in the protein fraction.

It is assumed that all the sites of the RNA of exponentially growing cells are saturated by amino acids formed endogeneously and that the replacement of the bound amino acids by free (or activated) radioactive amino acids depends upon protein formation.

Therefore the RNA-amino acid complex may be considered as an intermediate of part (if not all) of the protein synthesized by *E. coli*.

1. Introduction

In recent years two reactions of considerable theoretical interest have been discovered in the course of studies on amino acid incorporation into the protein of tissue homogenates. The first one, the activation of amino acids by specific enzymes in the presence of ATP (Hoagland, 1955; Hoagland, Keller & Zamecnik, 1956; Berg, 1956) leads to the formation of enzyme-adenyl-amino acid complexes. The second, a transfer of the activated amino acids to a special ribonucleic acid (RNA) fraction (S-RNA) (Hoagland, Zamecnik & Stephenson, 1957; Hoagland, 1958; Hoagland, Stephenson, Scott, Hecht & Zamecnik, 1958), is catalyzed also by the "activating enzymes" and gives rise to the formation of an RNA-amino acid complex. Despite the large number of investigations on the nature of these enzymatic steps, little is known about their potential role in protein synthesis.

With regard to the first reaction, the fact that all the naturally occurring amino acids have been found to be activated by these enzymes suggests that this may be the first step in the formation of proteins. Further support for the role of amino acid activating enzymes in protein synthesis is given by the observation that only those

† This work has been aided by a grant from the Jane Coffin Memorial Fund and from the Commissariat à l'Energie Atomique.

‡ Graduate student from the Rockefeller University of New York.

amino acid analogues which are capable of catalysing an exchange between ATP and pyrophosphate can be incorporated into proteins (Sharon & Lipmann, 1957).

The idea that S-RNA participates in protein synthesis is supported by the observation that amino acids are directly transferred from S-RNA to microsomal proteins in preparations from liver (Hoagland *et al.*, 1957) and from *E. coli* (Zillig & Corquodale, 1958).

However, in order to make a better evaluation of the role of RNA-amino acid complexes as obligatory intermediates in protein formation, a study of their behaviour *in vivo* was undertaken. Previously, only limited work has been done on this aspect of the problem, but the observation by Hoagland *et al.* (1958), that in Ascites tumor cells S-RNA becomes labeled *in vivo* earlier than other cellular RNA and protein, is significant.

In the present study some metabolic properties of the RNA-amino acid complexes have been examined. In particular, a study has been made of the relationship between the renewal of the amino acids bound to RNA and the rate of protein formation.

2. Materials and Methods

(a) *Growth of bacteria*

To determine the size of the pool of RNA-bound amino acids, cells of *E. coli* in the logarithmic phase are labeled with a radioactive amino acid, their RNA is extracted without breaking the bonds between amino acids and RNA, and the radioactivity associated with this fraction is measured. Amino acids not convertible to purines or pyrimidines were used in these experiments.

The bacteria taken from an inoculum of an overnight culture grown in a mineral medium "63" (Monod, Cohen-Bazire & Cohn, 1951) were cultivated at 37°C in the same medium with 0·2% glucose as carbon source. When the bacterial population corresponded to 0·2 mg dry weight per ml., usually after about three divisions, the culture was distributed in 50 ml. portions into flasks which were shaken at 20°C in a water bath. After 30 to 60 min growth a radioactive amino acid (specific activity between 2 and 10 μc per μmole) was added.

(b) *Extraction of RNA-amino acid complexes from intact cells*

Two methods of extraction were used. Both are derived from those described by Hoagland *et al.* (1957) to isolate the RNA-amino acid complexes from liver tissues.

Method 1: *extraction by hot saline solution*

Except where noted otherwise, this method has been used in all the experiments to be described.

The incorporation of the radioactive amino acid was arrested by acidifying to pH 1·0 with HCl. The sample was then centrifuged in the cold and the bacteria were resuspended in a measured volume of distilled water. A fraction of the suspension, about a tenth, was set aside for the determination of total RNA by the method of Albaum & Umbreit (1947). The remaining material, after addition of trichloroacetic acid (TCA) to a final concentration of 5%, was again centrifuged. The bacterial residues were washed twice more with 5% TCA, once with alcohol, and finally with a mixture of alcohol and ether. After drying, the solid residue obtained was suspended in 2 ml. of a 10% solution of NaCl. The nucleic acids were extracted by heating the suspension at 100°C for 30 min. After cooling and centrifuging, the residue was again extracted by heating in 1 ml. of saline for 20 min. In this way, 90% of the bacterial RNA passes into solution. After combining the extracts, the nucleic acids were precipitated at −10°C by addition of alcohol, to a final concentration of 60% by volume. The precipitate was dissolved in a dilute solution of NaCl and reprecipitated with alcohol. Finally, the nucleic acids were dissolved in water. The RNA content and the radioactivity were determined in portions of this solution. By multiplying

the specific radioactivity by the total amount of RNA contained in the bacteria, a measure of the total pool was obtained for the amino acid considered.

Method 2: *extraction with phenol*

This method was used in some cases, to see if the size of the RNA-amino acid pool was affected by the procedure used in method 1 (see section 3(a)). After incorporation of radioactive amino acids, the bacteria were washed, suspended in 0·002 M-Tris buffer pH 7·2 containing 0·005 M-$MgCl_2$, and lysed by ultrasonic vibration. Cellular debris was removed by centrifugation and the DNA was destroyed by treatment with deoxyribonuclease (DNase). The lysate was then deproteinized by shaking with 90% phenol, as described by Hoagland *et al.* (1957). RNA was finally precipitated by alcohol at −10°C. The precipitate was dissolved in water and the solution dialysed against distilled water. Determination was then made of the specific radioactivity expressed in terms of RNA.

(c) *Separation of the soluble RNA from bacterial extracts*

In some experiments involving tracer incorporation into RNA, we had to fractionate the cells in order to separate the "soluble" from the "particulate" RNA. Usually bacteria were washed with Tris buffer (0·002 M-Tris, pH 7·4 + 0·005 M-$MgCl_2$) at 0°C for 10 min, then ground with three times their wet weight of alumina A 301, † and finally extracted with this dilute Tris buffer. After centrifugation in the cold at 15,000 ***g*** for 15 min to remove alumina and cell debris, the supernatant was incubated with 10 μg/ml. of crystalline DNase at 20°C for 20 min. The extract, free of DNA, was centrifuged at 40,000 rev/min in a Spinco ultracentrifuge (Model L) at 0°C for 2 hr. The subsequent operations were carried out at 0°C. The upper four-fifths of the supernatant (Fraction A) and the remaining one-fifth were drawn off separately with a syringe. The pellet was allowed to drain thoroughly, and was then resuspended in Tris buffer (Fraction B).

The specific radioactivities of the "soluble" and the "particulate" RNA were determined in the following way. Fraction A was brought to pH 4·0 by careful addition of 0·1 M-acetic acid; the precipitate was washed twice in 5% cold TCA, and its RNA extracted by hot TCA. To Fraction "B" TCA was added; the precipitate thus obtained was washed twice with 5% TCA, and the RNA extracted with hot 5% TCA. Both TCA extracts containing soluble or particulate RNA were analyzed for their RNA content by the method of Albaum & Umbreit (1947). Radioactivities were determined on diluted samples.

(d) *Radioactive products*

The [^{14}C]valine, [^{14}C]phenylalanine, and [^{35}S]methionine were synthetic products obtained from the Commissariat à l'Energie Atomique which furnished us also with radioactive [^{35}S]sulfate. We have also used radioactive methionine obtained from the Radiochemical Centre, Amersham, Bucks, England. [^{14}C]leucine, [^{14}C]proline, and [^{14}C]arginine were prepared by the Service des Radioisotopes of the Institut Pasteur.

The [8-^{14}C]adenine was a product of Schwartz and Co. Deoxyribonuclease was obtained from the Worthington Biochemical Corporation, Freehold, New Jersey, U.S.A.

3. Results

(a) *Comparison between the measurements of pool size obtained using different extraction procedures*

Upon incorporation of any given radioactive amino acid into a culture of *E. coli*, the fraction corresponding to nucleic acids and devoid of proteins exhibits an appreciable amount of radioactivity. This activity remains constant on further purification by precipitation with alcohol.

As indicated in Table 1, the specific radioactivity of the bacterial RNA is independent of the nature of the procedure used to extract the nucleic acids. Thus, the

† Manufactured by the Aluminium Company of America.

TABLE 1

Independence of the size of the pool of RNA-bound amino acids and the extraction procedure

[^{14}C]DL-phenylalanine was added to 100 ml. of a culture of *E. coli* ML 308 in medium "63" plus glucose at 20°C (final concentration 0·03 mM; specific activity : 3·5 μc per μmole). After 10 min, the culture was quickly cooled to 0°C and divided into two portions, A and B. A undergoes saline extraction (procedure 1); B is lysed and deproteinized with phenol (procedure 2). The same experiment is done in the second column but there is an incubation with an excess of [^{12}C]phenylalanine for 3 min following the 10 min labeling period.

Extraction procedure	Specific radioactivity (μmoles phenylalanine/mg RNA)	
	After labeling with [^{14}C]phenylalanine	After labeling, followed by displacement with [^{12}C]phenylalanine
A. NaCl method	0·097	0·012
B. Phenol method	0·085	0·012

incorporation of amino acid indicates the formation of a well-defined pool composed of one or several substances linked to the RNA. We shall examine presently the nature of this material and the type of linkage with the nucleic acid.

(b) *Nature of the radioactive substances present in the nucleic acid fraction*

The radioactive substance associated with the nucleic acids is not dialysable (Table 2); neither is it soluble in cold TCA. Consequently the pool in question does

TABLE 2

Behavior on dialysis of the radioactivity associated with the "nucleic acid" fraction after incorporation of radioactive sulfate: effect of ribonuclease

The RNA is prepared after incorporation of radioactive ^{35}S by a culture of *E. coli* ML 308 and purified according to Procedure 1. The solution is divided into 3 portions: A: non-dialysed control; B: 1 ml. solution + 0·1 ml. water; C: 1 ml. solution + 0·05 ml. 0·2 M-NaCl + 0·05 ml. RNase (2 mg/ml.), incubated 3 hr at 37°C. One ml. of B and C are dialysed for 40 hr at 3°C against 9 ml. of distilled water.

	Radioactivity total activity in counts/min			Total absorption at 260 mμ		
	A	B	C	A	B	C
Solution	8,480	8,480	2,620	25·5	21·7	8·0
Dialysate		270	5,760		1·4	18·4

Percentage of substance dialysable			
Radioactivity		RNA (260 mμ absorption)	
untreated B	RNase-treated C	untreated B	RNase-treated C
3·1	69·0	6·2	69·4

not consist of free amino acids or peptides. That it does not consist of proteins either, is shown by the almost complete solubility of the radioactive substance linked to the nucleic acid fraction in *hot* TCA, which parallels the behavior of nucleic acids, as opposed to that of proteins.

The conclusion that we are dealing with a substance actually linked to the nucleic acids is supported by the following properties of the material.

(1) The radioactive substance is not dissociated from the nucleic acids by electrophoresis (Fig. 1).

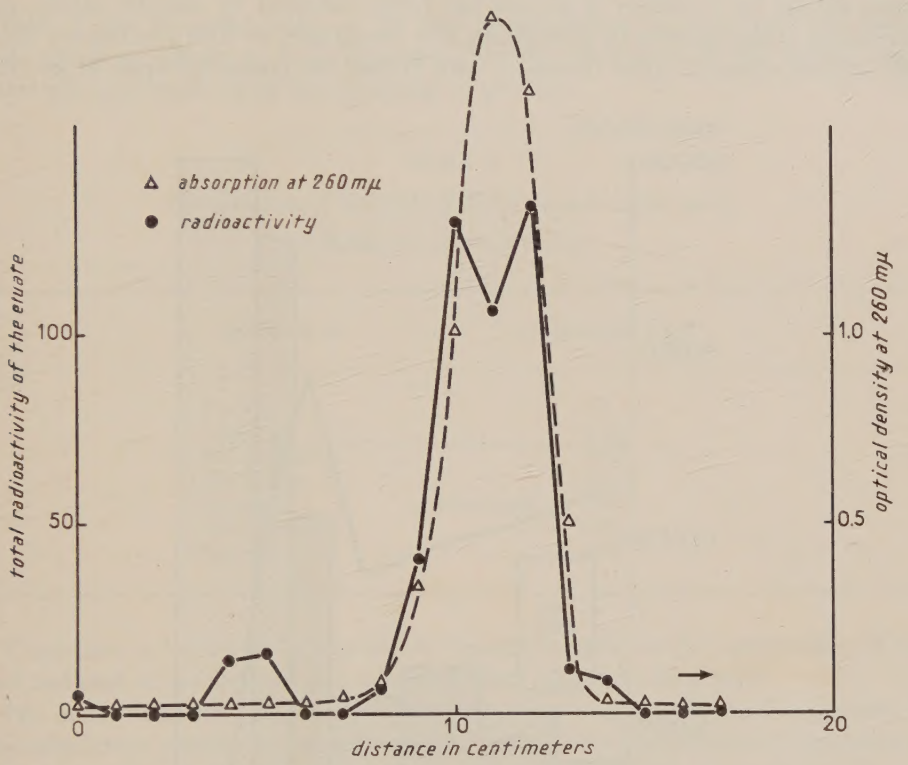

FIG. 1. Agar electrophoresis of the "RNA fraction" after labeling by incorporation of radioactive sulfate.

Electrophoresis is carried out for 7·5 hr at 4°C as described by Bussard & Perrin (1955). Voltage: 3·2 v/cm. Buffer: 0·02 M-ammonium formate-formic acid at pH 4·3. For the elution, sections of agar 1 cm wide are cut and eluted for 24 hr in 3 ml. of cold water.

(2) When the radioactive extract is digested with ribonuclease, about 70% of the radioactive substance becomes dialysable; the same as the proportion of RNA itself which becomes dialysable (see Table 2).

(3) As in the case of the RNA-amino acid complex studied by Hoagland, the radioactivity due to the amino acid can be detached by brief treatment with alkali, without hydrolysis of the RNA itself. Under these conditions, 80 to 90% of the radioactive substance becomes dialysable and soluble in cold TCA.

We have analysed the nature of the dialysable substance obtained after mild alkaline treatment in a case in which the radioactivity resulted from the incorporation of [^{35}S]methionine. The dialysate, after the removal of salt, was concentrated and analysed by paper chromatography. Two spots appeared, one corresponding to

methionine and one to methionine sulfoxide, which was probably produced from free methionine under the influence of dilute alkali. We have thus demonstrated that the pool isolated from cells which have incorporated radioactive amino acids consists of a complex of RNA and amino acids.

(c) *Nature of the RNA linked to the amino acids*

The results so far quoted do not determine whether all the RNA, or only a certain fraction of it, is combined in this fashion with the amino acids.

The following experiment answers this question. After the incorporation of radioactive sulfate by a culture of *E. coli*, the lysate obtained by osmotic shock, after conversion of the bacteria to protoplasts, was centrifuged at 7000 *g* to remove debris and unlysed material. After treatment with DNase, the lysate was spun in an ultra-

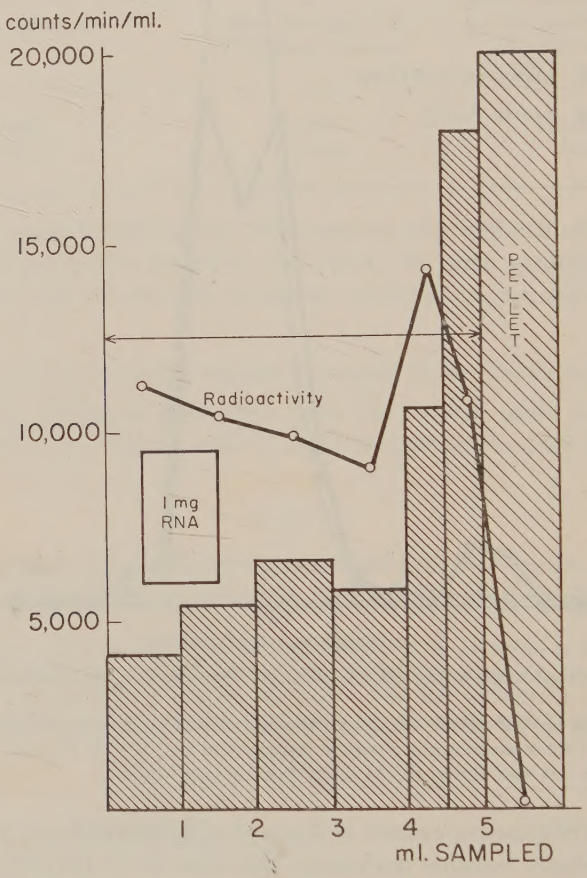

FIG. 2. Distribution of the RNA-bound radioactivity after ultracentrifugation of an extract of *E. coli* K 12, labeled with ^{35}S.

Bacteria are labeled by growing for 12 min at 20°C in a medium of low sulfate content, containing [^{35}S]sulphuric acid (1 μc/ml.). After cooling, bacteria are harvested, washed in cold 0·005 M-Tris buffer, pH 7·6, and resuspended in the same buffer. Lysozyme and sucrose are added, and bacteria are converted to protoplasts by the method of Sistrom (1958). After osmotic shock, the lysate is freed of DNA by treatment with DNase and centrifuged at 100,000 *g* for 2 hr (in the swinging bucket Spinco ultracentrifuge). Samples of the supernatant fluid are drawn off separately with a syringe. TCA (5%) is added to each sample and to the suspension of the pellet. The radioactivity of the amino acid-RNA fraction is determined according to procedure A. Corrections are made for the loss of RNA during the extraction.

centrifuge for 2 hr at 105,000 *g*. Successive layers of the supernatant fluid were withdrawn with the aid of a syringe. Each layer, and also the sediment, was analysed both for its RNA content and its specific radioactivity resulting from the presence of sulfur-containing amino acids linked to RNA. As shown in Fig. 2 practically all the RNA-amino acid complex is found in the non-sedimentable fraction of the bacterial RNA, a fraction which usually represents about 10% of the total RNA. This observation agrees with early observations by Hoagland *et al.* (1957, 1958).

(d) *Composition and dimensions of the pool of RNA linked to amino acid*

Table 3 lists the composition of the pool at saturation, for seven different amino acids which are known to be incorporated into the proteins of *E. coli* without prior metabolic conversion (with the exception of proline).

TABLE 3

Composition of the pool of RNA-bound amino acids

(Measured at saturation)

Amino acid	mμmoles/mg RNA
Proline	0·8
Arginine	0·18
Phenylalanine	0·12
Methionine	0·15
Valine	0·20
*Iso*leucine	0·27
Leucine	0·19

There does not seem to be any direct correlation between the composition of the pool and that of the proteins as a whole for these different amino acids.

The mean value for the content of any one amino acid in the pool (excluding in this calculation proline, which is present to a markedly greater extent) corresponds to 0·2 mμmoles/mg of RNA. If it is assumed that the RNA extracted by the salt method (see section on techniques) represents the total RNA, it can be calculated that at saturation the RNA-amino acid pool contains one specific amino acid per 1000 nucleotides, or one amino acid of any kind per 50 nucleotides, that is per equivalent molecular weight of acceptor RNA equal to 15,000. Such a result, based on a rough estimation, is in rather good agreement with the calculations of Hoagland (1958) and of Berg & Ofengand (1958), derived from data obtained with *in vitro* systems.

Proline seems to be a special case; it is possible that more than one molecule of this amino acid may be fixed on a single RNA acceptor molecule, or that a large amount of this amino acid is bound to the "particulate" RNA.

(e) *Kinetics of formation and turnover of the pool*

The kinetics of incorporation of a given amino acid are described by a saturation-type curve. Saturation is generally attained after 3 to 5 min in bacteria growing exponentially at 20°C (Fig. 3). Under such conditions it usually takes between 10 and 15 min for the free amino acid pool to be completely saturated.

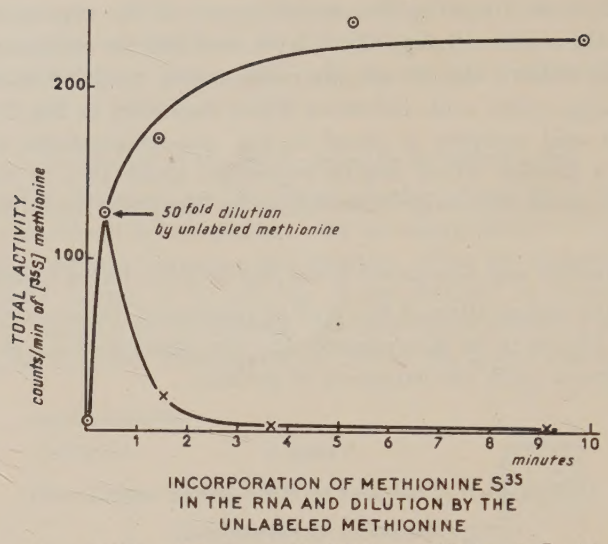

FIG. 3. Incorporation of [^{35}S]methionine in the RNA and dilution by unlabeled methionine.
To *E. coli* K12 growing exponentially at 20°C (Medium 63 plus succinate) [^{35}S]DL-methionine (2 μc/mole) is added at zero time. Final concentration: 0·2 mM; 50 ml. samples are taken at intervals and analyzed according to the procedure of extraction in hot saline solution described under "Materials and Methods."

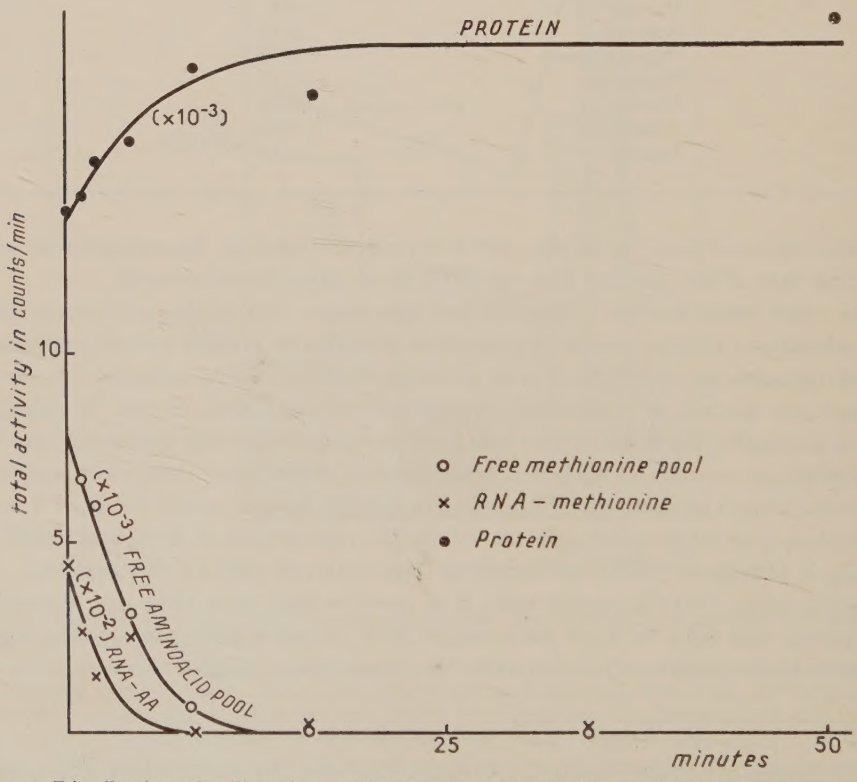

FIG. 4. Distribution of radioactive methionine from the "RNA pool" labeled previously by a short exposure to [^{35}S]methionine.
Exposure 2 min to [^{35}S]DL-methionine (0·02 mM), at 20°C. After harvesting and washing, cells are resuspended in medium 63 without carbon source; equilibration 5 min at 20°C. Glucose added at zero time. Sampling at intervals for determination of radioactivity in the free methionine pool (Cohen & Rickenberg, 1956), the RNA-methionine pool, and the proteins.

The amino acids of the pool undergo a very rapid turnover. Thus, it is possible to displace radioactive amino acids quantitatively from the pool by adding an excess of the same amino acids in a non-radioactive form (Fig. 3).

If, after a very brief labeling with a radioactive amino acid, the bacteria are washed to remove the amino acid and resuspended in a growth medium, the radioactivity of the pool soon becomes negligible. This demonstrates again a very rapid utilization of the amino acids present in the pool (Fig. 4).

(f) *Relationship between the turnover of amino acids in the pool and protein synthesis*

The turnover of amino acids that we have just described could depend on one or both of the following mechanisms:

(1) An exchange reaction of the type:

$$\text{amino acids} \rightleftharpoons \text{adenyl-amino acids}$$

$$\text{adenyl-amino acids} + \text{S-RNA} \rightleftharpoons \text{RNA-amino acid} + \text{AMP} \qquad (1)$$

(2) A reaction or series of reactions leading, in one direction, to the utilization of the pool RNA amino acids for protein synthesis:

$$\text{amino acids} + \text{S-RNA} \rightarrow \text{RNA-amino acids} \rightarrow \text{S-RNA} + \text{protein} \qquad (2)$$

It is possible to distinguish between these two mechanisms by varying the rate of protein synthesis and observing how this affects the rate of renewal of the RNA-bound amino acids. According to scheme (1), variation in the rate of protein synthesis should have no effect, whereas according to scheme (2), it should be affected considerably.

We have therefore compared the turnover of the RNA-bound amino acids both under normal conditions (bacteria in exponential growth) and under conditions of reduced protein synthesis.

Chloromycetin (Fig. 5) diminishes considerably the speed of incorporation of radioactive amino acids into the RNA. The initial rate of labeling is reduced by 80%. On the other hand, the equilibrium level of labeling is the same in the presence as in the absence of the inhibitor. Specific starvation of autotrophic bacteria for an essential amino acid gave qualitatively the same effect as chloromycetin: reduction in the initial rate of incorporation without alteration of the equilibrium state (Fig. 6). In a similar fashion chloromycetin reduces the rate of displacement of radioactive amino acids in the pool by non-radioactive amino acids (Fig. 7).

Generally, then, the turnover of amino acids bound to RNA is slower when the synthesis of proteins is inhibited. This behavior would be expected if in exponentially growing bacteria all the RNA acceptor sites were saturated by amino acids (aa) and the liberation of these sites depended on protein synthesis.

The equation:

$$\text{aa} + \text{S-RNA} \rightleftharpoons \text{RNA-aa} \rightarrow \text{S-RNA} + \text{protein}$$

would account for the observed behaviour.

(g) *Exchange reactions between amino acids linked to RNA and free amino acids*

It is observed that chloromycetin only diminishes the rate of turnover and does not completely eliminate it. The slow incorporation of amino acids which remains could be explained in two ways:

(1) By an exchange reaction of the type:

$$\text{adenyl-amino acid} + \text{S-RNA} \rightleftharpoons \text{RNA-aa} + \text{AMP} \qquad (3)$$

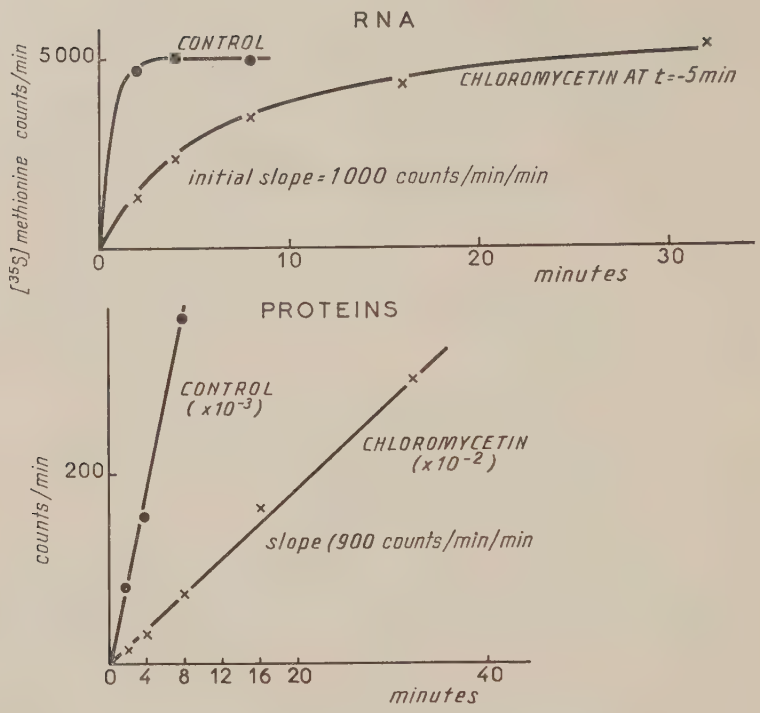

Fig. 5. Effect of chloromycetin on the incorporation of [^{35}S]methionine into the RNA and protein of *E. coli* ML 30.

E. coli ML 30 is cultivated in medium 63 plus glucose (0·2%) at 20°C. Chloromycetin (20 μg/ml.) [^{35}S]DL-methionine (final concentration 0·04 mM).

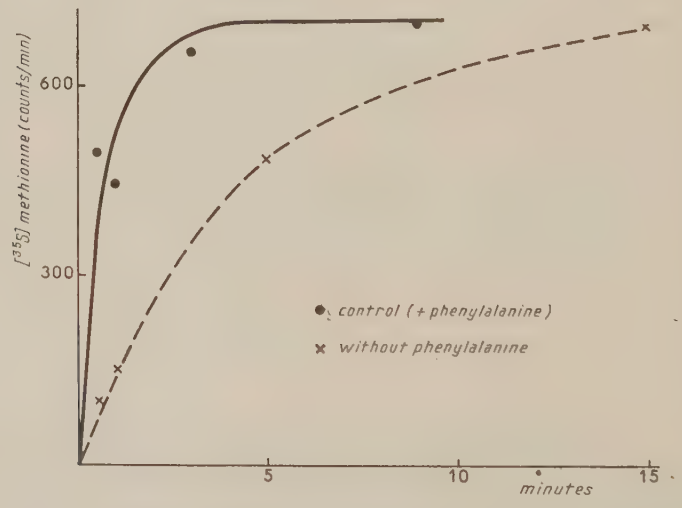

Fig. 6. Formation of the "RNA methionine" pool in cells previously starved for phenylalanine.

E. coli M 83–5 is grown in medium 63 plus glucose plus L-phenylalanine (10^{-4}M), the cells are harvested, washed twice and starved 3 hr for phenylalanine. At zero time [^{35}S]DL-methionine is added (0·1 mM), with or without phenylalanine 0·1 mM (control curve).

(2) By a slow renewal of the pool dependent on residual protein synthesis which occurs in the presence of chloromycetin at about 10% of the normal rate.

Further experimental results seem to support the first hypothesis. On the one hand, when very high concentrations of chloromycetin are used, for example 200 μg/ml., residual protein synthesis is about half as great as in the case previously mentioned when chloromycetin at 20 μg/ml. was used; however, the rate of incorporation of amino acids into the S-RNA is the same.

On the other hand, when chloromycetin, instead of being added to the culture at the same time as radioactive amino acids, is added 90 minutes before, this preincubation taking place at 37°C, the initial rate of incorporation of amino acid into the

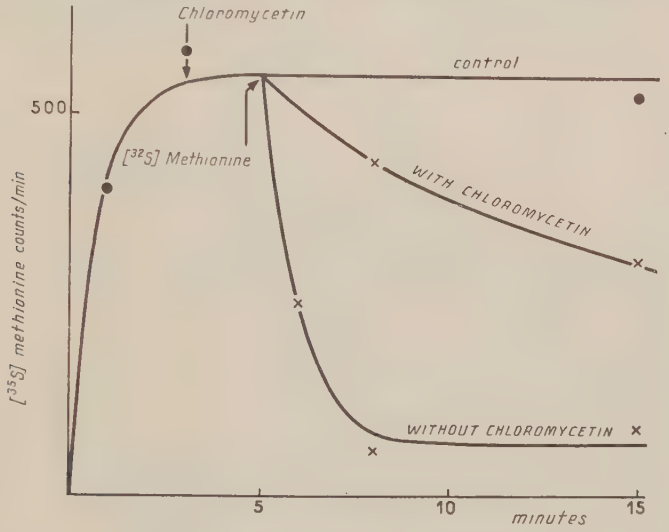

FIG. 7. Effect of chloromycetin on the dilution of [^{35}S]methionine in the "RNA pool" after addition of non-labeled methionine.

E. coli ML 30 labeled with 0·04 mM [^{35}S]DL-methionine at 20°C. After 5 min, excess of unlabeled DL-methionine (0·004 M) is added in the presence or absence of chloromycetin (20 μg/ml.).

RNA is the same, whereas the rate of protein synthesis is further reduced to less than half of the rate after simultaneous addition (Fig. 8). It may be noticed that the saturation level of the pool is greater in this instance owing to the synthesis of additional acceptor RNA by the bacteria during the preincubation in the presence of chloromycetin.

The slow incorporation of amino acid into the RNA in the presence of chloromycetin probably depends therefore on an exchange reaction involving reversibility of the process of fixation of activated amino acids onto soluble RNA (Equation 3).

(h) *Specificity of the acceptor sites for the amino acids*

Fixation of amino acids onto the RNA appears to involve specific sites. Addition to a culture of any amino acid in excess influences neither the rate nor the level of incorporation of another amino acid. The different amino acids are, therefore, incorporated in an additive fashion.

Amino acid analogues can be incorporated into the S-RNA. For instance after addition of [^{14}C]*para*fluorophenylalanine to a culture of *E. coli* the RNA pool is found to be labeled, and to contain on a molar basis the same quantity of analogue

that is obtained when [^{14}C]phenylalanine is used under the same conditions. There is a possibility that *para*fluorophenylalanine may occupy the same site on the RNA as phenylalanine. In preliminary experiments carried out in collaboration with Dr. A. Ullman, a "pH 5 enzyme" preparation of *E. coli* was incubated with [^{14}C]phenylalanine, and also with a mixture of [^{14}C]phenylalanine and non-radioactive *para*fluorophenylalanine in a ratio of one to four. Measurements of the incorporation of radioactivity into S-RNA revealed that the initial rate of incorporation was reduced by about 1/4 in the presence of the analogue. When the analogue was replaced by non-radioactive tyrosine, the rate of incorporation of [^{14}C]phenylalanine was not affected. Experiments are in progress to determine whether the competition takes place at the level of the activation by ATP, or at the fixation on the S-RNA.

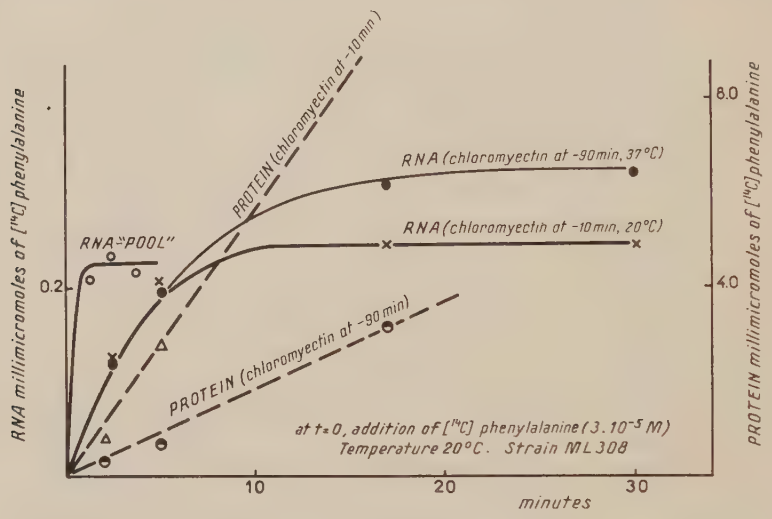

FIG. 8. Incorporation of [^{14}C]phenylalanine into RNA and protein in the presence of chloromycetin.

For details see text. The suspension of cells treated with chloromycetin for 90 min at 37°C is equilibrated 5 min at 20°C before addition of [^{14}C]phenylalanine.

(i) *Liberation of specific sites on the acceptor RNA*

Until now, we have been considering only prototrophic bacteria during exponential growth, that is those in which the acceptor RNA is constantly saturated by amino acids. Let us turn our attention to the case where free sites are present on the RNA and study the manner of fixation of a given amino acid onto these sites.

Let us consider an auxotroph unable to synthesize one of the amino acids. When this auxotroph is grown in the presence of its essential amino acid, the acceptor RNA will be saturated for all the amino acids. Now we remove the essential amino acid and submit the auxotroph to prolonged starvation. If the incorporation of each amino acid into the RNA is independent of the presence of the others, and if the RNA-bound amino acid is actually a direct precursor of protein, it is clear that after the starvation all the sites of the RNA will be saturated, except those corresponding to the missing amino acid. One would then expect that the fixation of this amino acid onto the free site would be independent of the rate of protein synthesis.

Experiments were performed with two types of mutant having double requirements: phenylalanine-tyrosine and methionine-histidine. The organisms were starved

for several hours, after which the fixation of [^{14}C]phenylalanine in the first case, and [^{35}S]methionine in the second case, was studied both in the absence and presence of the other essential amino acid. Fig. 9 shows, for the methionine-histidine auxotroph, that the speed of incorporation of the [^{35}S]methionine is the same in the presence or absence of radioactive histidine. Furthermore, the speed of incorporation of methionine in the presence of histidine is not influenced by chloromycetin. However, the incorporation into the RNA of valine, an amino acid for which the mutant was not starved, occurs much more slowly if the methionine or histidine is omitted than in the presence of these essential amino acids. Finally, it is observed that after the

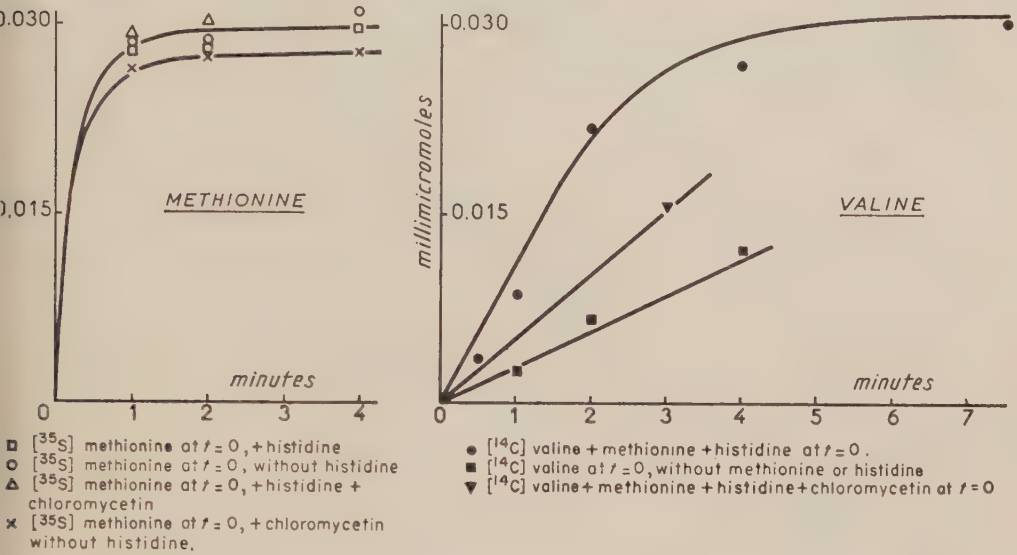
0.030
0.015
METHIONINE
minutes
0 1 2 3 4
0.030
millimicromoles
0.015
VALINE
minutes
0 1 2 3 4 5 6 7
□ [35S] methionine at t = 0, + histidine
○ [35S] methionine at t = 0, without histidine
△ [35S] methionine at t = 0, + histidine + chloromycetin
× [35S] methionine at t = 0, + chloromycetin without histidine.
● [14C] valine + methionine + histidine at t = 0.
■ [14C] valine at t = 0, without methionine or histidine
▼ [14C] valine + methionine + histidine + chloromycetin at t = 0

FIG. 9. Comparison between the rate of formation of the RNA-methionine and RNA-valine pools, in a strain requiring methionine and histidine, after simultaneous starvation for these amino acids. For details see text.

double starvation, the RNA is saturated in less than one minute by methionine, whereas saturation takes five times as long in the case of valine. Results of the same type were obtained with the phenylalanine-tyrosine auxotroph, in studying the fixation of [^{14}C]phenylalanine.

These experiments show that:

1. Fixation of an amino acid onto its "free" site on the RNA is very rapid (less than one minute required at 20°C).

2. Each amino acid can be incorporated independently into the RNA. For example, methionine is incorporated as quickly, and to the same extent, whether histidine is present or absent from its site. The fact that amino acid attachment is additive has already been reported by Hoagland (1958) and by Berg & Ofengand (1958) in their studies on incorporation of amino acids into S-RNA, in the presence of pH 5·0 enzyme fraction, or purified activating enzymes.

3. Direct attachment of an amino acid onto its site is independent of protein synthesis.

(j) *Transfer of amino acids from RNA-amino acid complexes to protein*

After starving the mutant requiring methionine and histidine, the RNA-pool of the bacteria is labeled by adding [^{35}S]methionine in the absence of histidine. Then

an excess of unlabeled methionine is added along with histidine, in order to permit the synthesis of proteins. There is observed an almost complete loss of radioactivity from the pool at the same time as proteins, which were only slightly labeled in the absence of histidine, continue to incorporate radioactivity (despite a one hundredfold dilution of the free radioactive amino acid due to the addition of unlabeled methionine). Table 4 shows fairly good agreement between the activity lost by the RNA-amino acid fraction and the activity incorporated into proteins after dilution of the

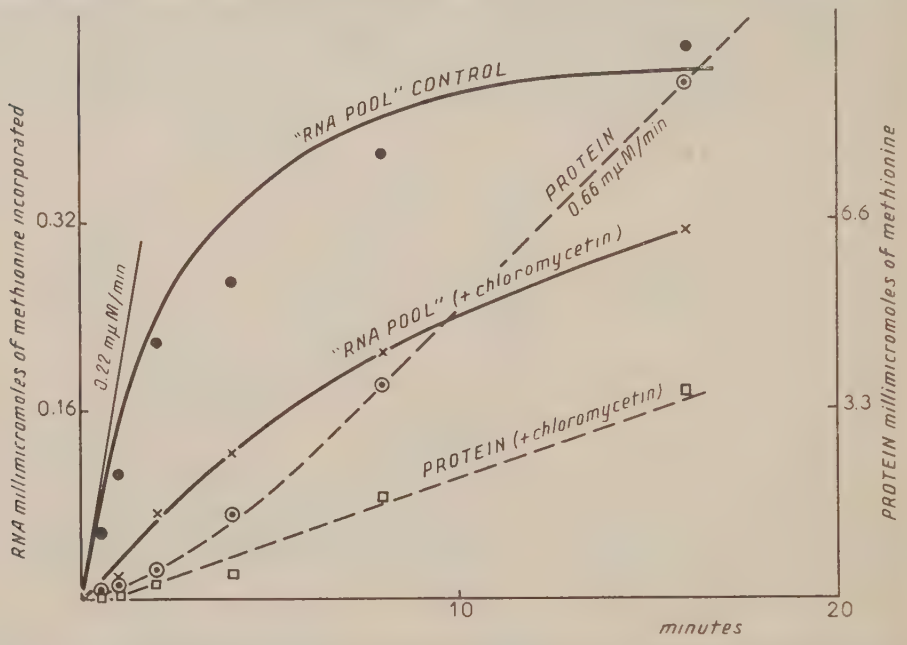

FIG. 10. Comparative rate of incorporation of methionine into the RNA-methionine complex and into protein. For details see text.

isotope. This experiment is compatible with the hypothesis of a direct transfer to the protein fraction of amino acids linked to RNA;† and is also in accord with early observations by Hoagland *et al.* (1958), that S-RNA labeled by an amino acid can transfer its radioactivity direct to the protein of microsomes, in *in vitro* preparations.

(k) *Relationship between the rate of turnover of the pool and the rate of protein synthesis*

The facts we have just described suggest a definite relationship between the turnover of RNA-bound amino acids and protein synthesis. They lead one to believe that amino acids in general might be fixed onto the soluble RNA before being incorporated into peptide chains.

We have therefore investigated whether the rate of renewal of amino acids in the RNA pool was compatible with the maximum rate of protein synthesis or not. The

† This is true, however, only at temperatures greater than 20°C. If the temperature is lowered to 10 to 15°C there is less of a correspondence between the loss of radioactivity from the pool and its increase in the proteins. In effect, the lowering of the temperature seems to affect much less the replacement of radioactive amino acid in the pool than its rate of incorporation into the protein fraction. This may be explained by recognizing that the incorporation of amino acids into RNA represents two processes: a replacement of amino acids due to their being used for protein synthesis and an exchange reaction independent of protein synthesis. It would appear, then, that the exchange reaction is affected much less by lowering the temperature than is the reaction incorporating these amino acids into protein.

experiment with a culture growing at 10°C shows (Fig. 10) that the maximum speed of incorporation of amino acids into the pool (evaluated by taking the tangent to the curve at the origin) is about two to three times *less* than the maximum rate of incorporation of the amino acids into the proteins. This point will be considered further in the discussion.

(l) *Kinetics of labeling of the soluble RNA by [^{14}C]adenine*

The amino acids are linked to a non-sedimentable fraction of the cellular RNA. One might wonder whether this fraction, which in *E. coli* corresponds to 10% of the total RNA, shows any peculiar metabolic behaviour.

To study this we have compared the kinetics of incorporation of a radioactive purine base, adenine, into the S-RNA on the one hand and into the particulate RNA on the other.

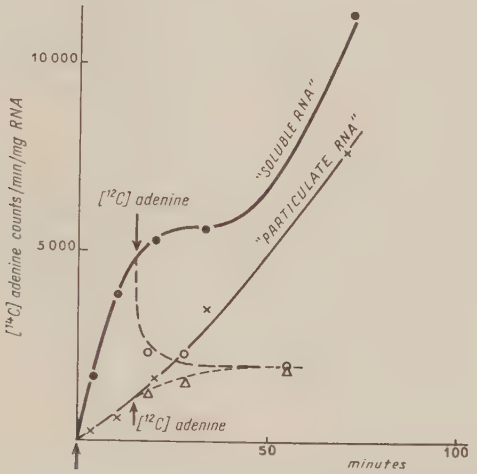

FIG. 11. Rates of incorporation of [^{14}C]adenine into the soluble and particulate RNA.
At time zero [^{14}C]adenine (10 μg/ml. and 300 counts/min/μg) is added to a culture of *E. coli* ML 308 growing at 18°C in medium 63 plus glucose; 200 ml. of culture containing 300 μg of cells (dry weight) per ml. are sampled at intervals and cooled rapidly to 0°C. Soluble and particulate RNA are fractionated according to the procedure described in "Materials and Methods."

The adenine is found to be incorporated much more quickly by the S-RNA than by the particulate RNA. Furthermore, while the incorporation into particulate RNA shows a steady rise, the kinetics of incorporation into the S-RNA are more complicated. At first it gives a saturation type curve. Once the plateau is attained (at about 20 min in an experiment at 18°C), there is a further steady rise beginning at about 30 min. At that time the rates of incorporation into the soluble and particulate forms of RNA are similar (Fig. 11).

If after incorporation of [^{14}C]adenine an excess of non-radioactive adenine is added, there is a rapid and substantial decrease in the specific activity of the S-RNA while that of the particulate RNA continues to increase.

(m) *Fixation of nucleotides at the end of the chain of soluble RNA*

It was of interest to see if the rapid labeling of the S-RNA observed in our experiments might not be explained, at least in part, by a mechanism of fixation of nucleotides in terminal positions, mechanisms of the type described previously by Hecht,

Zamenick, Stephenson & Scott (1958). According to these authors the attachment of amino acids to S-RNA requires the prior fixation to the end of the chain of two cytidylic residues and one adenylic residue.

$$\text{S-RNA} + 2\ \text{CTP} + \text{ATP} \rightleftharpoons \text{adenyl-cytidyl-cytidyl-S-RNA} + 3\ \text{PP}$$

Some experiments on this point are in progress in collaboration with Dr. Naono, and will be reported in detail in a future publication. Preliminary results show that after *in vivo* labeling of S-RNA by [^{14}C] adenine, an important proportion of the radioactivity (30% following 30 min labeling at 18°C) is found as adenosine upon alkali hydrolysis. The rapid labeling of the S-RNA, observed in the *in vivo* experiments reported above, must therefore result in part from the incorporation of adenylic acid at the end of the chain.

(n) *Fate of the pool RNA-bound amino acids after starvation for uracil*

Although terminal attachment of adenylic acid might explain in part the fast labeling of the S-RNA from [^{14}C]adenine, the possibility was not excluded that

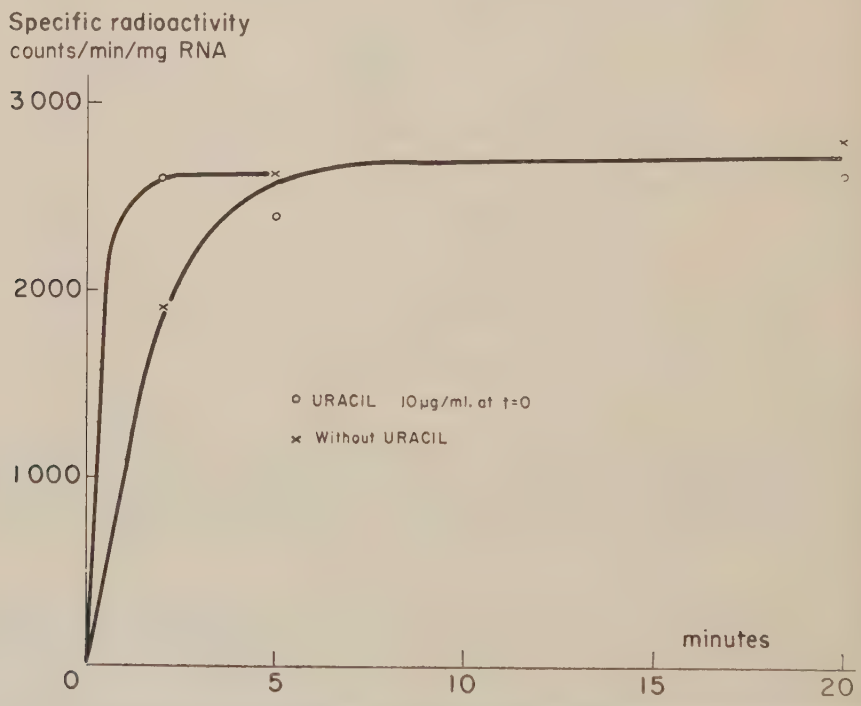

FIG. 12. Formation of the RNA-valine pool in *E. coli* W-63·86, after starvation for uracil.

S-RNA is a precursor of the particulate RNA, and that it would therefore become labeled before the particulate RNA. If there is a transformation of S-RNA into particulate RNA, the bacterial content of S-RNA in growing cells must result from an equilibrium between the formation and utilization of this substance. When production is rendered impossible, following, for example, a specific starvation for uracil, the S-RNA content ought to drop to a negligible value. To the extent that the RNA acceptor of amino acids is identical with the total S-RNA, starvation for uracil ought to result in the disappearance of this acceptor RNA. A measurement of the RNA-amino acid pool for a given amino acid should confirm this point.

The experiment was performed by submitting the mutant W 63–86 (uracil-requiring) to prolonged starvation for uracil and comparing the dimensions of the RNA-methionine pool before and after starvation. The results pictured in Fig. 12 demonstrate that the starvation decreased the rate of incorporation but did not influence the equilibrium level; that is, starvation did not modify the dimensions of the acceptor RNA pool.

This result makes improbable a direct conversion of amino acid-receptor RNA into particulate RNA.

4. Discussion

It has been demonstrated in this paper that the addition of single amino acids to growing cultures of *E. coli* results in the formation of an RNA-amino acid complex between these amino acids and RNA, involving mainly the non-sedimentable fraction of RNA. It seems likely that endogenously synthesized amino acids also combine with RNA. This is suggested by the fact that in bacteria grown in a medium containing radioactive sulfate the S-RNA is labeled, the label being presumably due to complexes of S-RNA with cystine or methionine.

Judging from the amount of complexes formed with the seven amino acids studied, it is possible to estimate the size of the total pool of bound amino acids. This corresponds to about 0·005% of the bacterial mass and to about 1/20 of the pool of free, endogenously formed amino acids (Mandelstam, 1956).

That each amino acid is attached to a specific site on the RNA is shown by the absence of competition among amino acids, even structurally related ones, in regard to rate and degree of incorporation into the RNA. In addition it has been shown that attachment of one amino acid to its free site does not require the presence of others.

All these results of *in vivo* studies are in good agreement with those previously obtained with *in vitro* systems (Hoagland *et al.*, 1957; Hoagland, 1958; Hoagland *et al.*, 1958; Berg & Ofengand, 1958; Schweet, Bovard, Allen & Glassman, 1958).

In addition to the mode of formation of the RNA-amino acid complexes, their role in protein synthesis has also been investigated in the present work. The evidence allows these RNA-amino acid complexes to be considered as intermediates in protein synthesis inasmuch as in growing bacteria renewal of amino acids in the complex depends for the most part on protein synthesis. In the absence of protein synthesis, renewal occurs four times more slowly, apparently by an exchange reaction between activated amino acids and acceptor RNA. This situation is represented schematically as follows:

$$\text{aa} + \text{S-RNA} \underset{3}{\overset{1}{\rightleftharpoons}} \text{RNA-aa} \xrightarrow{2} \text{proteins} + \text{S-RNA}$$

In this equation, reaction 3 is assumed to be slower than reaction 2 for the regeneration of acceptor RNA.

Furthermore, after incorporation by the bacteria of a radioactive amino acid, followed by its dilution by a large excess of unlabeled amino acid, there is observed, following the dilution, an increase in the radioactivity of the proteins corresponding to the loss observed in the fraction of this amino acid bound to the RNA (see Table 4). Gale's recent work on the incorporation of amino acids by disrupted staphylococcal cells (Gale, Shepherd & Folkes, 1958) leads to similar conclusions. These observations,

although they do not present direct evidence, are nevertheless compatible with the hypothesis that the RNA-amino acid is an intermediate between free amino acid and protein.

TABLE 4

Transfer of a radioactive amino acid from the "RNA-amino acid" pool to the "protein fraction"

A culture of the auxotroph *E. coli* M-191 (methionine-histidine) is starved for 4 hr at 32°C. [^{35}S] methionine (0·02 mM) is then added and allowed to label the "RNA pool" for 5 min, in the absence of histidine; at the end of this period, a large excess of non-radioactive methionine (0·004 M) is added to the culture. The total radioactivity of the "RNA pool", and of the proteins, is measured at the time of addition of the unlabeled amino acid and 8 min later.

		Loss of radioactivity from the "RNA pool" (in 8 min) in counts/min	Increase in radioactivity of the proteins (in 8 min) in counts/min
Experiment 1	Control	2,700	2,400
	Chloromycetin	1,600	1,000
Experiment 2		2,140	1,500
Experiment 3		3,100	2,100

Such a hypothesis, however, encounters one difficulty. As we have indicated, the maximal rate of renewal of the pool of bound amino acids is two to three times less than the maximal rate of incorporation of the amino acids into protein. It is possible that the extraction procedures result in a loss and hence underestimation of the pool under study. Such a situation seems improbable, however, since the same values for the pool size are obtained with two very different procedures (see the experiment described in Table 1). The discrepancy mentioned above would then appear to be due to other causes which could include the following:

(1) A heterogeneity of the pool, a consequence of which would be that a fraction of the pool would have an actual turnover considerably more rapid than the observed rate.

(2) A certain number of cellular proteins would be formed *directly* from free amino acids or intermediates other than the RNA-amino acid complexes. It is believed, for example, that cell wall proteins are formed by a mechanism different from that responsible for cytoplasmic proteins, since their synthesis is not blocked by chloromycetin (Crathorn & Hunter, 1958).

(3) All the cellular proteins would involve the same mechanism of synthesis, but only a certain fraction of the amino acids would pass via the "activation enzymes-S-RNA" path; another fraction of the amino acids would be incorporated into peptide linkage without passing through this step, viz.

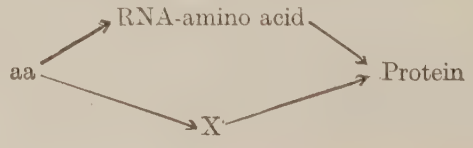

In regard to the manner of formation of proteins from the RNA-amino acids there are so far only hypotheses. The most attractive one seems to be that proposed by Crick (1958). According to him a fraction of the S-RNA resulting from its cleavage would "sterically" adapt the amino acids linked to it to certain "loci" of a matrix of high molecular weight. After condensation of the amino acids into peptide linkage, the S-RNA would be reconstituted from the various fragments (or "adaptors").

The results of the present work demonstrate precisely that, in a cellular population in a steady state, the synthesis of protein limits the availability of sites capable of fixing amino acids. There is, then, compatibility on this point between the experimental data and the hypothesis of an acceptor-RNA that can be regenerated *after* protein synthesis as proposed by Crick.

Another important aspect of the problem presented by the very existence of the apparently low molecular weight RNA is its relationship to the rest of the RNA, that is to say, to the particulate RNA. It is known from the work of Schachman, Pardee & Stanier (1952) and that of Tissières & Watson (1958), as well as that of Roberts, Britten & Bolton (1958), that the majority of the RNA in *E. coli* is linked to proteins in the form of sedimentable particles. About 90% of the *E. coli* RNA is particulate while 10% exists in soluble form.

One may wonder whether the S-RNA acceptor of amino acids is perhaps a precursor of particulate RNA.

We have seen that bacteria incorporate nucleic acid precursors, such as adenine, much more rapidly into this S-RNA than into the high molecular weight RNA. Similar results have been obtained recently using ^{32}P by Naono (1959, unpublished results). It was tempting to suppose that the rapidity of labeling of the S-RNA was related to its role as precursor of another, less metabolically active, fraction of RNA. Let us examine this possibility. If it is supposed that the acceptor RNA is transformed into particulate RNA after having transferred its amino acid to peptide linkage one arrives at a mechanism of the type:

$$\text{S-RNA-aa} \rightarrow \text{RNA} + \text{proteins}$$

Apart from general arguments which make a mechanism of "cosynthesis" of nucleic acid and protein not plausible, there are several specific facts which do not fit this hypothesis. For instance, the S-RNA differs from the particulate RNA in the proportion of the bases (Spahr & Tissières, personal communication, 1959) and moreover contains atypical bases almost absent in the particulate RNA (Dunn, 1959). Also it has been shown in this paper that in uracil-starved cells the amino acid acceptor RNA does not disappear. This would not be expected, if the S-RNA was converted irreversibly to a metabolically stable fraction.

Therefore the observed fast labeling of the S-RNA starting with [^{14}C]adenine probably reflects the attachment of nucleotides to the end of the chain, as has also been observed in *in vitro* systems by Hecht *et al.* (1958) and by Canellakis (1957).

REFERENCES

Albaum, G. & Umbreit, W. W. (1947). *J. Biol. Chem.* **153**, 408.
Berg, P. (1956). *J. Biol. Chem.* **222**, 1025.
Berg, P. & Ofengand, E. J. (1958). *Proc. Nat. Acad. Sci., Wash.* **44**, 78.
Bussard, A. & Perrin, D. (1955). *J. Lab. Clin. Med.* **46**, 689.
Cannellakis, E. S. (1957). *Biochim. biophys. Acta*, **25**, 217.
Cohen, G. N. & Rickenberg, H. V. (1956). *Ann. Inst. Pasteur*, **91**, 693.

Crathorn, A. R. & Hunter, G. D. (1958). *Biochem. J.* **69**, 47.
Crick, F. H. C. (1958). *Symp. Soc. Biol.* **12**, 138.
Dunn, D. B. (1959). *Biochim. biophys. Acta*, **34**, 286.
Gale, E. F., Shepherd, C. J. & Folkes, J. P. (1958). *Nature*, **182**, 592.
Hecht, L. I., Zamecnik, P. C., Stephenson, M. L. & Scott, J. F. (1958). *J. Biol. Chem.* **233**, 954.
Hoagland, M. B. (1955). *Biochim. biophys. Acta*, **16**, 288.
Hoagland, M. B. (1958). *4th Int. Cong. of Biochem.* (*Vienna*), *Symposium* **8**.
Hoagland, M. B., Keller, E. B. & Zamecnik, P. C. (1956). *J. Biol. Chem.* **218**, 345.
Hoagland, M. B., Zamecnik, P. C. & Stephenson, M. L. (1957). *Biochim. biophys. Acta*, **24**, 215.
Hoagland M. B., Stephenson, M. L., Scott, J. F., Hecht, L. I. & Zamecnik, P. C. (1958). *J. Biol. Chem.* **231**, 241.
Mandelstam, J. (1956). *Biochem. J.* **64**, 55.
Monod, J., Cohen-Bazire, G. & Cohn, M. (1951). *Biochim. biophys. Acta*, **7**, 585.
Roberts, R. D., Britten, R. J. & Bolton, E. T. (1958). *Microsomal Particles and Protein synthesis*, p. 84. Washington: Pergamon Press.
Schachman, H. K., Pardee, A. B. & Stanier, R. Y. (1952). *Arch. Biochem. Biophys.* **28**, 245.
Schweet, R. S., Bovard, F. C., Allen, E. & Glassman, E. (1958). *Proc. Nat. Acad. Sci., Wash.* **44**, 173.
Sharon, N. & Lipmann, F. (1957). *Fed. Proc.* **16**, 246.
Sistrom, W. R. (1958). *Biochim. biophys. Acta*, **29**, 579.
Tissières, A. & Watson, J. D. (1958). *Nature*, **182**, 778.
Zillig, N. & Corqodale, D. J. (1958). *Abstracts of the IVth Internat. Cong. of Biochem.* 76.

J. Mol. Biol. (1959) **1**, 321-328

Partition Cell Analysis of Infective Tobacco Mosaic Virus Nucleic Acid†‡

Benjamin S. Friesen and Robert L. Sinsheimer

Division of Biology, California Institute of Technology, Pasadena, California, U.S.A.

(*Received 13 July 1959*)

The infective principle of ribonucleic acid (RNA) isolated from tobacco mosaic virus (TMV), either by Duponol C or water-saturated phenol, has a sedimentation constant of 19·6 Svedberg units at 5°C in 0·02 M-phosphate, pH 7·3, as determined by partition cell ultracentrifugal analysis. This corresponds to an S_{20} of 30.

In fresh samples of RNA, the bulk of the material has the above sedimentation rate. The weight average molecular weight of such samples is 2×10^6 as determined by light scattering.

The sedimentation rate of the infective principle in samples degraded at room temperature to various fractions of residual activity remains the same, although the bulk of the material sediments at a much slower rate. It is therefore concluded that the smaller components do not carry a detectable amount of the infectivity.

1. Introduction

Since the discovery of the infectivity of RNA from TMV (Gierer & Schramm, 1956*a*; Gierer & Schramm, 1956*b*; Fraenkel-Conrat, 1956), conflicting values have been reported for the size of the basic infective unit (Fraenkel-Conrat, Singer & Williams, 1957; Fraenkel-Conrat & Williams, 1957; Gierer, 1958; Ginoza & Norman, 1957; Schuster & Schramm, 1958). A preliminary report of the determination of the sedimentation rate of the infective unit by partition cell experiments has been given (Cheo, Friesen & Sinsheimer, 1959). In this paper a detailed account of these and additional experiments upon the properties of this RNA is given.

2. Materials and Methods

(a) *Preparation of virus stocks*

All virus stocks were of the common variety of TMV, obtained originally from Dr. Wildman of the University of California at Los Angeles. Turkish tobacco plants (*Nicotiana tobacum* var. Turkish) were inoculated by lightly rubbing the leaves with pads of cheese cloth dipped into a 1·0 μg/ml. suspension of TMV containing 20 mg/ml. carborundum. Approximately one month later the leaves were harvested and stored at − 14°C.

The virus was purified by a method developed by Dr. Norman S. Simmons of the University of California at Los Angeles Medical Center (personal communication). This method, which involves the use of ion-exchange resins to effect the deionization of the expressed tobacco juice, routinely yielded monodisperse solutions of virus.§

† The research reported in this paper was performed at the California Institute of Technology, but also formed a major part of the Ph.D. dissertation of B. S. F., submitted to Iowa State College.

‡ The research reported in this paper was supported in part by grants from the American Cancer Society, U.S. Public Health Service and the California Division of the American Cancer Society.

§ The criterion for monodispersity was the presence of a single boundary of 182 *S* when the virus preparation was centrifuged at 3 mg/ml. in 0·02 M-phosphate, pH 7·5, at 17,250 rev/min. The presence of small amounts of dimerized, 224 *S*, or fragmented TMV could be readily detected under these conditions.

The procedure consisted of blending 100 g frozen and pulverized, infected tobacco leaves with 100 ml. of cold 0·01 M-NH_4OH in an Omnimix blender for 2 to 3 min. Capryl alcohol was added whenever needed to prevent foaming. To the blended material, while stirred at the pH meter with a mechanical stirrer, 25 g of Amberlite IRC-50 (16 to 50 mesh) in hydrogen form was added. The pH was quickly brought to pH 7·3 by the addition of Dowex 1-X8, 50 to 100 mesh, in the hydroxyl form. The pH was kept at pH 7·3 ± 0·2 by the periodic addition of Dowex-1. After the reaction was essentially complete (approximately 30 min), the pulp and resins were sedimented at 4,000 *g* for 30 min. To the supernatant, after filtration through fluted S. & S. 410 paper, was added 0·1 volume of 0·1 M-versene, pH 7·0. The solution was immediately adjusted to pH 7·5 with 1·0 M-sodium hydroxide, and the virus sedimented in a 30 rotor (refrigerated Spinco Model L centrifuge) at 28,000 rev/min for 45 min.

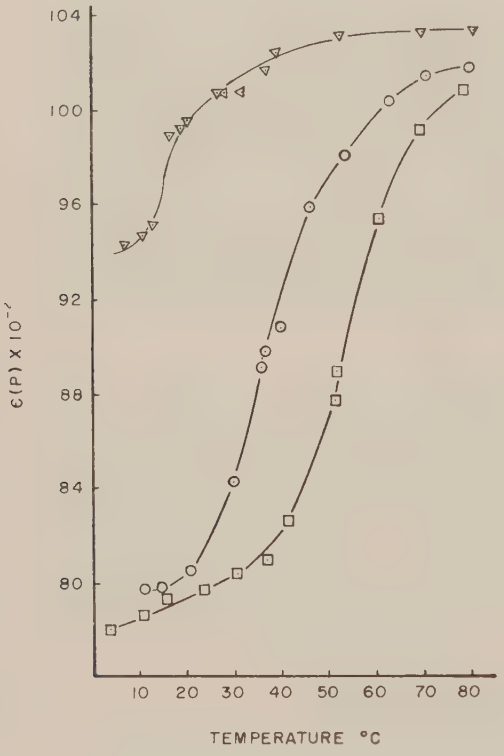

Fig. 1. The extinction of detergent-prepared RNA at 275 mμ as a function of temperature.
▽ RNA in de-ionized distilled H_2O
⊙ RNA in 0·2 M-phosphate, pH 7·3
⊡ RNA in 0·2 M-NaCl + 0·001 M-phosphate, pH 7·5.

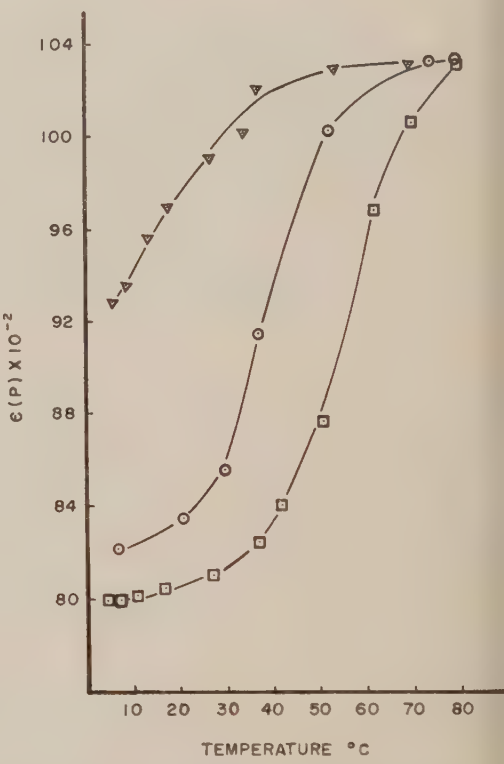

Fig. 2. The extinction of phenol-prepared RNA at 257 mμ as a function of temperature.
▽ RNA in de-ionized distilled H_2O
⊙ RNA in 0·02 M-phosphate, pH 7·3
⊡ RNA in 0·2 M-NaCl + 0·001 M-phosphate, pH 7·5.

Green debris was removed from the pellet by shaking in the lusteroid tube, vigorously by hand, with a portion of the supernatant. This supernatant was then discarded, usually leaving a transparent virus pellet. The virus was resuspended in 0·001 M-versene, pH 7·5, and subjected to a centrifugation for 30 min at 12,000 rev/min in the refrigerated Spinco Model L to remove debris. The high and low speed centrifugations were repeated; the virus was then stored at 10 mg/ml. in 0·001 M-versene, pH 7·5, at 4°C until use.

(b) *Preparation of RNA*

RNA was isolated from the protein either by the phenol method of Gierer & Schramm (1956*a*), or by the detergent method of Fraenkel-Conrat (Fraenkel-Conrat, Singer & Williams, 1957). In later experiments, the Gierer & Schramm isolation procedure was

modified to include four alcohol precipitations from 0·02 M-phosphate, pH 7·3. Such preparations were considerably more stable at room temperature than those in which these precipitations were omitted. RNA samples were frozen in tubes in a dry ice-acetone bath at 1·2 mg/ml. and stored at — 60°C until used.

The concentration of the RNA was determined by absorbance as measured in a Beckman DK2 spectrophotometer at a known temperature. The appropriate extinction coefficient was obtained from Fig. 1 or Fig. 2. The absorbance as a function of temperature was obtained from a sample of detergent-prepared RNA of which the phosphorus content had been determined by a modification of the method of Allen (1940). The extinction coefficients for the phenol-prepared RNA were determined on the basis of the sugar content of such a preparation, relative to that of a detergent-prepared RNA, as determined by the phloroglucinol method (von Euler & Hahn, 1946).

The bulk of RNA, freshly isolated either by detergent or phenol, had a sedimentation constant of 30 S in 0·02 M-phosphate, pH 7·3 at 20°C, and a molecular weight of 2×10^6 as determined by light scattering. The reciprocal of the weight average molecular weight of the RNA increased linearly with time, when it was kept at 25°C. Incubation with $1{\cdot}5 \times 10^{-2}$ μg/ml. of ribonuclease for 1 hr at room temperature routinely abolished the infectivity of the preparation.

In those experiments requiring partially degraded samples, the RNA, in the presence of a drop of chloroform to prevent bacterial growth, was incubated at 25°C or 37°C for an appropriate period of time. The RNA was then cooled below 5°C before further experiments were initiated. The residual infectivity of degraded RNA was determined by assaying it against an aliquot of the same sample kept at a temperature below 5°C after removal from the deep freeze.

(c) *Biological assay system*

Biological assays were performed on the leaves of *Phaseolus vulgaris L*, var. Pinto, *Nicotiana tobacum L*, var. Xanthi nc, and the Holmes hybrid L.L. The pinto beans were grown in vermiculite under climate controlled conditions in the Earhart Laboratories, after it was discovered that this environment increased their sensitivity to RNA twenty-fold. The temperature was maintained at 26°C for 9 hr, followed by 15 hr at 20°C. Auxiliary lights were used to provide a 16 hr day and an 8 hr night. Twenty-four hours before use the pinto beans were placed in the dark. Just prior to infection, the leaves were dusted uniformly with carborundum. One drop of the test solution, kept in test tubes immersed in an ice bath until inoculation, was placed in the centre of the leaf by means of a glass capillary and spread evenly over the surface of the leaf with a glass spatula. The opposite leaf received the same treatment with the control solution.

Xanthi and Holmes L.L. seeds, generously supplied by Dr. Takahashi from the University of California and by Dr. Newmark from the University of Kansas, respectively, were germinated in flats containing vermiculite. Plants were used approximately 4 weeks after the seedlings had been transplanted from the flats. The assay procedure was the same as that described above except that adjacent half leaves were used for test and control solutions.

Concentrations of fresh RNA employed for assay were from 0·2 to 0·5 μg/ml. when tobacco plants were used, and from 0·5 to 1·0 μg/ml. when pinto beans grown in the Earhart Laboratories were used. Twenty times this amount was needed for pinto beans grown under more usual greenhouse conditions.

(d) *Partition cell centrifugation*

All analytical centrifugation was performed with the Model E Spinco Ultracentrifuge. RNA was centrifuged at 5°C, either in 0·02 M-phosphate, pH 7·3, or in 0·2 M-sodium chloride plus 0·001 M-phosphate, pH 7·5. It was found experimentally, in agreement with expectation, that the S at 5°C had to be multiplied by 1·5 to obtain the S at 20°C. Centrifugation was performed at a concentration either of 1 to 1·4 mg/ml. with the use of schlieren optics, or of 20 to 50 μg/ml. with the use of ultraviolet light absorption optics. Yphantis-Waugh partition cell experiments were performed as described by Yphantis & Waugh (1956*a*, 1956*b*).

It was observed that the centerpiece of the Yphantis-Waugh cell inactivated RNA placed in contact with it. By immersing the centerpiece for one minute in "desicote" (Beckman Instrument Company), rinsing with carbon tetrachloride, and allowing it to air dry, this difficulty was overcome for work at RNA concentrations greater than 1mg/ml. The biological activity of RNA placed in the "desicoted" cell at 1·2 mg/ml. for 2 hr at 5°C was statistically identical to that of a control solution. The assembled cell was periodically checked in this manner.

After centrifugation at 56,100 rev/min as described by Yphantis & Waugh,† two dilutions of the supernatant (material remaining above the partition) were assayed against an appropriate dilution of the original RNA solution as a control. Usually the dilution of the supernatant was chosen to be approximately Q‡ and $2Q$ times that of the control solution.

The optical densities of separate portions of the supernatant, subnatant (material remaining below the partition), and the original solution were determined for the calculation of the recovery of ultraviolet-absorbing material and the corresponding sedimentation constant.

From Q, the radius of the meniscus, the radius of the partition plate, at rest, and the graphical integration of $\omega^2 dt$ (Yphantis & Waugh, 1956*a*), the sedimentation rate of the infective unit was calculated.

At RNA concentrations of 20 to 50 μg/ml. erratic inactivation by the partition cell and the containers was a critical problem. The rubber springs and centerpiece of the partition cell, microabsorption cells, and occasional test tubes were found to inactivate severely. Although techniques were finally developed which greatly reduced the inactivation, it could not be eliminated entirely, and rigorous control experiments were performed to provide appropriate corrections.

To reduce inactivation, the centerpiece of the Yphantis-Waugh cell was given two additional coats of "desicote". The cell was always assembled and soaked with 0·1 M-versene, pH 7, for 24 hr before use. It was then disassembled, washed with distilled water, rinsed thoroughly with de-ionized water, air dried, and reassembled for immediate use. Tweezers, covered with surgical tubing, were used to place the spring and the partition in the cell. All glassware, including pipettes and absorption cells, were soaked in nitric acid for 24 hr, rinsed with de-ionized distilled water, and air-dried before use. In addition micropipettes and microabsorption cells were rinsed with de-ionized distilled water, followed by distilled alcohol, and air dried under aspiration immediately before and after use.

The centrifuge runs were carried out at a speed of 42,040 rev/min, when 20 to 50 μg/ml. concentrations were used. § Control experiments were performed immediately before and after each analytical centrifugation by subjecting portions of the original solution to every procedure used in the analytical run itself, save one. The difference was that the control solutions were spun at 4,000 rev/min, a speed at which the partition moved to the bottom of the cell, but which produced no appreciable sedimentation. As nearly as possible the time spans were made identical to those of the analytical run itself. The original solution was then assayed against the supernatants of the two control experiments in addition to the supernatant of the test run.

† At the end of the run, slow brake was used from 56,000 rev/min to 39,500 rev/min, medium brake from 39,500 rev/min to 28,000 rev/min, fast brake from 28,000 rev/min to 6,000 rev/min, and slow brake from 6,000 rev/min to rest.

‡ Q (Yphantis & Waugh, 1956*a*), the average fractional supernatant concentration, is defined by the relation

$$Q = \frac{\int_a^{r_p} c(r,t)\ r dr}{\int_a^{r_p} c_0\ r dr} = \frac{r_p^2 - a^2 - r_p^2\left(1 - e^{-2s\int_0^t \omega^2 dt}\right)}{r_p^2 - a^2}$$

where c_0 is the original solute concentration, $c(r,t)$ is the solute concentration at radius r and time t (t is the effective time of the end of the sedimentation), a is the radius of the meniscus, r_p is the rest radius of the separation plate of the partition cell, ω is the angular velocity during any time interval dt, and s is the sedimentation coefficient of the solute.

§ The braking speeds at the end of the run were changed at 29,000 rev/min, 21,000 rev/min and 6,000 rev/min from slow to medium, medium to fast, and fast to slow, respectively.

It was found that the exposures of ultraviolet light necessary for absorption photography during centrifugation were sufficient to reduce the infectivity. As a consequence, conventional sedimentation constants were determined from separate portions of the original RNA solutions.

3. Results

(a) *Partition cell experiments at 1·0 to 1·4 mg/ml. RNA concentration*

For a given sample of RNA, three sedimentation rates could be calculated. These were obtained from the proportion of ultraviolet light-absorbing material remaining above the partition (Q_{UV}), from the biological activity remaining above the partition ($Q_{INF.}$), and the rate of sedimentation of the schlieren boundary.† Undegraded RNA and RNA with residual infectivities ranging from 4 to 61% of the initial value were analyzed. The results of these experiments are recorded in Table 1.

(b) *Partition cell experiments at 50 μg/ml.RNA concentration*

In these experiments the $Q_{INF.}$ value used for the calculation of sedimentation rates had to include correction for inactivation of the RNA during the centrifugation, by the experimental procedure described. The residual infectivity (R) was determined by dividing the average infectivities of the supernatants of the two control runs (made at 4,000 rev/min) by that of the initial uncentrifuged sample. On the assumption that the RNA in the supernatant of the test (42,040 rev/min) run was inactivated by the same amount, the Q value obtained experimentally from the test solution would be R times smaller than the value that would have been obtained in the absence of inactivation. Therefore, the experimental Q value was divided by R to obtain $Q_{INF.}$ The data obtained from these experiments are recorded in Table 2.

4. Discussion

The possibility that the use of the Yphantis-Waugh partition cell might not be valid for RNA was investigated by sedimenting all the material below the rest position of the partition, allowing the partition to return, and checking the supernatant for residual ultraviolet light-absorbing materials and for infectivity. The absorption of the supernatant accounted for less than 0·4% of that of the solution (1·2 mg/ml.) initially placed in the cell. The spectrum of this supernatant was not that of RNA. No infectivity could be demonstrated in the supernatant. In addition, the sedimenting peak appeared undisturbed after the plate had returned past it. The general procedure was also checked with TMV. A value of 208 S was obtained for the biological activity of TMV as compared to 189 S for the photographic boundary of this same sample. These are in agreement within the statistical variation to be expected in the biological assay.

† At a concentration of 1 mg/ml., over 85% of the RNA appears under a single schlieren peak, while the remainder trails at lesser sedimentation rate. The S (Boundary) of Table 1 is the sedimentation rate of this leading component.

At a concentration of 50 μgm/ml., 60 to 75% of the RNA appears as a distinct leading centrifugal component (Boedtker, 1959), while the remainder trials with a spread of lesser sedimentation rate. The sedimentation rate of the leading component was determined, from densitometer traces of the ultraviolet light photographs, from the successive positions of the 50% (of the leading 60 to 75%) point. The S (Boundary) of Table 2 is the sedimentation rate of this leading component.

The S (UV) of Tables 1 and 2 has been determined from the Q_{UV} and, since it is weighted by inclusion of the slower-sedimenting components, will always be less than the S (Boundary).

TABLE 1

Results of partition cell experiments on infective RNA at 1 mg/ml.

A	B	C	D	E	F	G	H	I	J		
									S (5°C)		
Preparation	Per cent storage survival	Per cent recovery of UV absorption	r_m (cm)	$\int\omega^2 dt \times 10^{10}$	Ratio† of lesions for Q	Dilution‡	$Q_{INF.}$§	Q_{UV}	Boundary	UV	INF
1. Phenol	100	91	5·963	4·52	6982/8518	2·0	0·410	0·420	12·6	11·1	11·3
2. Phenol	100	101	5·884	6·38	2473/3143	4·0	0·197	0·245	12·7	11·5	12·3
3. Phenol	100	100	5·865	3·80	169/227	2·0	0·372	0·571	12·2	10·9	16·3
					541/1501	1·0	0·360				16·7
4. Phenol	100	99·7	5·874	5·65	227/185	4·0	0·307	0·346	11·9	11·3	12·0
5. SDS	100	92·4	5·832	6·70	678/1340	4·0	0·126	0·187	14·7	12·9	14·0
					1045/5263	1·35	0·147				13·7
6. Phenol	10		5·902	6·29	394/1949	3·65	0·055	0·353	11·6	9·6	14·5
7. Phenol	54		5·846	6·70	1784/1924	3·65	0·254		12·4		11·6
					671/1196	2·0	0·280				11·1
8. Phenol	61	110	5·888	5·71	48/319	4·0	0·038	0·509	12·2	8·1	16·7
					124/326	2·0	0·190				13·8
9. SDS	59	100	5·884	5·91	1322/1682	3·0	0·262	0·546		7·2	12·1
					300/825	1·5	0·242				12·5
10. SDS	43	97	5·888	6·52	195/575	2·0	0·170	0·421	12·0	8·4	12·4
11. SDS	4	113	5·879	6·19	11/80	3·0	0·046	0·512	11·5	7·5	15·5
					12/71	1·5	0·113				14·3
12. SDS	40	94	5·864	6·20	187/1177	3·0	0·053	0·570	12·9	6·8	15·6
					59/333	1·5	0·118				14·5
								Average	12·46		13·7

† The ratio is given as the total number of lesions obtained from the supernatant over the total number of lesions produced by the initial sample.
‡ The dilution is given as the factor by which the dilution of the control exceeds that of the test solution.
§ $Q_{INF.}$ = Column F/Column G.

TABLE 2

Results of partition cell experiments on fresh infective phenol RNA at 50 μg/ml.

A	B	C	D	E	F	G	H	I	J		
									S (5°C)		
Experiment	Per cent recovery of UV absorption	r_m (cm)	$\int\omega^2 dt \times 10^{10}$	Ratio† of lesions for controls	Ratio‡ of lesions for Q	Dilution §	$Q_{INF.}$‖	Q_{UV}	Boundary	UV	INF
1.	95	5·867	2·22	6750/8700	4821/3134	4	0·496	0·592	18·8	18	22
					1573/3166	1	0·640				16
2.¶	100	5·869	3·36	2210/3145	853/1211	4	0·251	0·550		13	22
					481/1009	2	0·340				20
3.	90	5·979	3·49	4162/6941	712/3817	4	0·078	0·395	19·6	14	22
					614/4552	1·35	0·167				20
4.		5·833	3·93	3222/4367	2166/2115	5	0·278	0·441	18·9	15	19
					1055/1488	2·5	0·385				16
5.		5·928	4·19	1412/3697	580/1671	6	0·151	0·343	18·7	14	18
		5·983	2·27	56/204	83/237	3	0·425				20
								Average	19·0	15	19·4

† Ratio is given as total number of lesions obtained from both control supernatants divided by the total number of lesions produced by the initial sample.
‡ Ratio is given as total number of lesions obtained from test supernatant divided by total number produced by the initial sample.
§ The control or initial sample was diluted the factor given times as much as the supernatant.
‖ $Q_{INF.}$ = Column F/(Column E) · (Column G).
¶ This sample was badly degraded for unknown reasons.

Theoretically, the subnatant could be used as an added check on the sedimentation rate, but RNA sedimented against the bottom of the cell and resuspended was totally inactivated, and velocity sedimentation photographs demonstrated its physical disintegration.

It is well known that duplicate assays for TMV and RNA may vary as much as 10 to 20%. For this reason it was necessary to design experiments so that the $Q_{INF.}$ values were below 0·4, preferably between 0·1 and 0·25. In this range of Q values, a relatively large statistical error in $Q_{INF.}$ produces a relatively small error in the calculated S. For example, if $Q_{INF.}$ equals $0{\cdot}25 \pm 20\%$, $S = 13 \pm 7\%$. However, at very low values of $Q_{INF.}$, insufficient material remained above the partition for an assay of the above stated accuracy.

It was desirable to determine the sedimentation rate for as great a range in $Q_{INF.}$ as possible in order to establish whether infective units of various sizes existed. As a compromise, values of $Q_{INF.}$ between 0·05 and 0·5 were used. It is clear that not all experiments recorded in the tables are equally reliable. It is significant that the most reliable experiments in general showed the greatest agreement with the boundary sedimentation rates.

The fact that the sedimentation rate of the infective unit is approximately 30 S. irrespective of the degree of degradation of the RNA, suggests strongly that only the high molecular weight material is infective and that the smaller components do not carry a demonstrable amount of activity. The method of preparation has no effect on the minimal size of the infective unit, in contrast to the reported findings of Fraenkel-Conrat (Fraenkel-Conrat & Williams, 1957). On the basis of the physical characterization of the undegraded RNA mentioned above, it would appear that the molecular weight of the 30 S infective material is of the order of 2×10^6 in agreement with the work of Gierer (1958).

It is a pleasure to acknowledge the able technical assistance of Miss Barbara Starman and Mr. Robert Bradford. Financial support to one of us (B. S. F.) from the Arthur McCollum Fund is gratefully acknowledged.

REFERENCES

Allen, R. J. L. (1940). *Biochem. J.* **34**, 858.
Boedtker, H. (1959). *Biochim. biophys. Acta*, **32**, 519.
Cheo, P., Friesen, B. & Sinsheimer, R. L. (1959). *Proc. Nat. Acad. Sci., Wash.* **45**, 305.
Fraenkel-Conrat, H. (1956). *J. Amer. Chem. Soc.* **78**, 882.
Fraenkel-Conrat, H., Singer, B. & Williams, R. C. (1957). *Biochim. biophys. Acta*, **25**, 87.
Fraenkel-Conrat, H. & Williams, R. C. (1957). *N.Y. Acad. Sci. Spec. Publ.* V, 217.
Gierer, A. & Schramm, G. (1956*a*). *Nature*, **177**, 702.
Gierer, A. & Schramm, G. (1956*b*). *Z. Naturf.* **11***b*, 138.
Gierer, A. (1958). *Z. Naturf.* **13***b*, 485.
Ginoza, W. & Norman, A. (1957). *Nature*, **179**, 520.
Schuster, H. & Schramm, G. (1958). *Z. Naturf.* **13***b*, 697.
von Euler, H. & Hahn, L. (1946). *Svensk Kem. Tidskr.* **58**, 251.
Yphantis, D. A. & Waugh, D. F. (1956*a*). *J. Phys. Chem.* **60**, 623.
Yphantis, D. A. & Waugh, D. F. (1956*b*). *J. Phys. Chem.* **60**, 630.

J. Mol. Biol. (1959) **1**, 329-332

Electron Microscopy of Ribonucleoprotein Particles from *E. Coli*

C. E. Hall and H. S. Slayter

Department of Biology, Massachusetts Institute of Technology, Cambridge, Massachusetts, U.S.A.

(*Received 8 August 1959*)

Four kinds of ribonucleoprotein particles from *E. coli* characterized by the sedimentation constants 30, 50, 70 and 100 *S* were observed in shadow cast specimens and measured. The 30 and 50 *S* particles are apparently produced by a splitting of the 70 *S*, while the 100 *S* material consists of dimers of the 70 *S* which form at high concentrations of Mg^{++}. As dried and prepared for electron microscopy, 30 *S* particles are asymmetric, representable by a prolate ellipsoid 95 × 170 Å. The 50 *S* particles are more nearly spherical and represented by an oblate ellipsoid 170 × 140 Å. Volumes calculated from these dimensions are in excellent agreement with those deduced from physical chemical data. 70 *S* particles exhibit an undefined substructure and are not closely representable as ellipsoids, but the diameter and height are estimated to be approximately 200 and 170 Å respectively. The results in general confirm and supplement the physical chemical studies of Tissières and co-workers on these same materials.

1. Introduction

Tissières & Watson (1958) and Tissières, Watson, Schlessinger & Hollingworth (1959) have described the isolation of ribonucleoprotein (RNP) particles from *E. coli* and the separation of this material into four components characterized by sedimentation constants of 30, 50, 70 and 100 *S*. We report here electron microscopic observations of samples of these materials made concurrently with the studies which they have described.

2. Materials and Methods

Samples suspended in magnesium acetate prepared by Tissières *et al.* (1959) were transported packed in ice immediately after isolation and prepared for electron microscopy by a spray drop method (Hall, 1956) within a few hours. Polystyrene latex spheres with an average diameter of 880 Å were added to the preparations to provide an internal standard for measuring the shadow-to-height ratio. Specimens were shadow cast with platinum at an angle of about 5 : 1.

Initial experiments indicated that the particles were relatively unstable in time and that their stability was also a function of Mg^{++} concentration (Tissières & Watson, 1958). The results to be described were obtained from materials suspended in various concentrations of magnesium acetate, though we generally use volatile salts in this spray method. Although magnesium acetate is non-volatile, its presence did not cause noticeable deterioration of the images in the concentrations used, which were 5×10^{-3} M and less.

3. Observations and Results

(a) *Morphology of the RNP particles*

Electron micrographs of the four components are shown in Plate I. The 30 *S* component is the smallest and consists to a large extent of particles which are rod-shaped as indicated by the arrow in Plate I(a). The 50 *S* component shown in Plate

I(b) is more nearly spherical in appearance. The 70 *S* specimens always contained an appreciable number of particles similar in size to those in the 30 and 50 *S* materials as well as some larger particles indicated by the arrows in Plate I(c). These latter particles show a complexity of structure as though they were made up of subunits, but the appearance is so variable that a unique morphology has not been determined. The 100 *S* preparation contained a large number of diploid particles as indicated by the arrow in Plate I(d). In many instances these particles show one or more small granules lodged in between the two larger symmetrical units. This appearance is to be seen in an exaggerated fashion in the particle in the lower right hand corner of Plate I(d) where we see a diploid stretched out, showing two large particles separated by two smaller subunits, all in a line.

(b) *Measurements of 30, 50 and 70 S preparations*

In the case of the 50 and 70 *S* particles two measurements were made from electron micrographic prints (at about 100,000 ×): (a) widths perpendicular to the shadow

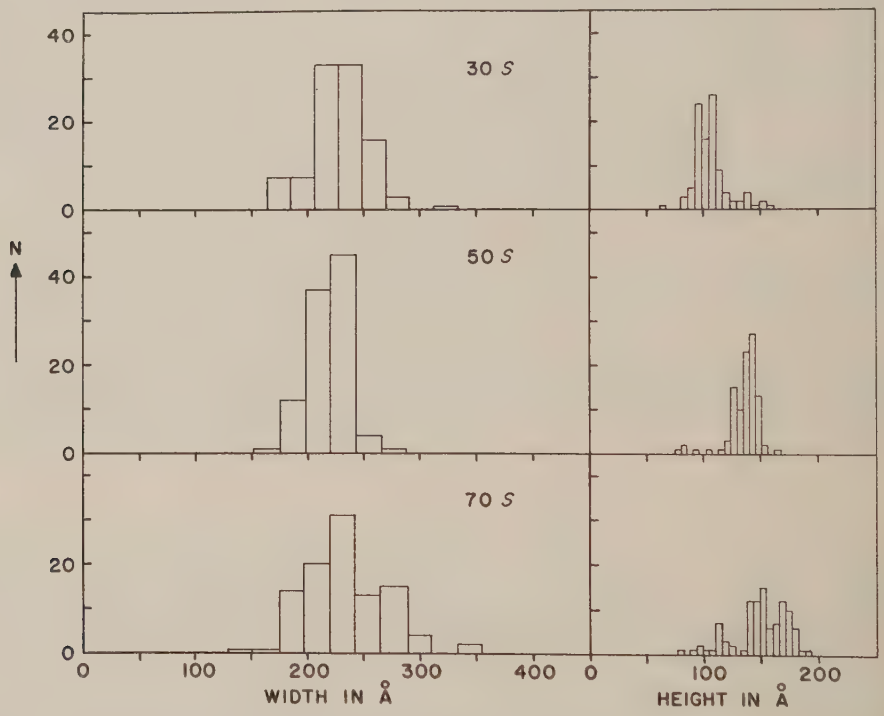

Fig. 1. Histograms showing widths and heights of platinum-shadowed ribonucleoprotein particles from *E. coli*, characterized by their sedimentation constants. In the case of the 30 *S* particles the "width" refers to the long axis and for the other two the width is measured perpendicular to the shadow direction. The widths include a cap of metal which is estimated to exaggerate this dimension by about 60 Å.

direction and (b) shadow lengths from which particle heights can be calculated. In the case of the 30 *S* particles which are somewhat rod-shaped as indicated by the arrow in Plate I(a) the longest dimension was measured rather than the width perpendicular to the shadow direction. Results of these two measurements for about 100 particles in each case are shown in Fig. 1 for 30, 50 and 70 *S* preparations. The apparent width is about the same for the 30 and 50 *S* particles. In the 70 *S* preparation

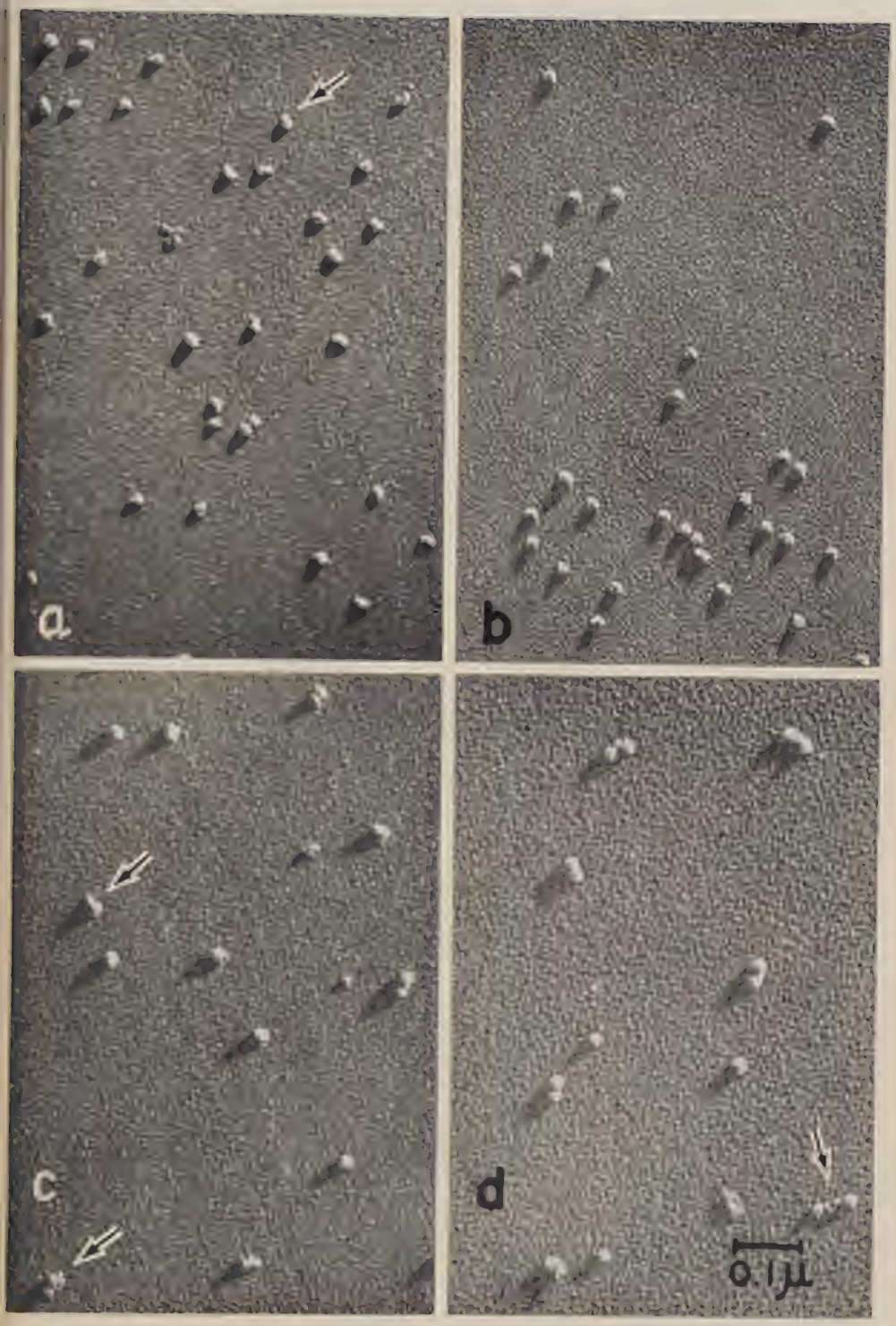

PLATE I. Ribonucleoprotein particles from *E. coli*. Magnification 100,000 ×.

(a) RNP particles from a 30 s preparation. The arrow indicates a typical asymmetrical particle.

(b) RNP particles from a 50 s preparation.

(c) RNP particles from a 70 s preparation. These specimens also show 30 and 50 s particles. The 70 s particles, such as are indicated by arrows, show a substructure as though they consisted of two or more granules.

(d) RNP particles from a 100 s preparation. The 100 s particles are believed to be dimers of th 70 s.

[*To face page* 330

there is also a large number with about the same width as the others, but there is a significant number with a greater width. The height of the 30 *S* particles is significantly smaller than the height of the 50 *S*. The 70 *S* shows a relatively wide distribution of heights, some about the same as the 30 and 50 *S* and some which are significantly higher. The 70 *S* preparation apparently contains breakdown products resulting from preparative procedures for electron microscopy (EM). The distribution of measurements can be accounted for by considering it to consist of a mixture of 30 *S* and 50 *S* particles and a third larger component, presumably 70 *S*. The experiment shown in Fig. 1 was repeated on a second set of materials with practically identical results.

From measurements of a number of spherical molecules of known molecular weight we have found that the measured shadow lengths are a good measure of the true particle heights and that apparent widths are too great in our method by about 60 Å due to the cap of shadowing metal. With these considerations in mind the analysis of the results yields two figures, a height and a width (corrected for metal), which figures we assume to be the major axes of equivalent ellipsoids for the purpose of calculating molecular volumes for comparison with the data of Tissières *et al.* (1959). For the 70 *S* particles we have selected the dimensions of the larger particles in the field, ignoring the smaller particles of about the dimensions of the 30 and 50 *S* preparations. Figures for the 30 and 50 *S* particles are averages and include more particles than are represented in Fig. 1. A summary of average dimensions is shown in Table 1

Table 1

Sedimentation constant	Mg^{++}	EM Dimensions Å	EM M.W. $\times 10^{-6}$	Tissières *et al.* M.W. $\times 10^{-6}$
30 *S*	2×10^{-4}M	Prolate 95 × 170	0·76	0·70
50 *S*	$2{\cdot}5 \times 10^{-4}$M	Oblate 170 × 140	2·0	1·80
70 *S*	10^{-3}M	Oblate 200 × 170	3·4	2·63

where the partial specific volume 0·64 is used to convert calculated molecular volume to molecular weight. Since the volume is quite sensitive to linear dimensions the agreement between EM and physical chemical methods is very good for the 30 and 50 *S* particles though the EM value is 10% high in both cases. In the case of the 70 *S* preparation the EM value is too high in comparison with the physical chemical data and also 20% greater than the sum of the 30 and 50 *S* weights from electron microscopy. We take this to mean that the 70 *S* particles are not accurately representable as a solid ellipsoid. It is not clear in detail from the micrographs how the 30 and 50 *S* particles might be put together to form a 70 *S*. They are probably not to be thought of as rigid structures that retain exactly the same shape when they separate.

(c) *Comparison of 70 and 100 S preparations*

Two samples containing fairly high Mg^{++} and characterized by the sedimentation constants 70 *S* and 100 *S* respectively were examined. Both of these preparations showed two peaks in the ultracentrifuge and are characterized by the constant for the larger peak (Tissières & Watson, 1958). Micrographs of both of these preparations

showed a relatively large number of double particles as indicated by the arrow in Plate I(d) as well as single particles such as one sees in 70*S* preparations. Fields were selected at random and counts were made of the number of single and double particles present in both preparations. The relative amount of material present in the two forms is shown in Table 2 for each preparation, on the assumption that a double

Table 2

Material	Mg^{++}	N counted	Fraction of material† in: single particles	double particles
"70*S*"	0·002 M	406	65%	35%
"100*S*"	0·005 M	229	39%	61%

†Assuming that the mass of a double particle is twice that of a single.

particle has twice the mass of a single. (This is not strictly accurate since there are some single particles smaller than those identified as 70*S*.) The increase in double particles at the higher Mg^{++} concentration leaves little doubt that the 100*S* peak in the centrifuge is to be identified with the double particles. Particle volumes for the dimers estimated from shadow lengths and widths are about twice the volume of the 70*S* particles.

4. Conclusions

In general, the observations confirm the results of Tissières *et al.* (1959) on the existence and weights of the four components of RNP designated 30, 50, 70 and 100*S*. In addition, we observe aspects of the particle morphology which supplements the evidence from physical chemical methods. The 30*S* particles have a high degree of asymmetry (axial ratio about 2 : 1.) The 50*S* particles are more nearly spherical. (The slight oblateness observed may be partly caused by a flattening against the supporting surface.) The 70*S* particles exhibit a substructure which is not sufficiently well-defined to show clearly how the 30 and 50*S* fragments are related when combined in the 70*S*. Due to irregularities in shape, the 70*S* particles are not closely representable by a solid ellipsoid with axes corresponding to the major dimensions. The 100*S* particles appear clearly to consist of two 70*S* particles combined.

This investigation was supported by a research grant C-2171 (C6 & 7) from the National Cancer Institute of the National Institutes of Health, United States Public Health Service.

REFERENCES

Hall, C. E. (1956). *J. Biophys. Biochem. Cytol.* **2**, 625.
Tissières, H. & Watson, J. D. (1958). *Nature*, **182**, 778.
Tissières, A., Watson, J. D., Schlessinger, D. & Hollingworth, B. R. (1959). *J. Mol. Biol.* **1**, 221.

J. Mol. Biol. (1959) **1**, 333-338

Electron Microscope Studies of the Development and Structure of Poliomyelitis Virus

R. W. Horne
Electron Microscope Group, Cavendish Laboratory, University of Cambridge, England

J. Nagington
Public Health Laboratory Service, Cambridge, England

(*Received 13 August 1959*)

The application of the potassium phosphotungstate negative staining technique to fragments of HeLa cells infected with poliovirus is described.

The assembly of virus particles from subunits, within a containing membrane, is observed from high resolution electron micrographs. Preliminary studies have revealed the presence of three kinds of virus particle—complete, incomplete and empty shells.

The subunit arrangement of the protein shell appears to be consistent with the icosahedral symmetry (532) predicted by X-ray diffraction investigations. All three antigenic types of poliovirus appear to be 300 Å in diameter with protein subunits approximately 60 Å in diameter.

1. Introduction

Poliomyelitis virus particles were first measured by electron microscopy in 1954 by Sabin, Hennessen & Warren, who examined particles from infected tissue culture and estimated the virus to have an approximate diameter of 250 Å. Purified virus preparations were studied by Schwerdt, Williams, Stanley, Schaffer & McClain (1954) who obtained a diameter of 310 Å for air-dried particles and 270 Å after freeze-drying. They considered the latter figure to be the most reliable. Further studies using particle density estimations by Schwerdt & Schaffer (1955) gave a particle diameter in the range 220 Å to 280 Å, and suggested that the larger value represented a more reliable estimate of the particle size. From the chemical and physical studies they concluded that polioviruses contained nucleoprotein of the RNA type, which comprised one fourth to one third of the mass of the particle.

Sjöstrand & Polson (1958), using the technique of ultra-thin sections, examined packed pellets of poliovirus fixed in osmium tetroxide. A particle diameter corresponding to the lower figure of 220 Å given by Schwerdt & Schaffer was estimated from the electron micrographs, but some evidence of compression distortion was obtained, together with possible shrinkage effects from fixation, which may offer a possible explanation of the small diameter they measured. Steere & Schaffer (1958) employed frozen replica techniques to study fractured crystals of purified poliovirus in the electron microscope and got a particle diameter of 273 Å, which is in good agreement with the value given by Schwerdt *et al.* (1954) for frozen dried particles. More recently, Finch & Klug (1959) have used X-ray diffraction methods to study the structure of poliovirus from wet crystals. From the subunit spacing and particle symmetry they concluded that the diameter of the individual particles is approximately 300 Å.

The estimated size and symmetry is similar to the particles found in preparations of turnip yellow mosaic virus (TYM) by Cosslett & Markham (1948), Cosentino, Paigen & Steere (1956) and others. X-ray diffraction studies of TYM by Klug, Finch & Franklin (1957) suggested that the particles had icosahedral symmetry (532) with the subunits placed at the vertices of a snub dodecahedron. Further investigations by Finch & Klug (1959) on poliovirus revealed 532 symmetry of the protein particle subunits and it was concluded that the two viruses are structurally similar.

In the present electron microscope studies the new negative staining technique with potassium phosphotungstate, developed by Brenner & Horne (1959; Horne & Brenner, 1958), has been used. It will be seen that the high resolution electron micrographs obtainable by this method reveal the presence of the virus subunits and their possible arrangement to form the outer protein component of the particles; the particle diameter measured from these preparations is estimated to be 300 Å. No previous electron microscope studies on the subunit arrangement of the external structure of poliovirus particles appear to have been reported.

As the technique allows the study of growing virus in tissue culture, some information has also been made available on the morphology of the intracellular growth of the virus.

2. Materials and Methods

(a) *Growth of virus*

The classical strains of poliovirus, Brunhilde (Type 1), MEF-I and Y-SK (Type 2) and a strain of Type 3, were grown in HeLa cell monolayers in Pyrex feeding bottles. After the addition of enough virus to infect all the cells they were maintained in Hanks' balanced salt solution (Weller, Enders, Robbins & Stoddard, 1952) with either 5% horse or 5% calf serum. The cells were harvested at intervals during the growth cycle up to 7 hr. They were washed with phosphate-buffered saline (Dulbecco & Vogt, 1954) and removed from the glass after exposure to 1 : 5000 versene for 5 min at 37°C.

The suspension was centrifuged at 1000 rev/min for 3 to 4 min, the supernatant completely removed and the pellet frozen immediately to — 20°C in an alcohol bath.

(b) *Electron microscopy*

For electron microscopy a procedure based on that of Brenner & Horne (1959) was used. The frozen pellet was rapidly thawed at 37°C and suspended in 4% aqueous ammonium acetate to give a concentration of 5×10^7 cells per ml. To this was added 5 volumes of 3% potassium phosphotungstate adjusted to pH 6·2. It was found that this was the highest pH value which could be used without causing an increase in the viscosity of the nucleoprotein sufficient to prevent spraying of the suspension. Damage to the cells by hypotonic solutions and repeated freezing and thawing tends to increase the effect of potassium phosphotungstate on the viscosity of the suspension, presumably by rendering the nucleoprotein more accessible to it.

To spray the suspensions onto carbon-coated grids without contaminating the atmosphere with live virus, a Vaponefrin atomiser spray gun was connected to a plastic box into which a removable slide containing the grids could be inserted (Fig. 1). The excess vapour was drawn through a wash bottle into another bottle of 2 to 3 l. volume which acted as a reservoir, and then through a Bunsen flame by means of a narrow bore tube fastened immediately above the burner jet. The wash bottle placed between the reservoir and the plastic box served as an indicator for the presence of leaks. The effluent was drawn off and burnt and the negative pressure enabled removal of the slide and repeated spraying to be carried out in safety. All joints were made airtight with vacuum grease and a valve was inserted between the atomiser and pressure bulb in order to prevent any vapour being drawn back into the bulb.

This technique enables droplets of up to 20μ diameter to be sprayed, although the average droplet size is considerably smaller. For the study of the intracellular development

of virus it was found that cell fragments produced by a single cycle of freezing and thawing were the most useful. The sprayed droplets dry quickly; the phosphotungstate seems to exert a supporting action so that drying distortion is negligible and excellent preservation of the intracellular structures is achieved.

Specimen grids sprayed with poliovirus were inserted in standard electron microscope specimen holders. These were transferred to the microscope specimen chamber by screwing them onto the removable locking insert, located in the air lock system, thus preventing any direct contact with the supporting grid or holders. Air was admitted to the specimen chamber through the leak valve mechanism before the specimens were removed in order to avoid rupture of the carbon substrate which might have caused contamination of the microscope. A few experiments on specimens removed from the microscope failed to demonstrate the presence of living virus and it is probable that these were sterilised by the vacuum and the electron beam.

The specimens were examined in a Siemens Elmiskop electron microscope at instrumental magnifications of $\times 40{,}000$ to $\times 80{,}000$ using double condenser illumination.

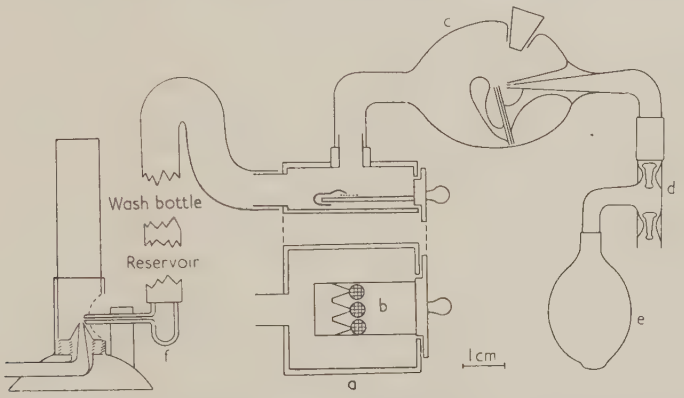

Fig. 1. (a) Perspex box. (b) Removable slide of Perspex with metal clip to hold the carbon-coated grids in place. (c) Spray gun. (d) Glass valve. (e) Rubber bulb. (f) Narrow bore metal tube attachment, with end above the gas jet of a Bunsen burner.

3. Results and Discussion

(a) *The development of the virus*

Examination of electron micrographs obtained from cell fragments shows that particles with a definite resemblance to virus in shape and size are not distinguishable until approximately 4 to $4\frac{1}{2}$ hr after infection of the cells. This is soon after the beginning of the production of infective virus which can first be detected at about 3 hr (Ackermann, 1958; Kallman, Williams, Dulbecco & Vogt, 1958; Ledinko, 1958). The concentration of mature virus before 4 to $4\frac{1}{2}$ hr is probably too small for particles to be detected by the methods described in this communication, except as a rare event. A number of preparations examined $3\frac{1}{2}$ to 4 hr after infection revealed the existence of bodies of the shape and size of that shown in Plate I. Some evidence of loosely packed subunits can be seen within the body. These subunits have dimensions similar to those of the subunits found in individual virus particles studied at higher magnification.

The recognisable virus particles were frequently observed enclosed in these well-defined bodies bounded by a membrane. Measurements made from the electron micrographs show a variation in the size of the bodies from approximately 300 Å diameter to more than 1 μ (Plate II); it is possible that they may reach larger dimensions but fail to survive the spraying procedure. Many of the bodies contained about

10 virus particles in different stages of development. The largest contained over 500 particles and might have been visible by light microscopy (Plate VII). Both large and small bodies containing virus can be seen at about 5½ hr and they probably represent asynchronous development of the virus in individual HeLa cells.

Large intracellular structures appearing at the time that infective virus starts to be produced have been observed on several previous occasions, although most observations have been made very much later in the cycle.

Tenenbaum (1957), using fluorescent microscopy, saw markedly increased RNA fluorescence in the cytoplasm approximately 4 hr after infection, and also observed the onset of a process of discarding fragments of this material into the medium. At the same time she saw increased DNA activity in the nucleus.

Electron micrographs of ultra-thin sections of monkey kidney cells at this time also show increased density of the central cytoplasm (Kallman *et al.*, 1958) which can be seen with phase contrast (Barski, Robineaux & Endo, 1955), and is probably the same as the eosinophilic mass about the size of a nucleus observed by Reissig, Howes & Melnick (1956) and others.

A little later in the cycle, i.e. 5 to 6 hr, dense bodies about 1200 to 1300 Å in diameter were seen in sections by Kallman *et al.* (1958) who suggested that these bodies, which they named "U-bodies", might represent dense material which forms or invades some kind of canalicular system in the cell. They were unable to see any virus particles in these preparations, possibly owing to the loss of definition in stained sections and the high instrumental magnification required to detect the individual virus particle. In none of these studies has the intracellular location of the virus particles been defined.

From approximately 5 to 5½ hr after infection three kinds of virus particle can be readily distinguished (Plate III). There are incomplete particles which appear to have a partially assembled shell of subunits, empty shells or "ghost" particles, and complete or nearly complete particles. The proportion of complete, incomplete and empty particles seen inside the large bodies is about the same as for particles lying free, and this suggests that the free particles have probably been released from disrupted large bodies.

The percentage of empty shells observed depends on how readily the complete and incomplete particles can be distinguished. The highest counts were recorded at 5½ hr when 11 to 14% were seen. By 6½ hr the number had fallen slightly to 3 to 8% and this value seems to remain fairly constant for 24 hr or more. The fall in numbers may be due to the failure of the empty shells to survive intact. They may be somewhat unstable without the whole RNA core of complete particles.

It is highly probable that the three kinds of particle correspond to the fractions which have been identified in sucrose density gradients (Le Bouvier, Schwerdt & Schaffer, 1957); that is, the complete particles may correspond to the infective virus and the incomplete and empty shells to the non-infective. The empty shells are comparable with the "top component" of TYM preparations.

After 6½ hr the large bodies containing the virus particles are seen very infrequently (Plate VII), and it is possible that they may break down during the changes which accompany cytotransudation, which starts at about this time (Ackermann, 1958). This would be consistent with migration of the virus particles across the cytoplasm, and their appearance in the extracellular fluid at about 7 hr with the onset of the phase of virus release.

In an attempt to produce non-infectious virus by means of proflavin it was hoped to see if morphologically different virus could be distinguished. The addition of

PLATE I. Large body (1μ across) embedded in phosphotungstate. From HeLa cells infected with Type 1 poliovirus 4 hr earlier. No recognizable virus particles are visible, but small particles forming the internal structure are of the same size as the subunits seen in virus particles.

[*To face page* 336

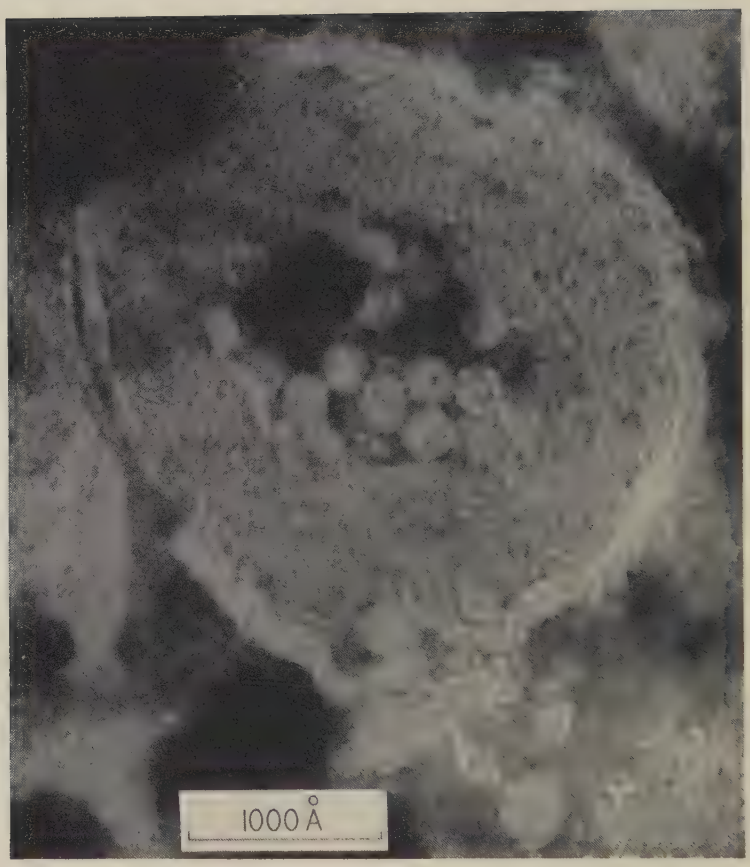

PLATE II. Relatively small body (4000 Å) seen at 4½ hr after infection. Virus particles in various stages of assembly are visible. The body is bounded by a membrane.

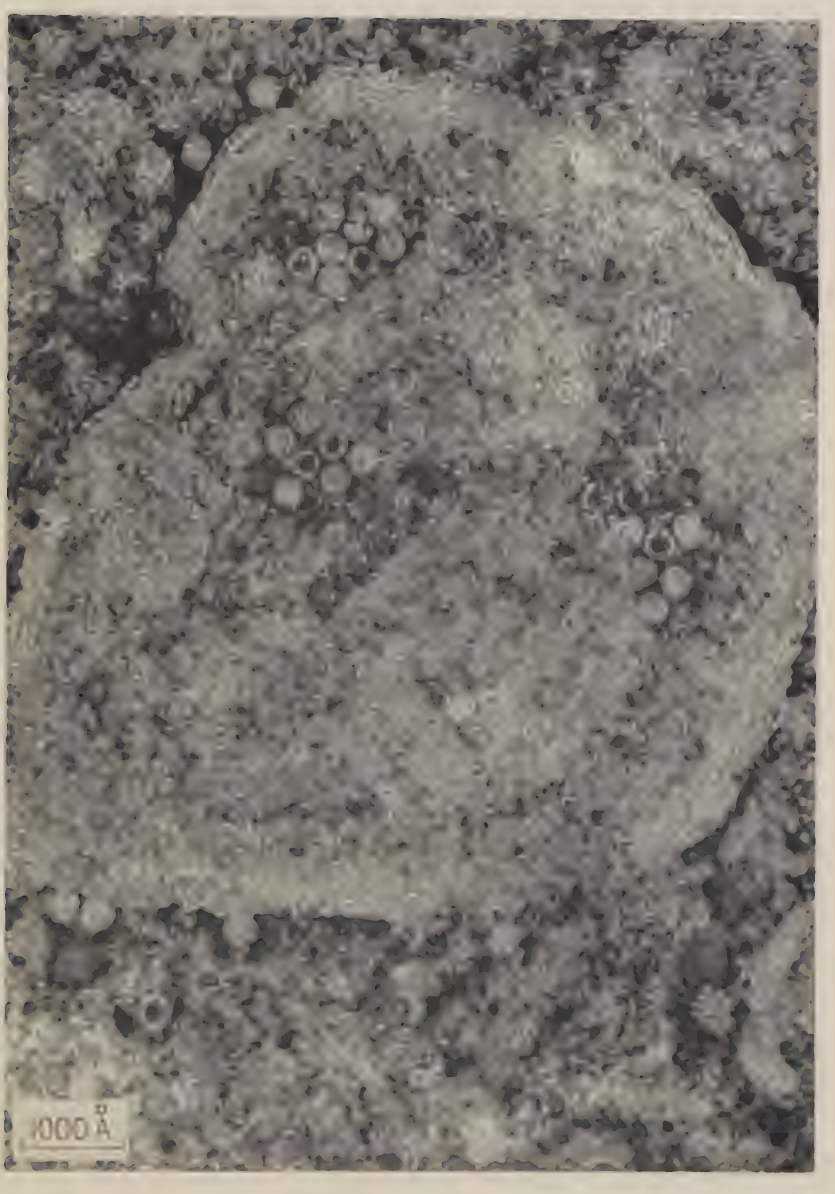

PLATE III. Large body approximately 1μ diameter, showing three areas where virus seems to be in various stages of assembly. Note the presence of empty protein shells. 5½ hr.

PLATE IV. Higher magnification of body (5000 Å) showing subunits both in virus particles and surrounding stroma. The central region shows virus particles overlapping where they are more than one layer deep.

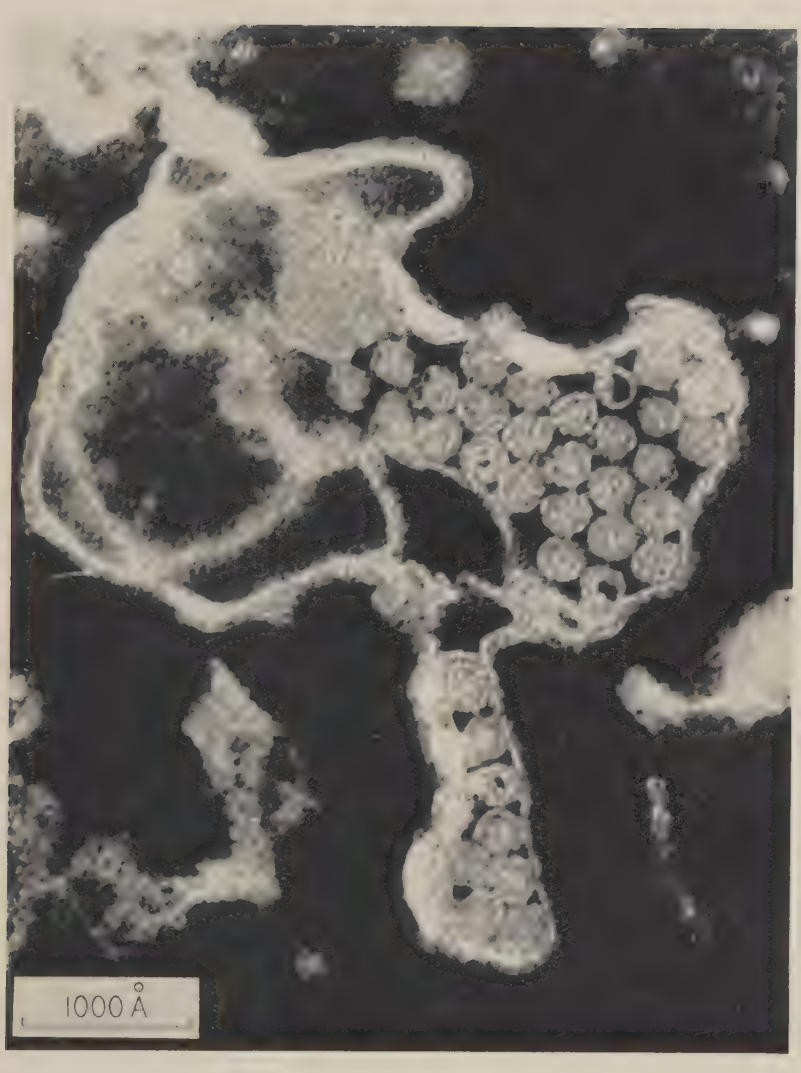

PLATE V. Body showing virus particles in later stage of assembly at 5½ hr. Subunits are clearly visible in both complete and incomplete particles.

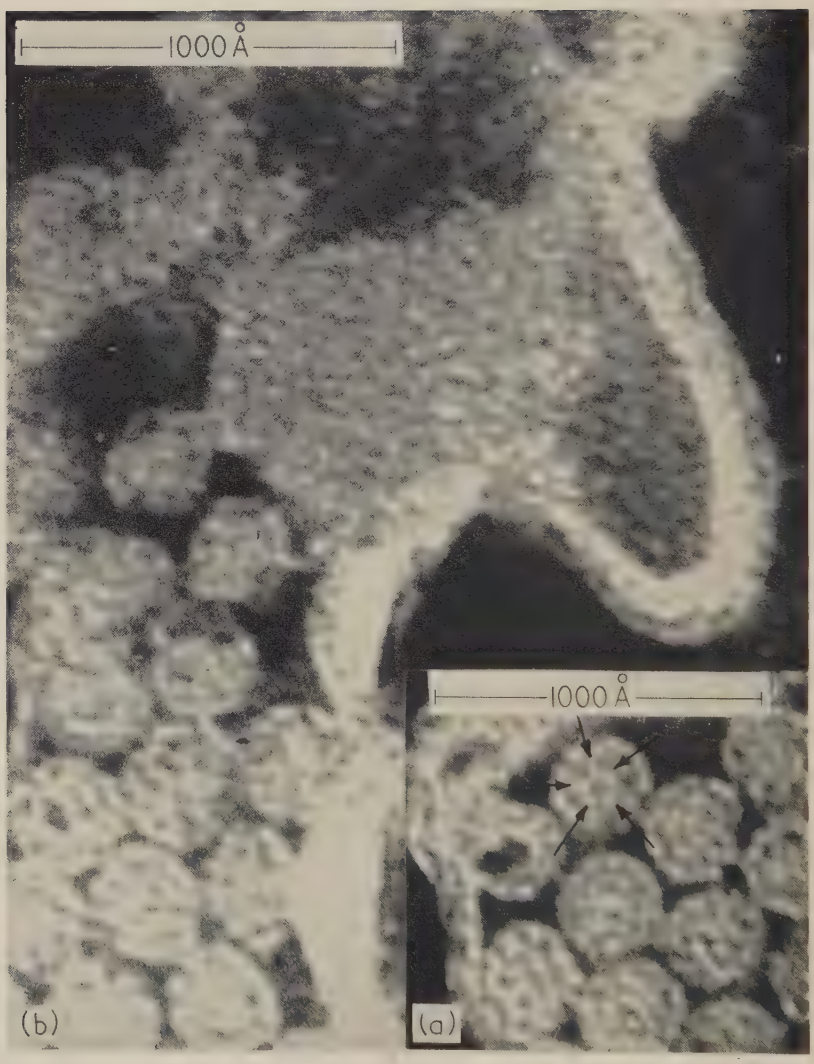

PLATE VI. (a) Region from Plate V with virus in suitable orientation to show possible 5-fold arrangement of the subunits. (b) High magnification of region from plate V showing partly formed virus particles linked to undifferentiated subunit stroma.

PLATE VII. Area approximately 1μ across showing mass of virus particles without limiting membrane.

2·5 μg/ml. of proflavin (diaminoacridinium monohydrogen sulphate) to virus cultures, 1 hr after infection, gave rise to the production of mainly non-infectious virus as described by Ledinko (1958), but it was not possible to distinguish any morphological difference between the virus particles in these preparations and those made in the absence of proflavin.

(b) *The structure of the virus*

Finch & Klug (1959) have recently examined crystals of purified poliovirus by X-ray diffraction methods. Their results suggest that the protein shell is similar to that of TYM, possessing icosahedral symmetry (532), and being built up from 60 protein subunits each 60 Å in diameter. From the X-ray evidence it was not possible to deduce the precise way in which the 60 subunits forming the protein shell were arranged. It was suggested that a compact arrangement would be a consequence of the ratio of the virus particle diameter to the estimated distance between the subunits; and that with icosahedral symmetry, each subunit would probably be in contact with four or five neighbouring subunits.

The electron micrographs taken at high magnification show individual virus particles, apparently in various stages of assembly, and the subunits can be clearly seen (Plates IV and V). Measurements made from particles seen inside the large bodies, and from particles free in the cytoplasm, show them both to be 300 Å in diameter. These dimensions compare well with those predicted from the X-ray diffraction studies.

It is difficult to resolve the arrangement of individual subunits, probably because they are close-packed as predicted, but particles lying in favourable orientations show groups of subunits around a hollow centre. In Plate VI(a) a group of 5 such subunits can be resolved and each subunit is estimated to be approximately 50 Å in diameter. The thickness of the walls of the empty shells seen in the electron micrographs is also estimated to be 50 to 60 Å. This is similar to the subunit size determined by Finch & Klug (1959) who made the centre-to-centre distance 60 to 65 Å. Sjöstrand & Polson (1958) were able to distinguish an opaque central core in their preparation, and estimated its diameter as 160 Å and the thickness of the outer shell as 30 Å.

Small structures, approximately 50 Å in diameter, can be resolved in concentrated masses, forming the internal component of the large bodies, and these can be seen closely associated with the virus particles, in the various stages of development (Plate VI(b)).

It is interesting to note that all these measurements relate to *unfixed* poliovirus. Potassium phosphotungstate, in the concentrations used, has no appreciable action on the viability of poliovirus, either in solution for 24 hr at + 4°C or after spraying and drying in the usual way.

All the above measurements were found to be the same for each of the three antigenic types of poliovirus.

We wish to thank Dr. P. Wildy and Dr. S. Brenner for valuable discussions throughout. The electron microscopy was carried out in the Electron Miscroscope Section of the Cavendish Laboratory under the direction of Dr. V. E. Cosslett. The Siemens microscope was purchased by a generous grant from the Nuffield Foundation.

REFERENCES

Ackermann, W. W. (1958). *Bact. Rev.* **22**, 233.
Barski, G., Robineaux, R. & Endo, M. (1955). *Proc. Soc. Exp. Biol. N.Y.* **88**, 57.

Brenner, S. & Horne, R. W. (1959). *Biochim. biophys. Acta*, **34**, 103.
Cosentino, V., Paigen, K. & Steere, R. L. (1956). *Virology*, **2**, 139.
Cosslett, V. E. & Markham, R. (1948). *Nature*, **161**, 250.
Dulbecco, R. & Vogt, M. (1954). *J. Exp. Med.* **99**, 167.
Finch, J. T. & Klug, A. (1959). *Nature*, **183**, 1709.
Horne R. W. & Brenner, S. (1958). IVth International Conf. on Electron Microscopy, Berlin.
Kallman, F., Williams, R. C., Dulbecco, R. & Vogt, M. (1958). *J. Biophys. Biochem. Cytol.* **4**, 307.
Klug, A., Finch, J. T. & Franklin, R. E. (1957). *Biochim. biophys. Acta*, **25**, 242.
Le Bouvier, G. L., Schwerdt, C. E. & Schaffer, F. L. (1957). *Virology*, **4**, 590.
Ledinko, N. (1958). *Virology*, **6**, 512.
Reissig, M., Howes, D. W. & Melnick, J. L. (1956). *J. Exp. Med.* **104**, 289.
Sabin, A. B., Hennessen, W. A. & Warren, J. (1954). *Proc. Soc. Exp. Biol. N.Y.* **85**, 359.
Schwerdt, C. E. & Schaffer, F. L. (1955). *Ann. N.Y. Acad. Sci.* **61**, 740.
Schwerdt, C. E., Williams, R. C., Stanley, W. M., Schaffer, F. L. & McClain, M. E. (1954). *Proc. Soc. Exp. Biol. N.Y.* **86**, 310.
Sjöstrand, F. S. & Polson, A. (1958). *J. Ultrastruc. Res.* **1**, 365.
Steere, R. L. & Schaffer, F. L. (1958). *Biochim. biophys. Acta*, **28**, 241.
Tenenbaum, E. (1957). *Nature*, **180**, 1044.
Weller, T. H., Enders, J. F., Robbins, F. C. & Stoddard, M. B. (1952). *J. Immunol.* **69**, 645.

J. Mol. Biol. (1959) **1**, 339-349

The Histidine Residue in the Active Centre of Ribonuclease

I. A Specific Reaction with Bromoacetic Acid

E. A. Barnard and W. D. Stein

Department of Zoology, University of London King's College, Strand, London, England

(*Received 14 August 1959*)

Bromoacetic acid reacts readily with ribonuclease to form an inactive derivative in which, at pH 7, one carboxymethyl group has been introduced per molecule of enzyme. The sole residue in the enzyme so substituted is shown to be one of the four histidines in the molecule. The rate of reaction of this histidine with bromoacetic acid is far greater than that of free histidine, the residue in the enzyme being, therefore, activated. The reaction with bromoacetic acid is slowed down greatly in the presence of cytidylic acid, a competitive inhibitor of the enzyme, suggesting that the histidine residue concerned is situated in the active centre of the enzyme.

1. Introduction

Ribonuclease is the first enzyme whose primary (covalent-bonded) structure has been more or less completely established (Hirs, Stein & Moore, 1958; Anfinsen, 1958).† This achievement now opens the way to an attack on two major problems, namely (1) the identity and configuration of those parts of the molecule directly involved in the catalytic process, i.e., the so-called active centre of the enzyme, and (2) the nature of what can at present only be loosely defined as the activation of the amino acid residues involved, i.e., the pattern of electron distributions and steric relationships that determine the novel (catalytic) properties of the residues at the active centre. The solution of these problems (taken together with information on substrate specificity etc.) should lead to an interpretation in chemical terms of the mechanism of enzyme action.

One approach to these problems is a search for specific reagents whose reaction with particular groups in the active centre is related to the activation of those groups by their molecular environment, i.e., for cases where the participation of a group in enzymic activity is intrinsically related to an enhanced chemical reactivity of a particular type. This would provide a handle for identifying the group concerned. (That such a behaviour can in practice be obtained is shown, for example, by phenomena found in the highly specific reaction of certain organo-phosphate reagents, e.g., di-*iso*propylfluorophosphate (Balls & Jansen, 1952) with a group of proteases and esterases.)

The present work reports an activation of this type, of a histidine residue in ribonuclease. It is known from the work of Weil & Seibles (1955) that a histidine residue may be essential for ribonuclease activity; those authors found that on photo-oxidation the loss of enzymic activity was accompanied by the destruction of histidine

† Note added in proof: For the complete covalent structure, see Hirs, C. H. W., Moore, S. & Stein, W. H., *J. Biol. Chem.* (1960) (in press); Spackman, D. H., Stein, W. H. & Moore, S., *J. Biol. Chem.* (1960) (in press).

residues in ribonuclease, and that the stoicheiometric equivalent of one histidine residue was lost at 74% inactivation.

Taking into account existing knowledge on the chemical reactivity of histidine residues in proteins (Barnard & Stein, 1958) and simple hypothetical models for the catalysis, it was thought that the desired reactivity might be obtained with an alkylating agent, and in particular, on account of its charge and size, with bromoacetic acid. This reagent, introduced for protein alkylations by Korman & Clarke (1955*a*,*b*) is an analogue of the iodoacetic acid reagent long in use for SH group alkylations, but possessing some reactivity advantages for the present purposes over the latter compound. Bromoacetic acid introduces stable carboxymethyl (Cm —) groups into a number of reactive sites in proteins, by reactions of the type:

$$-RH + BrCH_2COO^- \longrightarrow -RCH_2COO^- + HBr$$

In the present work, such a reaction has been obtained with ribonuclease and the effects on the activity and structure of the enzyme have been determined.

2. Experimental

(a) *Ribonuclease*

Crystalline bovine pancreatic ribonuclease (Armour Laboratories, batch no. BL 0871; moisture content 7·8%) was used in all experiments, without further purification. (Reactions at pH 7 and pH 9, and the cytidilic acid experiment were, in addition, performed using batch no. 23673, in preliminary studies. This material also gave essentially the same results as those reported here.)

(b) *Substrate solution*

Ribonucleic acid (RNA) (Nutritional Biochemical Corpn. Inc.), was purified as follows: RNA (0·5 g) was dissolved in 100 ml. sodium acetate buffer (0·1 M, pH 5·3) and precipitated from solution by a mixture of ethanol (3 vols) and acetic acid (0·2 vols). This procedure was repeated and the precipitate finally dissolved in 0·1 M-acetate buffer (200 ml.) with final adjustment to pH 5·3, to give the standard RNA solution.

(c) *Enzymic assay*

The method employed was the spectroscopic measurement of hydrolytic products, in the form due to Dickman, Aroskar & Kropf (1956), with slight modifications as follows. To the ribonuclease sample (0·1 ml. containing 0 to 1 μg) at 37°C was added standard RNA solution (1 ml.) at 37°C and incubated (at pH 5·3 in all cases) for exactly 10 min, when 3 ml. of the precipitant (*tert*-butanol-acetic acid, 2 : 1) was added. After standing at room temperature for 15 min, followed by centrifugation (2000 *g*, 30 min), the supernatant was removed and mixed; 1 ml. was diluted with 5 ml. water, and the optical density of this solution at 260 mμ read in a Uvispek spectrophotometer (1 cm silica cells). The optical density due to a control incubation (enzyme omitted), treated simultaneously, is subtracted to give E_{260}.

A divergence from the results of Dickman *et al.* (1956) was observed in one respect: whereas those authors found E_{260} increased linearly with ribonuclease concentration only up to 0·25 μg (in 1 ml. incubation mixture, at pH 5·0), in the present case this increase is linear from 0 to 1·0 μg (in 1·1 ml. at pH 5·3). Ionic strength is 0·1 in both cases. At the ribonuclease level of 1 μg, E_{260} lies here in the range 0·8 to 1·1, the exact value depending on the actual RNA concentration used (and proportionately for smaller amounts of enzyme). Such a difference may be due to substrate differences. Lower values, with less satisfactory reproducibility, were obtained with three commercial samples of RNA from other sources, purified similarly. One of these was further purified by dialysis (24 hr) without adequate improvement. Some evidence for substrate inhibition was found when RNA concentration was varied, as observed also by Dickman & Ring (1958). Gelatin was found to given no advantage in the assay medium in this range and was omitted. Blank and standard tubes were run with each experimental assay reported.

(d) *Reactions with bromoacetic acid*

Bromoacetic acid (British Drug Houses Ltd.) was dissolved in water immediately before use, neutralised with the required amount of NaOH to bring to the desired pH and placed in appropriate buffer solution. The concentration was checked, on samples of the bromoacetic acid solutions in water, by acidimetric titration. The buffered bromoacetic acid solution, and a solution of ribonuclease in the same buffer, were brought to 37°C, mixed, and incubated with occasional stirring. The concentrations after mixing were 0·31 M and 0·06 mg/ml. respectively, unless stated otherwise. The pH was checked with a glass electrode (temperature-compensated) before and during the reaction. At known times, samples (usually 0·5 ml.) were withdrawn and diluted with ice-cold acetate buffer, pH 4, to give a ribonuclease concentration of 10 μg/ml. Approximately 90 sec after sampling 0·1 ml. of the diluted solution was transferred to a tube at 37°C, and the assay reaction was started 30 sec later.

The reaction media were: pH 7·1 and 6·7, 0·12 M-phosphate buffer; pH 9·0, 0·17M-carbonate-bicarbonate buffer; pH 5·3 and 4·2, 0·1 M-acetate buffer.†

Control solutions of ribonuclease, incubated (about 4 hr) without bromoacetic acid in the same buffers and assayed under identical conditions, showed no decrease in enzyme activity. Samples from a control bromoacetic acid solution, incubated without ribonuclease, gave the normal blank value in the enzyme assay. Bromoacetic acid, incubated without buffer and held at approximately constant pH by titration with 0·1 N-NaOH, showed a hydrolytic decomposition rate (as measured by proton liberation) of approximately 0·2% per hr at 37°C at pH 7, and less still at pH 5; the reagent concentration is taken to be constant within experimental error during the incubations with ribonuclease.

Cytidilic acid (L. Light and Co., Ltd.) was neutralised, placed in the appropriate buffer and mixed with the ribonuclease solution prior to the addition of bromoacetic acid. The optical densities in the assays here were corrected for the absorption of the cytidilic acid present.

(e) *^{14}C-labelled preparations*

Reaction was carried out at pH 7 in the standard manner, using [2-^{14}C]bromoacetic acid (Radiochemical Centre, Amersham) in two experiments (Table 1). At the end of the reaction period, a considerable excess of acetic acid and carrier bromoacetic acid was added to bring the pH to approximately 4. The mixture was dialysed (Visking cellophane, 20/32) against a large volume of stirred distilled water at 4°C (12 hr) and then against running distilled water at room temperature. Portions were taken for radioactivity measurements after a total dialysis period of 40 hr (experiment 1) and after 20 hr and 60 hr (experiment 2). The amount of protein present in these samples was obtained in experiment 1 by correction for overall losses in the dialysis procedures (maximum 15%), as measured (by optical density at 277 mμ, *cf.* below) in a parallel non-radioactive preparation dialysed similarly. In experiment 2 the amount of protein present was determined directly (by optical density at 277 mμ) on the radioactive samples withdrawn. Samples were deposited on filter paper planchets and counted with an end-window Geiger-Müller tube (with correction for background), with calibration by similar samples of sodium [^{14}C]bromoacetate standards.

(f) *Ultra-violet spectroscopy*

All measurements were made in a Hilger Uvispek spectrophotometer using silica cells.

After reaction in the standard way at pH 7 (3 hr), followed by exhaustive dialysis, the carboxymethylated protein (Cm-ribonuclease) was obtained as a freeze-dried white powder. The spectra were determined on solutions in water of this material, and of untreated

† When a preliminary report (Stein & Barnard, 1958; *cf.* also Barnard & Stein, 1959*a*) was made of part of this work, at the IVth International Congress of Biochemistry, Vienna, September 1958, including the results of reactions at pH 7·1 and 9·0, Dr. Stanford Moore very kindly informed us that in recent unpublished work in his laboratory an inactivation of ribonuclease by iodoacetic acid, also involving histidine, had been observed, and that this iodoacetate reaction proceeded faster at pH 5 than at pH 8·5. Our rate determinations at pH values below 7 were carried out subsequently, in the light of this helpful communication.

ribonuclease, after adjustment of pH to the measured values with acetic acid or with sodium hydroxide. The concentrations are not corrected for moisture content.

Reaction of ribonuclease (0·6 mg/ml.) with bromoacetic acid was carried out at pH 5·3 as before and samples were withdrawn for direct measurement of u.v. absorption as follows:

(i) immediately after mixing at 20°C,

(ii) after 1½ hr incubation at 37°C,

(iii) after 2 hr at 20°C.

(g) *Diazonium coupling reaction*

Diazobenzenesulphonic acid was prepared from sulphanilic acid (AR) and nitrous acid at 2°C; the moist crystals were washed with 0·1 N-HCl, neutralised and dissolved in cold 0·1% $NaHCO_3$ to give a 1% (w/v) solution, which was used immediately. A solution of Cm-ribonuclease, prepared under standard conditions at pH 7, was dialysed exhaustively. This solution, and a solution of pure ribonuclease in water, were adjusted to identical concentrations, utilising their optical densities at 277 mμ and the spectroscopic data reported below.

The method used was a modified version of that of MacPherson (1942). 5 ml. of each solution were diluted to 17 ml. and 1 ml. of diazo reagent was added; after 5 min, 3 ml. 20% Na_2CO_3, 2 ml. ethanol and water to a final volume of 25 ml. were added and, after standing at room temperature 15 min, the optical density was measured in a Hilger Spekker spectrophotometer with a green (No. 3) filter. In the main experiments reported, the 5 ml. portion of each of the two protein solutions was first made 8 M with respect to urea in a total volume of 18 ml., and allowed to stand 1 hr at 20°C, prior to the addition of 1 ml. diazo reagent; further treatment was as before, but 8 M-urea was used in place of water in the final dilution. The optical densities were corrected for that due to a blank solution (protein omitted) treated identically in each case. In a similar experiment on a further preparation of Cm-ribonuclease, the urea was added during the course of the coupling reaction.

3. Results

(a) *Inactivation of ribonuclease by bromoacetic acid*

The effect on the enzymic activity was followed during reaction at various pH values. Initially it was observed that the reaction with bromoacetate inactivates

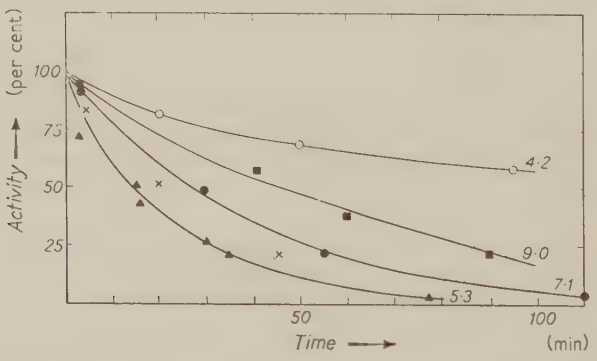

Fig. 1. Inhibition of ribonuclease activity by reaction with bromoacetic acid at different pH values.

○, pH 4·2; ▲, pH 5·3; ×, pH 6·7; ●, pH 7·1; ■, pH 9·0.

ribonuclease, and that the inactivation rates at pH 7·1 and pH 9·0 are of the same order, with the former rather faster (Fig. 1). The inactivation at pH 7·1 is virtually complete after reaction for 2 hr at 37°C. Very similar curves were obtained at pH 7·1 for reactions where the concentration of ribonuclease ranged from 0·03 to 1·0 mg/ml.

From the results of Korman & Clarke (1955*a*,*b*) bromoacetate may react with proteins (at pH 9, with magnesium oxide buffer) at several types of group present, namely SH, amino (lysine and N-terminal), phenolic (tyrosine) and imidazole (histidine) groups. Ribonuclease contains no SH groups; if one or more of the other three types of group is involved here, it would be expected from pK considerations that the reaction would be greatly retarded at pH below 7. In practice, when the pH was lowered an anomalous behaviour was found (Fig. 1), with a considerable increase in rate at pH 5·3, followed by a further decrease in more acid solution.

When the reaction at pH 7·1 was repeated in the presence of cytidilic acid (0·025 M), the inactivation was very considerably slowed (Fig. 2). Cytidilic acid is known to be a

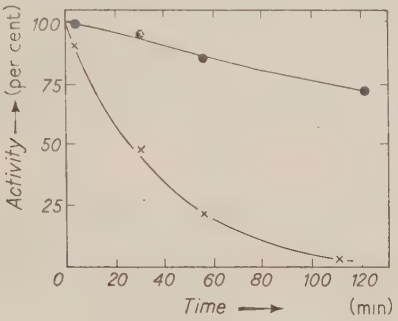

FIG. 2. Inactivation of ribonuclease by bromoacetic acid at pH 7·1, in the presence (●) and absence (X) of cytidilic acid (0·025 M).

strong competitive inhibitor of ribonuclease (Davis & Allen, 1955). The phenomenon of protection by a competitive inhibitor from an inactivating reagent (*cf.* Hopkins, Morgan & Lutwak-Mann, 1938; Rapkine, Rapkine & Trpinac, 1939) may reasonably be taken as evidence that the reagent attacks a group at or very close to the active centre of the enzyme.

(b) *Characterisation of Cm-ribonuclease*

The product of the reaction of ribonuclease with bromoacetate at pH 7 was examined to gain information on the changes in the enzyme molecule giving rise to the inactivation.

In the two experiments where [2-^{14}C]bromoacetic acid was used and the product analysed, the number of carboxymethyl groups introduced per molecule of ribonuclease by this reaction was determined (Table 1). This value lay in all cases in the range $\frac{1}{2}$ to $1\frac{1}{2}$ Cm groups per molecule. Under the more accurate conditions of experiment 2, this value became close to 1. This is after a reaction period when enzymic inhibition has been found to be virtually complete; hence it appears that the inhibited enzyme is formed by reaction of the ribonuclease molecule with a single molecule of bromoacetate. Small amounts of secondary reactions are not, however, excluded by the radioactivity data.

The u.v. spectra of a preparation of Cm-ribonuclease and of untreated ribonuclease are shown in Fig. 3. The spectra are very similar, and both have the reported absorption maximum (Shugar, 1952) close to 277 mμ in acid or neutral solution.

Ribonuclease shows the normal shift of absorption maximum in alkaline solutions, due to the ionisation of tyrosine residues, but 3 of the 6 tyrosines in the molecule contribute only above about pH 12 (Tanford, Hauenstein & Rands, 1955) when an

irreversible denaturation occurs (Sela & Anfisen, 1957). Cm-ribonuclease was found here to give the same behaviour in alkali (Fig. 3) as ribonuclease. The titration of the first three tyrosine residues in Cm-ribonuclease appears to proceed normally, as

TABLE 1

Amount of [^{14}C]bromoacetic acid reacting with ribonuclease at pH 7

Reaction mixture					Product	
Ribonuclease mg	Bromoacetic acid mg	Activity (μc)	Total volume ml.	Time of incubation hr	Purification	Specific activity 10^3 μc/μmole ribonuclease
Experiment 1						
15	750	50	15	3	Dialysed 48 hr	5·7†
						(9·3)‡
Experiment 2						
15	310	50	8·5	3	Dialysed 20 hr	32
					Re-dialysed further 40 hr	24
						(23)‡

† Mean value for five samples taken from this preparation (range 5·5 to 6·0).

‡ Theoretical value per group reacted, calculated for 1 carboxymethyl group introduced per molecule ribonuclease.

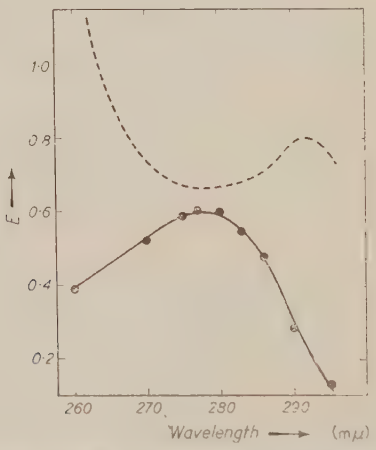

FIG. 3. Ultraviolet absorption spectra of solutions of Cm-ribonuclease (●) and ribonuclease (solid line) at pH 3·2; and of Cm-ribonuclease (broken line) at pH 12·3 (all at 0·65 mg/ml.).

judged spectroscopically, and the other tyrosine residues appear to titrate as usual above about pH 12 (although an exact equivalence of this second set in the two proteins was not, in practice, established, due to the time-dependence of the titration behaviour above pH 12). Had any of the tyrosine phenolic groups become carboxymethylated, this group would easily be recognised by its spectral characteristics. As expected for an O-alkylated phenolic group, the u.v. spectrum of O-carboxymethyl

tyrosine, both free and in protein (Korman & Clarke, 1955*a*,*b*), differs in several respects from that of the unsubstituted compound, and in particular the characteristic shift of absorption maximum in alkali is abolished. The spectra obtained here indicate that no tyrosine group has reacted with bromoacetate (although Cm-ribonuclease does show slight spectral differences, of unknown origin, from ribonuclease in alkali).

The diazonium reaction employed gives coloured products with tyrosine and histidine side chains, but not when these are alkylated. Under the conditions of diazonium reaction employed, a molecule of tyrosine is found to give 30% of the colour yield of a molecule of histidine. The situation is complicated by the question whether or not all of the tyrosine and histidine residues in native ribonuclease are available for the reaction. For this reason the proteins were denatured in 8 M-urea prior to reaction with the diazo reagent, a method found to give satisfactory results with ribonuclease in this reaction. Since ribonuclease contains four histidines and six tyrosines (Hirs, Moore & Stein, 1954) the total colour yield would be equivalent to 5·8 histidines. The decrease found (Table 2) in comparing ribonuclease with its

TABLE 2

Diazonium coupling of ribonuclease after reaction with bromoacetic acid at pH 7

	O.D. units†			
	Ribonuclease	Cm-ribonuclease	Difference %	Predicted difference % for 1 histidine blocked
Preparation 1	0·24	0·20	20	21
Preparation 2	0·62	0·52	19	

† Readings are directly comparable only within each experiment, since different amounts of material were used in preparations 1 and 2.

carboxymethylated derivative is close to that predicted for the loss of 1 histidine. Other allocations would be possible (i.e. loss of 3 tyrosines, or of fractional combinations) but are inconsistent with the results of the ^{14}C-binding and the spectroscopic data.

It may also be noted that parallel determinations on the proteins *without* the urea treatment gave results similarly consistent with one histidine blocked in Cm-ribonuclease, but the allocations here were complicated by the apparent non-availability of certain groups in both proteins to the diazonium reagent. Examination of the availability of groups in ribonuclease to this reagent (Barnard & Stein, unpublished) including diazonium coupling data on the products of total acid hydrolysis of ribonuclease and Cm-ribonuclease—where no such complications can arise—also gives results consistent with the above picture.

The close correspondence of the spectra of the two proteins, and of their change in alkaline solution, suggests that no gross denaturation of the ribonuclease molecule occurs during the reaction with bromoacetate at pH 7. A confirmatory experiment was performed at pH 5·3, where the inactivation is most rapid. No change in the normal absorption of ribonuclease could be detected at 277 mμ and 285 mμ, after reaction with bromoacetate for 2 hr at 20°C, nor after reaction for 1½ hr at 37°C, when assay

confirmed that inactivation was complete. The accuracy of these measurements was such that a change of 1% in the extinctions would have been detected. 277 mμ is the wavelength of maximum absorption, and 285 mμ is in the spectral region of the considerable change in optical density observed by Harrington & Schellman (1956) and by Sela & Anfinsen (1957) to be produced by the urea denaturation of ribonuclease. Similarly, Cm-ribonuclease in 8 M-urea solution has been found to give the same absorption change at 285 mμ as is given by ribonuclease in 8 M-urea (Barnard & Stein, 1959*b*, in preparation). Hence, in summary, it appears that denaturation, at least as assessed spectroscopically, does not occur appreciably in the carboxymethylation reaction, and that any change that is produced in the molecular structure is of a fairly subtle nature.

4. Discussion

It is apparent from these observations that a highly specific reaction can occur between ribonuclease and bromoacetic acid. Under the conditions employed, a single carboxymethyl group is introduced into the ribonuclease molecule (*cf.* Fig. 4), and

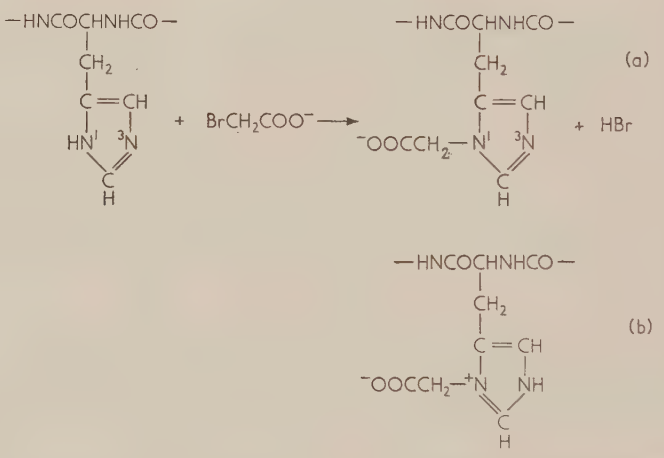

Fig. 4. Probable reaction of the histidine residue in question with bromoacetate. It is not possible, from present information, to specify whether the substitution in fact occurs at the 1 position (as shown) or at the 3 position, or what proportions of each isomer are present if a mixture is formed. It cannot be excluded, although from stability considerations it appears less probable, that a quaternary compound such as (b) is formed (at pH 7).

this modification completely removes the enzymic activity. The reaction is accompanied by the loss of one histidine residue and, so far as can be determined by the methods employed, by a change in no other residue. Data to be presented in the following paper, on the molecular location of the residue, incidentally provide confirmation of the latter conclusions.

It is conceivable that the inactivation of the enzyme is brought about only indirectly, in that the modification of a group *not* concerned in the catalysis might lead to structural changes in the protein affecting the "active centre".† However, the

† This term is employed here, as in most current usage, in the sense of the brief definition given in the Introduction. More exactly, we intend it to include groups (which may well be located in different segments of the amino acid sequence) that are involved directly in interactions with the substrate in the catalysis, or in activations directly related to these interactions, but not to include other groups which contribute structurally to some configuration of the protein essential for the integrity of this active centre.

evidence in the present case, in particular the effective protection afforded by a competitive inhibitor, indicates that a direct reaction at the active centre is involved.

This is in accordance with the singular reactivity of this histidine residue. Only one of the four histidines present reacts under these conditions; moreover, this is due to an elevation of the normal alkylation rate in the case of this one histidine, rather than to a depression of that rate at the other three histidines. This follows from comparison with the data of Korman & Clarke (1955*a*,*b*) on the rates of reaction of the histidine imidazole group, both in free histidine and in bovine serum albumin, with bromoacetic acid, using similar concentrations at 35 to 37°C at pH 9; that data would give a predicted rate for a "normal" histidine residue roughly 30 or more times slower than the rate found for the reaction here at pH 7.

A further remarkable feature of the reactivity of this group is the nature of the pH dependence which it exhibits. It is surprising that the reaction rate actually increases below pH 7, with a maximum somewhere in the neighbourhood of pH 5·3, where imidazole groups should normally be blocked by protonation. This might be taken to indicate that this particular group has an abnormally low dissociation constant (pK_a), due to special constraints introduced by its situation in the active centre. However, to explain the rates in acid solution, this pK_a would have to be somewhat below 5, and there is no indication that an imidazole in ribonuclease has such an abnormally low pK_a, so far as can be inferred from titration curve analysis (Tanford & Hauenstein, 1956). Moreover, an additional mechanism must then be invoked to explain the decrease (in place of the expected constancy) of reaction rate as the alkalinity increases. It has not been determined here whether histidine is similarly involved in the inactivation by bromoacetate at pH 9, but the data of Korman & Clarke would suggest that in any case normal lysine residues would react at an appreciable rate at pH 9.

In this context, valuable corroborative and additional evidence has now come from the concurrent results of Gundlach, Stein & Moore (1959) which the authors kindly made available to us while this manuscript was being completed. These authors, examining further the reaction of ribonuclease with iodoacetic acid (see the Note in Experimental Section above), have separated the products and made precise analyses on hydrolysates by ion-exchange resin chromatography. They find that the inactivation by iodoacetate shows a pH dependence very similar to that reported here, and that (i) at pH 5·5 the reaction is virtually confined to one histidine residue only; (ii) at pH 8·5 one to two lysine residues react but no histidine; (iii) at pH 2·8 several methionine residues react but again no histidine. The concordance of their results with those reported here is gratifying, and their extension of our knowledge of the inactivation reactions now permits a clearer picture of these to be drawn. Thus, it appears highly probable that the specific reaction with histidine in ribonuclease occurs with bromoacetic acid at pH 7 and at pH 5·3, and with iodoacetic acid at pH 5·5. The same general mechanism is presumed to operate throughout this range; the unusual nature of the pH dependence must derive from specific features in the active centre structure which are at present quite undefined. Above and below this range, this histidine residue ceases to react, although the reagents can still inactivate the enzyme by reactions (which may be less specific) at lysine and methionine residues respectively.

This histidine residue is, therefore, indeed endowed with a unique type of chemical reactivity in the enzyme, which must be presumed to derive from its position in the

constellation of groups that constitutes the active centre. Information on the latter should be obtainable by examination of the minimum structural requirements for this chemical reactivity (some studies on which are now in progress) and of the processes involved in the disappearance of this reactivity at pH above 7. The latter phenomenon we take to be probably related to the participation of a second group in a particular bonding at (or essential for the integrity of) the active centre.

Two further points may be remarked upon, emerging from a comparison of the bromoacetate and iodoacetate results. Firstly, the identification was made here on the intact protein, while Gundlach, Stein & Moore perform their identifications after hydrolysis. In fact, Cm-derivatives of histidine are quite stable to hydrolysis (Korman & Clarke, 1955*a*), but the comparison shows that the histidine residue is the site of the Cm-group in the enzyme, and not merely the final acceptor, after hydrolysis, from an initial, more labile bonding elsewhere. It is also of interest that Korman & Clarke found that the peptides glycylhistidine and alanylhistidine gave products with two Cm-groups on the imidazole ring, whereas the product from free histidine had one Cm-group on the ring. The ^{14}C-binding data of the present study indicate that in ribonuclease the latter behaviour is shown.

Secondly, since in the iodoacetate case the cytidine cyclic phosphate assay method has been employed, whereas we always used the RNA depolymerisation assay, it can be deduced that both stages of RNA hydrolysis, namely the RNA depolymerase action (i.e., a phosphodiesterase activity) and the subsequent, slower nucleoside cyclic phosphatase action (Markham & Smith, 1952), involve this histidine residue. The sites concerned are not necessarily identical in all respects, since there is some evidence that the two activities can be separated to some extent (Kalman, Linderstrøm-Lang, Ottesen & Richards, 1955), but this histidine residue at least appears to be essential to both. It may tentatively be suggested that the imidazole ring is involved in a phosphotransferase type of reaction in both cases.

We thank Dr. Stanford Moore for his courteous co-operation in informing us of results from his laboratory prior to publication. We wish to thank Mr. J. Marbrook of our laboratory for his competent help in the course of this work.

REFERENCES

Anfinsen, C. B. (1958). *Symposium on Protein Structure*, ed. by A. Neuberger, p. 223. London: Methuen.
Balls, A. K. & Jansen, E. F. (1952). *Advanc. Enzymol.* **13**, 321.
Barnard, E. A. & Stein, W. D. (1958). *Advanc. Enzymol.* **20**, 51.
Barnard, E. A. & Stein, W. D. (1959*a*). *Biochem. J.* **71**, 19 P.
Davis, F. F. & Allen, F. W. (1955). *J. Biol. Chem.* **217**, 13.
Dickman, S. R., Aroskar, J. P. & Kropf, R. R. (1956). *Biochim. biophys. Acta*, **21**, 539.
Dickman, S. R. & Ring, B. (1958). *J. Biol. Chem.* **231**, 741.
Gundlach, H. G., Stein, W. H. & Moore, S. (1959). *J. Biol. Chem.* **234**, 1754.
Harrington, W. F. & Schellman, J. A. (1956). *Compt. rend. Trav. Lab. Carlsberg (chim.)*, **30**, 21.
Hirs, C. H. W., Moore, S. & Stein, W. H. (1954). *J. Biol. Chem.* **211**, 941.
Hirs, C. H. W., Stein, W. H. & Moore, S. (1958). *Symposium on Protein Structure*, ed. by A. Neuberger, p. 211. London: Methuen.
Hopkins, F. G., Morgan, E. J. & Lutwak-Mann, C. (1938). *Biochem. J.* **32**, 1829.
Kalman, S. M., Linderstrøm-Lang, K., Ottesen, M. & Richards, F. M. (1955). *Biochim. biophys. Acta*, **20**, 408.
Korman, S. & Clarke, H. T. (1955*a*). *J. Biol. Chem.* **221**, 113.
Korman, S. & Clarke, H. T. (1955*b*). *J. Biol. Chem.* **221**, 133.

MacPherson, H. T. (1942). *Biochem. J.* **36**, 59.
Markham, R. & Smith, J. D. (1952). *Biochem. J.* **52**, 558.
Rapkine, L., Rapkine, S. M. & Trpinac, P. (1939). *C.R. Soc. Biol., Paris*, **209**, 253.
Sela, M. & Anfinsen, C. B. (1957). *Biochim. biophys. Acta*, **24**, 229.
Shugar, D. (1952). *Biochem. J.* **32**, 142.
Stein, W. D. & Barnard, E. A. (1958). Abs. Commun. IVth Internat. Cong. Biochem. (Vienna), p. 21.
Tanford, C., Hauenstein, J. D. & Rands, D. G. (1955). *J. Amer. Chem. Soc.* **77**, 6409.
Tanford, C. & Hauenstein, J. D. (1956). *J. Amer. Chem. Soc.* **78**, 5287.
Weil, L. & Seibles, T. S. (1955). *Arch. Biochem. Biophys.* **54**, 368.

J. Mol. Biol. (1959) **1**, 350-358

The Histidine Residue in the Active Centre of Ribonuclease

II. The Position of this Residue in the Primary Protein Chain

W. D. Stein and E. A. Barnard

Department of Zoology, University of London, King's College, Strand, London, England

(*Received 14 August 1959*)

The carboxymethyl derivative of ribonuclease, obtained by the reaction of bromoacetic acid with the enzyme, has been oxidised and digested with chymotrypsin. The peptides so formed have been separated by electrophoresis and chromatography and the peptide containing the introduced carboxymethyl group has been identified. This information locates the position in the protein chain of ribonuclease of the single histidine residue which reacts with bromoacetic acid, and hence locates at least a part of the active centre of this enzyme. The residue concerned is that histidine residue nearest to the C-terminal end of the protein chain (whose amino acid sequence is largely known). The result is considered in relation to other published evidence on primary structural requirements for ribonuclease activity. A start may be made on the task of constructing a model for the active centre of this enzyme.

1. Introduction

A stable, enzymically inactive derivative of ribonuclease (Cm-ribonuclease) has been obtained, in which one histidine residue carries a carboxymethyl (Cm) group on the imidazole ring, and in which no other amino acid residue has undergone reaction (Barnard & Stein, 1959). Such carboxymethyl groups are resistant to hydrolysis and hence can act as a label for the identification of the group concerned. It would be of considerable interest to determine which one of the four histidines in the ribonuclease molecule is so labelled, since it has been shown that this residue is at the active centre of the enzyme.

The behaviour of ribonuclease to disulphide oxidation and enzymic degradation to peptides has been recorded by Hirs, Moore & Stein (1956) and Hirs, Stein & Moore (1956). In the present work we have sought to split Cm-ribonuclease in this way and to identify the peptide carrying the Cm group, using isotopic labelling. If chymotrypsin (rather than trypsin or pepsin) is employed for the digestion, ribonuclease is split in such a way that each of the four histidine residues is contained in a separate peptide. The identification of that peptide which carries the Cm label will automatically locate the histidine residue so substituted in the protein chain, since the linear arrangement of these peptides has been unambiguously determined by Hirs *et al.*

We have not attempted to follow the elegant ion-exchange resin chromatographic methods for separating these peptides used by Hirs *et al.* In the present work, it has been sufficient to separate the peptides by paper electrophoresis, validated by subsequent chromatography (*cf.* Ingram's (1956) analysis by "finger-prints" of digests of haemoglobin), the labelled peptides being conveniently located by direct autoradiography.

2. Experimental

(a) *Protein preparations*

Materials and methods used were those described in the preceding paper. The preparation and subsequent purification by exhaustive dialysis of ^{14}C-labelled Cm-ribonuclease was that of the second ^{14}C experiment reported there. Ribonuclease and Cm-ribonuclease were oxidised with performic acid by the method of Hirs (1956), care being taken to keep the temperature at −10°C. After freeze-drying to a fine white powder, the latter was taken up in water (1 ml. per 10 mg) and digested with 0·01% chymotrypsin (Armour Laboratories) for 20 hr, the pH being kept at 7 by manual addition of a little triethylamine. The digested material was freeze-dried and redissolved in water (0·2 ml. per 10 mg) for electrophoresis.

(b) *Electrophoresis*

The hanging-strip method (Block, Durrum & Zweig, 1955) was used for the paper-electrophoretic separation of the peptides in a medium of 0·2 N-acetic acid. For two-dimensional separations, the paper was cut in the form of a thick T, the vertical bar of the T being rolled up for electrophoresis, and then unrolled for subsequent chromatography down the freshly-exposed region. The rolled-up portion required to be thoroughly saturated with solvent prior to the electrophoresis. Satisfactory separations were achieved only when the chymotryptic digestion was performed in the absence of buffer salts. Failure to observe this precaution resulted in a distortion of the electrophoretogram with a large amount of ninhydrin-positive material held at the origin. Each run required an amount of the peptides resulting from 0·5 to 2 mg of oxidised ribonuclease. With a gradient of 22 v/cm, 4 hr electrophoresis gave a satisfactory resolution of the peptides. The paper was freed of acetic acid by drying at 60°C for 15 min, and the peptides visualised by the ninhydrin method.

(c) *Chromatography*

(i) *Solvents*

"Collidine-lutidine": 10 ml. of each of 2 : 4 : 6-collidine, 2 : 6-lutidine and water were mixed with 2 drops diethylamine and well shaken. After a 15 min equilibration time, 24 hr separation by the ascending method gave a satisfactory resolution of the peptides.

"Butanol : acetic acid : water": the liquids were mixed in the ratio of 4 : 1 : 1 and the solvent used with ½ hr equilibration time and overnight development. This gave a less satisfactory resolution of the peptides than did the collidine-lutidine solvent, but a more satisfactory background colour for the ninhydrin visualisation. It satisfactorily resolved the free amino acids studied.

The phenylthiohydantoin derivatives of the amino acids (see below) were identified following Sjoquist (1953), using his solvents "B" and "C" without modification.

(ii) *Identifications*

Amino acids and peptides were visualised by the ninhydrin method. For papers dried from collidine-lutidine, 1% (v/v) acetic acid was added to the ninhydrin reagent, which was 0·2% triketohydrindene hydrate in acetone. For papers dried from acetic acid, 1% (v/v) pyridine was added to the ninhydrin reagent of the above concentration. After dipping in the ninhydrin reagent, the papers were dried at 60°C for 20 min.

Tyrosine-, histidine-, and lysine-containing peptides were identified by dipping papers in a diazonium coupling reagent, prepared from equal volumes of 5% (v/v) amyl nitrite in alcohol and 0·5% *p*-nitroaniline in ethanolic HCl (1% v/v, conc. acid in ethanol) followed by a wash in ethanol and drying in air. Lysine-containing peptides give a yellow coloration at this stage. On spraying with 0·5% aqueous sodium carbonate, the yellow colour is removed and peptides containing tyrosine and histidine develop a green or purple coloration.

Phenylthiohydantoins were visualised by the method of Sjoquist (1953), using a spray of sodium azide and iodine in potassium iodide, without modification.

(iii) *Autoradiography*

Papers, after thorough drying in a current of air (but without exposure to the reagent sprays) were stapled to X-ray film (Ilford) at three points and set aside for 60 hr under pressure in the dark. After photographic development, the labelled Cm-peptides from a sample of Cm-ribonuclease equivalent to 5×10^{-4} μc of ^{14}C were clearly localised. By subsequent superimposition of paper and film (using the stapling marks), the ^{14}C-labelled material could be cut out for elution and further investigation.

(d) *Elution and examination of peptides*

The peptide which produced the strongest blackening of the X-ray film was cut out and eluted in 5·7 N-HCl on shaking for 2 hr at room temperature. Similarly, from the control preparation, that peptide which gave a strong positive reaction with the coupling reagent, but which was absent from electrophoretograms of the Cm-ribonuclease, was located by treatment with a weak ninhydrin solution (0·05%), cut out and eluted as above. A sufficient number of papers was used to obtain peptide equivalent to that from 2 mg of enzyme. The solution of the peptides in 5·7 N-HCl was heated at 110°C for 20 hr for hydrolysis. Hydrochloric acid was removed by repeated evaporation at the water pump and the amino acids then converted into their phenylthiohydantoin derivatives by reaction with phenyl *iso*thiocyanate in dioxane, following Edman (1950). The phenylthiohydantoins were extracted from their acidic solution into ethyl acetate (or benzene), a procedure which recovered the derivatives of all the amino acids other than arginine and histidine (which were not further investigated). A mixture of 10 μmoles of each of proline, histidine and phenylalanine, together with 20 μmoles of valine (corresponding to the composition of the suspected peptide) was similarly converted into the corresponding phenylthiohydantoins, as a marker. The test, control and marker preparations were chromatographed simultaneously (at 5 μg of each amino acid) using both of Sjoquist's solvents "B" and "C".

In a confirmatory experiment, a portion of the free amino acids in the HCl hydrolysate derived from this eluted peptide from ribonuclease was chromatographed in butanol: acetic acid : water, together with a marker of the above mixture of amino acids.

3. Results

The digests of oxidised ribonuclease and of oxidised Cm-ribonuclease, when examined by the method of electrophoresis in 0·2 N-acetic acid followed by chromatography in the second dimension using collidine : lutidine, as described, gave useful "finger-prints" showing a set of peptide spots satisfactorily separated. However, these showed that for all initial examinations it was sufficient to use the one-dimensional electrophoresis alone, which separates a series of single peptides or small groups of peptides.

Figure 1A is a typical tracing made from a one-dimensional electrophoretogram of the peptides resulting from the hydrolysis of oxidised ribonuclease. In such a strip, a ninhydrin spray reveals a pattern of spots occupying a large part of the region shown (and largely on the negative side). But only certain of these are further revealed by the diazonium reagent spray, which shows tyrosine- and histidine- containing peptides. It is these latter spots that are indicated in Fig. 1.

A sample of the peptides from Cm-ribonuclease, electrophoresed simultaneously, showed a very similar picture with significant modifications (Fig. 1B). The spot X in Fig. 1A (which gave an intense purple colour after ninhydrin and coupling) had completely disappeared from the Cm-sample. Present in the Cm-sample, but not in the control, were four new ninhydrin-positive spots, of varying intensity. Of these four, three produced a significant degree of blackening of the X-ray film on autoradiography (Plate I), one being very intense (Y in Fig 1B and Plate I) and the others

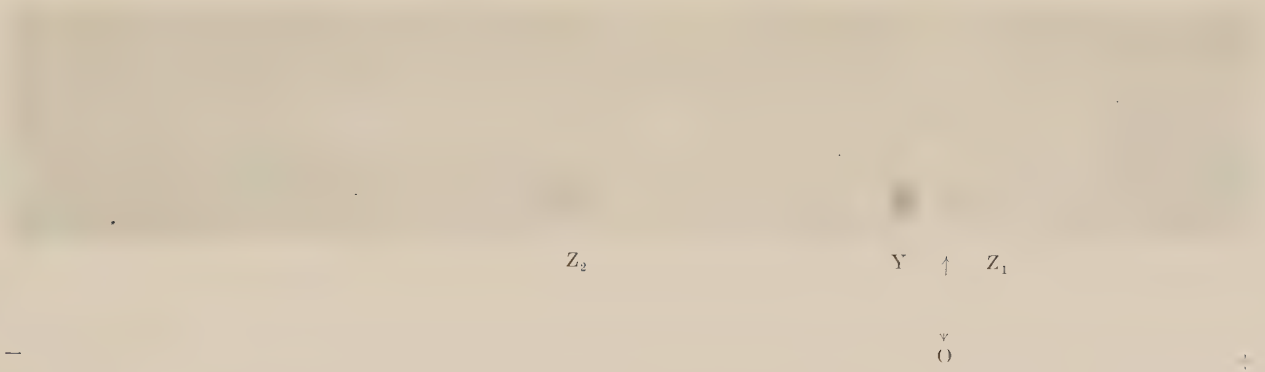

PLATE I. Autoradiograph of paper electrophoretogram of digest of oxidised [^{14}C]Cm-ribonuclease. Electrophoresis in 0.2 N-acetic acid for 4 hr at 22 v/cm. Y is the intense spot corresponding to a new ninhydrin-positive spot in the electrophoretogram. Two other, much fainter spots (Z_1, Z_2) which also correspond to new discrete ninhydrin-positive spots are present.

[*To face page* 352

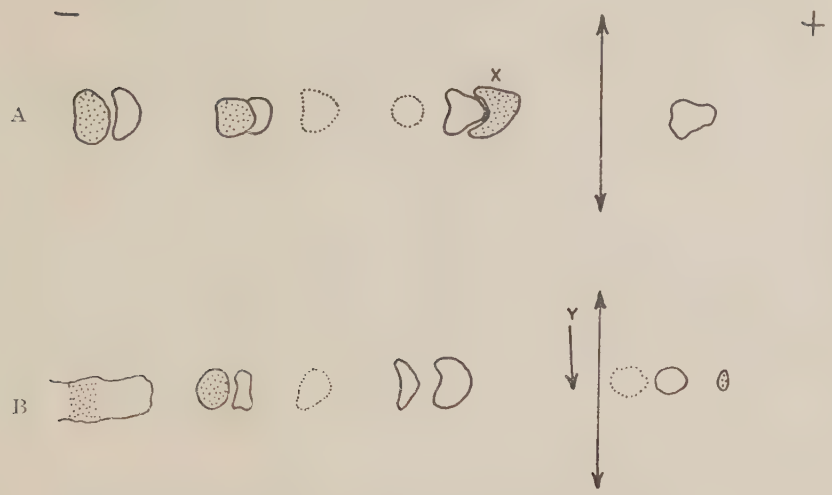

FIG. 1. Tracings from paper electrophoretograms of digests of oxidised ribonuclease (A) and of oxidised Cm-ribonuclease (B). Of the sets of ninhydrin-positive peptides present, only those revealed by the diazonium reagent spray are shown: spots are strong purple (dotted areas, solid boundary), green (solid boundary) or faint blue-green (broken boundary). Electrophoresis in 0·2N acetic acid for 4 h at 22 v./cm. The small arrow in B indicates the position of the spot (negative to the diazonium test) which gives the intense spot Y in the autoradiograph in Plate I.

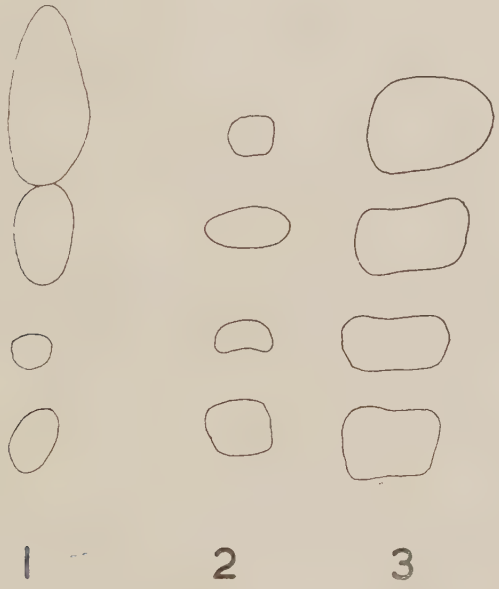

FIG. 2. Tracing from chromatogram showing amino acid composition of peptides under investigation. Peptide X from a digest of oxidised ribonuclease and peptide Y from a digest of oxidised Cm-ribonuclease, obtained by elution from the electrophoretograms, were hydrolysed to the free amino acids, which were converted to their phenylthiohydantoins, and these were extracted and separated by chromatography in solvent B. Column 3 is derived from X, column 2 from Y and column 1 from a mixture of His, Phe, Pro and Val_2. The R_Fs in the latter correspond in ascending order to derivatives of Phe, (artefact), Pro, Val. The derivative of histidine does not appear, in the procedure employed. The amounts of material applied in 2 and 3 are (due to the method of isolation of the peptides) unequal and unknown. Origins are at the marked figures.

considerably fainter. Two of the four new ninhydrin-positive spots could be visualised by coupling, one of these being coincident with one of the areas of fainter autoradiograph intensity, the other not being labelled by the ^{14}C.

Thus the spot X in the control sample had been replaced by a series of spots in the test sample, of which Y carried by far the greatest amount of the ^{14}C label. Neither X nor Y gave a yellow colour on coupling before alkali treatment, suggesting the absence of lysine in these spots.

Chromatography of such test and control strips in a direction at right angles to the direction of electrophoresis did not further resolve the spots X and Y, suggesting that these were single peptides. Thus one-dimensional electrophoresis under the present conditions was a sufficient treatment to prepare the peptides X and Y for subsequent study. The peptides X and Y were (as described in the experimental section) cut out from such electrophoretograms, eluted and hydrolysed in hydrochloric acid to their constituent amino acids. The amino acids were converted to their phenylthiohydantoin derivatives and identified by chromatography.

Figure 2 is a chromatogram of the phenylthiohydantoin derivatives of the amino acids obtained on hydrolysis of peptide X (column 3) and peptide Y (column 2), run alongside the marker, the latter being prepared from a mixture of proline, phenylalanine, histidine and valine in the molar proportions of 1 : 1 : 1 : 2 respectively, using the solvent system B of Sjoquist (1953).

The derivative of histidine is not recovered in this method, so that the presence of four rather than three spots in each column is presumably due to the degradation of part of one of the phenylthiohydantoins — a phenomenon met with elsewhere (*cf.* Fraenkel-Conrat, 1955; Stein, 1958). However, the composition of both the peptides X and Y appears to be similar to that of the synthetic marker used. A further sample of the phenylthiohydantoin mixture from peptide Y, and the marker mixture, when run side by side in Sjoquist's solvent C, gave chromatograms very similar to one another, with one spot at R_F 0·70 and a larger spot spreading from R_F 0·83 to 0·90 which could not be satisfactorily resolved. Nevertheless this result was sufficient to confirm that serine is absent (eliminating peptide O-Chy 21, see Discussion).

For further confirmation, the untreated free amino acids derived by hydrolysis from peptide X were separated by chromatography in butanol : acetic acid : water and identified as proline, phenylalanine, valine and histidine by comparison with simultaneously run markers, using ninhydrin development and in addition the diazonium reagent for histidine. The presence in X of histidine, in addition to the other 3 amino acids, was thus confirmed.

4. Discussion

(1) *The position of the activated histidine residue in the protein chain.*

From the careful work of Hirs, Moore & Stein, it is possible to list (Table 1) the composition of the histidine-containing peptides which are among the major constituents of a chymotryptic digest of ribonuclease. Column 4 is relevant in view of the following considerations. Introduction of a carboxymethyl group into the imidazole ring of histidine blocks the coupling reaction with diazotised *p*-nitroaniline, and could be expected to alter the electrophoretic and chromatographic behaviour of the peptide concerned. If such a peptide contained both a histidine and a tyrosine residue, then introduction of the Cm group into ribonuclease would not decrease the

number of coupling-positive peptides, but would alter the position of one of these. But if the reactive histidine was on a peptide which contained no tyrosine residue, the number of coupling-positive peptides would be decreased by one, and a new peptide, no longer positive to coupling, would be apparent. In the present work, quantitatively the major phenomenon was the disappearance of the coupling-positive peptide X from the digest of ribonuclease and the appearance of a new peptide Y, no longer positive to coupling and bearing the introduced ^{14}C label. (Three minor new constituents were also produced, however, two of which remained positive to coupling. It is considered that these represented the products of incomplete or atypical digestion, possibly arising from the introduction of the Cm group into the ribonuclease molecule or possibly from a trace of trypsin in the chymotrypsin. A small amount of bromoacetate reaction at another locus cannot be excluded.)

TABLE 1

Major expected histidine-containing peptides (chymotrypsin digest of oxidised ribonuclease)

Peptide†	Amino acids present	Probable charge in 0·2 N-acetic acid‡	Predicted diazonium coupling, after 1 His blocked
O-Chy 21	Arg, Asp, Glu_2, His, Met, Ser_3, Thr	+ 3	No
O-Chy 22	O-Chy 21 + Ala_2, $Asp(NH_2)$, Ser_3, Tyr	+ 3	Yes
O-Chy 16 (and O-Chy 15)	Ala_2, $Asp(NH_2)$, Cy-SO_3H, Glu, $Glu(NH_2)_2$, His, Leu, *Lys*, Ser_2, Val_3	+ 2	No
O-Chy 29	Ala, $Asp(NH_2)$, Cy-SO_3H, Glu, Gly, His, $Ileu_2$, *Lys*, Pro, Tyr, Val	+ 2	Yes
O-Chy 29 less O-Chy 3	*Lys*, His	+ 3	No
O-Chy 30	His, Phe, Pro, Val_2	+ 2	No

† Nomenclature of Hirs *et al.* (1956). Peptides shown by those authors to be present in very small amounts have been ignored.

‡ In deriving the "probable charge", the ionisation of carboxylic acid groups, which is low in this medium, is ignored. The observed migrations of the (largely electropositive) peptides of the total digests support the allocations on this basis.

This interpretation allows us to eliminate O-Chy 22 and 29 of Table 1 as candidates for peptide X. If it be remembered that neither X nor Y contained lysine, as judged by the absence of colour with the coupling reagent in acid, then peptides O-Chy 15, 16 and the split product "O-Chy 29 less O-Chy 3" are eliminated, and O-Chy 29 is also again eliminated. O-Chy 21 and O-Chy 30 remain for consideration. Now, taking the electrophoretic migrations, relative to the other peptides, as an approximate guide to the charge carried (in 0·2 N-acetic acid), both X and Y appeared to be positively charged, but neither is among the most heavily charged peptides. O-Chy 21 carries three positive charges and O-Chy 30 only two such charges. O-Chy 30 could thus be tentatively identified as the most likely candidate for X. This suggestion is fully substantiated by the chromatographic identification of the constituent free amino acids, and finally confirmed by the identification of the phenylthiohydantoins of these. The chromatographic evidence shows unequivocally that peptides X and Y are identical with (or derived from) peptide O-Chy 30.

It will be remembered that Y was located simply by being the point of greatest intensity of ^{14}C labelling. The fact that this spot corresponds to a peptide having a molecular composition derived from that of X (which was selected independently), both of them corresponding to the known peptide O-Chy 30, must largely validate our analysis of the situation.

Plate I shows that the major part of the ^{14}C label was concentrated in peptide Y, which, being derived from O-Chy 30, contains a single histidine residue. Thus, these results are consistent with the conclusion reached in the preceding paper, namely, that virtually only one histidine residue per ribonuclease molecule reacts with bromoacetic acid at pH 7.

Since peptide X is now identified with O-Chy 30, it follows that the single Cm residue in Cm-ribonuclease is on the imidazole ring of this peptide. The histidine residue involved is therefore (from the work of Hirs *et al.*) that histidine nearest to the C-terminal end of ribonuclease in the protein chain. The evidence presented in the preceding paper that this histidine is present in the active centre of ribonuclease thus locates the position in the primary chain of at least a part of the active centre of ribonuclease.

(2) *A consideration of the structure of the active centre of ribonuclease.*

This identification of the histidine residue of peptide O-Chy 30 as being at the active centre of ribonuclease is further evidence for the participation of the C-terminal tail of the enzyme in its activity. Thus, Anfinsen (1956) found that removal of the C-terminal tetrapeptide Asp.Ala.Ser.Val by limited pepsin digestion was accompanied by a loss of ribonuclease activity, the removal of this tetrapeptide being the only apparent modification in the covalent structure. Removal of only the three terminal residues by carboxypeptidase does not, however, appear to affect enzyme activity (Richards, Sela & Anfinsen, 1958) suggesting the importance of the aspartic acid residue (number 121). From other work it appears, as would indeed be expected, that it is not only the C-terminal tail that is of critical importance in enzyme function. The remarkable experiments of Richards (1958) show that the 20 residue-long N-terminal tail can be detached by subtilisin digestion and hence separated from the 104 residue-long remainder of the enzyme, both parts of which are inactive. Merely by mixing these two fractions, however, enzyme activity can be restored. The N-terminal tail can be replaced by oxidised ribonuclease which can restore activity to the 97 residue remainder. Thus part, at least, of the N-terminal tail is also required for enzyme function.

In addition, studies on the inactivation of ribonuclease by *O*-methyl-*iso*urea have led Klee & Richards (1957) (*cf.* also Geschwind & Li, 1957) to suggest that one lysine residue is of critical importance "in maintaining the integrity of the active centre region". There is no lysine residue in the C-terminal tail but 2 of the 10 lysines in the molecule are present in the N-terminal tail. It is of interest to note that the lysine implicated is *de*activated towards this reagent, by comparison with the other 9 lysines present. (The evidence does not also exclude the participation of any of the latter set in the active centre, since the conversion of amino to guanidino groups is not of necessity incompatible with such participation.) One to two lysine residues and more than one methionine residue per molecule of ribonuclease seem to be specifically labile to the attack, associated with some activity loss, of iodoacetic acid (above pH 8·5 and below pH 4 respectively) (Gundlach, Stein, & Moore, 1959). These residues, therefore, are essential, and they may be associated with the active centre, although the evidence does not yet permit the firm conclusion to be drawn

that they are, in fact, in and activated by the active centre. Again, no methionine is present in the C-terminal tail, but one residue is present in the N-terminal portion.

Zittle (1946) observed an inhibition of ribonuclease (assayed by acid group liberation) by small amounts of copper or zinc (but not mercury or silver) and suggested that this was due to reaction at SH groups (now known to be absent in this protein). (It may be mentioned that Zittle also reported then, that iodoacetic acid could inhibit ribonuclease.) When RNA is used, there might be complications due to metal interactions with the substrate (*cf.* Houck, 1957); however, Davis & Allen (1955) have further shown that when uridine cyclic phosphate is the substrate (at 3×10^{-2} M), considerable inhibition is obtained, specifically, with copper or zinc (at 2×10^{-4} M). It may be speculated that such an inhibition may arise from chelation of either of these two metals by, for example, an imidazole and another (? lysine amino) group in the neighbourhood of the active centre. A detailed examination of this system may thus be profitable.

In apparent contradiction to the conclusions of the present study (and to the earlier (Weil & Seibles, 1955) photo-oxidation evidence for histidine at the active centre of ribonuclease) are the results of Rogers & Kalnitsky (1957) on the digestion of ribonuclease by carboxypeptidase (containing proteolytic impurities). These authors report that limited digestion liberates a number of free amino acids including 4 out of 4 histidine molecules, while leaving 55 to 70% of the original ribonuclease activity intact. Histidine would not therefore appear to be essential for enzyme activity. Both Rogers & Kalnitsky and ourselves have measured the transphosphorylytic activity of ribonuclease and are therefore studying the same active centre. (Even so, the explanation suggested by Rogers & Kalnitsky for the discrepancy with the results of Weil & Seibles, namely that this arises because the latter authors measured instead the subsequent hydrolytic activity, is difficult to reconcile with the evidence that we have now discussed (Barnard & Stein, 1959) that this histidine is essential for both the activities of ribonuclease.) It is just possible that the contradiction arises from difficulties in the measurement of the liberated amino acids using paper chromatography. In their report, the histidine liberated in one test case at about 50% inactivation was determined as 2·6 moles/mole ribonuclease by quantitative paper chromatography but only 2·0 moles/mole when this was checked by the Moore & Stein (1954) ion-exchange method. If a difference of this size is systematically present in the experiments reported, then it might be difficult to distinguish between no histidine residues remaining and a sufficient fraction of 1 mole remaining to account for the residual activity. Another explanation, perhaps, is that Rogers & Kalnitsky have effected the deletion rather than the substitution of the histidine residue and it might be argued that it is the introduction of the negatively-charged Cm residue that inhibits the enzyme rather than that the imidazole itself plays any role. Against this, there is the observation that this one imidazole is itself markedly activated towards the action of bromoacetic acid (and also the peculiar pH dependence of this activation), a result which suggests the actual participation of this residue in the active centre.†

† It must also be noted that there are difficulties in reconciling this evidence of Rogers & Kalnitsky with the sequence that has been established for the polypeptide chain of ribonuclease (Hirs, Stein & Moore, 1958; Anfinsen, 1958). Taking only those portions of the molecule outside the disulphide-bridged structure, the known sequence requires that when all the 4 histidines are removed, a minimum of 2 aspartic acid and 2 phenylalanine residues must be removed from the covalent structure, in contrast to the 1·1 and 1·2 respectively found by Rogers & Kalnitsky to be lost in the active material which they find has lost 4·1 histidine residues. Similarly, the

It is not possible to review here the mass of evidence correlating enzymic activity in ribonuclease with modifications of the secondary and tertiary structure of the enzyme, all of which points to the critical importance of the distribution in space of the groups of the active centre. It is likely that other evidence of the type reported in the present study will locate the position in the primary chain of other groups of the active centre and will be of value in interpreting the data on secondary and tertiary structure. When that evidence is available, such a synthesis should lead to the formulation of precise chemical statements on the mechanism of action of ribonuclease.

REFERENCES

Anfinsen, C. B. (1956). *J. Biol. Chem.* **221**, 405.
Anfinsen, C. B. (1958). *Symposium on Protein Structure*, ed. by A. Neuberger, p. 223. London: Methuen.
Barnard, E. A. & Stein, W. D. (1959). *J. Mol. Biol.* **1**, 339.
Block, R. J., Durrum, E. L. & Zweig, G. (1955). *A Manual of Paper Chromatography and Paper Electrophoresis*. New York: Academic Press.
Davis, F. F. & Allen, F. W. (1955). *J. Biol. Chem.* **217**, 13.
Edman, P. (1950). *Acta chem. Scand.* **4**, 277.
Fraenkel-Conrat, H. (1955). *Methods of Biochemical Analysis*, ed. by D. Glick, II, p. 383. New York: Interscience.
Geschwind, I. I. & Li, C. H. (1957). *Biochim. biophys. Acta*, **25**, 171.
Gundlach, H. G., Stein, W. H. & Moore, S. (1959). *J. Biol. Chem.* **234**, 1754.
Hirs, C. H. W. (1956). *J. Biol. Chem.* **219**, 611.
Hirs, C. H. W., Moore, S. & Stein, W. H. (1956). *J. Biol. Chem.* **219**, 623.
Hirs, C. H. W., Stein, W. H. & Moore, S. (1956). *J. Biol. Chem.* **221**, 151.
Hirs, C. H. W., Stein, W. H. & Moore, S. (1958). *Symposium on Protein Structure*, ed. by A. Neuberger, p. 211. London: Methuen.
Houck, J. C. (1957). *Biochim. biophys. Acta*, **26**, 649.
Ingram, V. M. (1956). *Nature*, **178**, 792.
Klee, W. A. & Richards, F. M. (1957). *J. Biol. Chem.* **229**, 489.
Moore, S. & Stein, W. H. (1954). *J. Biol. Chem.* **211**, 893.
Richards, F. M. (1958). *Proc. Nat. Acad. Sci., Wash.* **44**, 162.
Richards, F. M., Sela, M. & Anfinsen, C. B. (1958). Quoted in Anfinsen, C. B. (1958).
Rogers, W. I. & Kalnitsky, G. (1957). *Biochim. biophys. Acta*, **23**, 525.
Sjoquist, J. (1953). *Acta chem. Scand.* **7**, 447.
Stein, W. D. (1958). *Ph.D. Thesis*, London.
Weil, L. & Seibles, T. S. (1955). *Arch. Biochem. Biophys.* **54**, 368.
Zittle, C. A. (1946). *J. Biol. Chem.* **163**, 111.

established sequence shows that the loss of all 4 histidines necessitates the removal of the C-terminal tetrapeptide, a step which, according to the evidence of Anfinsen quoted above, should lead to complete inactivation. It might possibly be argued, to overcome these objections, that certain peptides are formed by cleavage but can be bound very firmly to the protein residue by non-covalent bonds, but this interpretation would involve a number of further assumptions.

J. Mol. Biol. (1959) **1**, 359-364

Ultraviolet Absorption Spectra of Poly-L-Glutamic Acid

Kazutomo Imahori

Department of Chemistry, College of General Education, University of Tokyo, Japan

Jiro Tanaka

Institute for Solid State Physics, University of Tokyo, Japan

(*Received 5 May 1959, and in revised form 24 August 1959*)

The u.v. absorption spectra of poly-L-glutamic acid solutions at various pH's have been obtained.

It has become apparent that the optical density of peptide absorption increases as the molecule is transformed from helical to random coiled configuration, even after considering the effect of scattering and ionization of carboxyl groups of side chains. Thus it is possible to assess the helical content of a protein molecule from its u.v. absorption. We observed no splitting or broadening of the peptide absorption band of the helical form as predicted by Moffitt and by Evans respectively.

1 Introduction

Recently, Doty & Yang (1956) have extensively investigated the molecular configuration of polypeptides and proteins in various solvents, and have confirmed that the α-helix can exist in solution in equilibrium with the random coil or other states of aggregation. For example, in the case of poly-L-glutamic acid discussed in this paper, Doty, Wada, Yang & Blout (1957) have confirmed the helix-coil transition in water-dioxane solution by the methods of optical rotary dispersion, viscosity and infrared spectra. A change of ultraviolet absorption spectrum is also expected in this helix-coil transition, but only a little is known of the spectrum of polypeptides in the region characteristic of peptide absorption. Goldfarb & Saidel (1951) have observed spectral changes accompanying the denaturation of bovine serum albumin, but their measurements were made at the longer wavelength side of the characteristic peptide absorption.

In this study of the spectral changes of the peptide-characteristic absorption for a helix-coil transition we have examined the spectrum of poly-L-glutamic acid in the 1900 Å region in aqueous solution. This polymer has no conspicuous chromophoric amino acid residues other than the carboxyl group, and is well suited for this study of spectral changes in the peptide chromophore.

As a prelude, we must refer to the numerous studies of the ultraviolet absorption spectra of amides and polypeptides. Ham & Platt (1952) have measured the spectra of simple amides in the shorter ultraviolet region, and assign the 1850 Å band and 2100 Å band to π-π^* and n-π^* transitions respectively. Hunt & Simpson (1953) have determined the spectra of amides in the vacuum ultraviolet region and Peterson & Simpson (1956) have investigated the polarization of the 1850 Å band by measurements of crystalline spectra of myristiamide. Preiss & Setlow (1956) gave spectra of thin films of native proteins in the vacuum ultraviolet region.

From the theoretical point of view, Tanaka (1957) and Nagakura (in press) gave reasonable interpretations of features of amide spectra based on the charge transfer

theory in conjugated molecules. Electronic interactions in polypeptides, in which peptide bonds are arranged in regular positions, are of great importance from the theoretical point of view. Evans & Gergely (1949) have proposed a band model for the electronic structure of polypeptides linked by hydrogen bonding. Moffitt (1956 *a*,*b*) has shown that a helix has two transitions whose moments are respectively parallel and perpendicular to the screw axis, and has discussed the close relation between the splitting of excitation states and the optical rotatory power of a helix.

Thus it is also a purpose of the present paper to see if features of the absorption band such as those predicted by Moffitt or Evans will appear, by comparing the absorption spectra of helical forms to those of the random coil.

2. Experimental

(a) *The sample*

The sample of poly-L-glutamic acid was obtained by saponifying poly-γ-benzyl-L-glutamate which was presented through the courtesy of Dr. A. Wada of the Ochanomizu University of Tokyo and was the same sample as that used for his electric dipole moment work (Wada, 1959). Poly-γ-benzyl-L-glutamate was put in acetic acid saturated with dry hydrogen bromide, and was kept at 0°C for 7 hrs for debenzylation. The debenzylated sample was then put into water and precipitated with a mixture of methyl alcohol and ether. After this process had been repeated five times, the sample was dissolved into water and dialysed against water overnight. The final solution was lyophilized and the poly-L-glutamic acid sample was obtained as a white powder.

The debenzylation was shown to be complete by the fact that no absorption band could be obtained in the 2580 Å region. The molecular weight of the original poly-γ-benzyl-L-glutamate was found to be 50,000 from light scattering measurements. The molecular weight of poly-L-glutamic acid was not determined directly, but its intrinsic viscosity of 0·21 in 0·2 M-NaCl, pH 7, gave the value of about 11,000, based on the relation of Wada and Doty (unpublished). Since buffers were undesirable because of their absorption in the far ultraviolet region, the pH of the solution was adjusted by HCl and $NaHCO_3$ only. Concentration was determined by the Kjeldahl nitrogen method.

(b) *Spectra*

All spectral data were obtained with the Cary Recording Spectrophotometer Model 14. The wavelength range from 2600 to 1850 Å was especially carefully examined. Nitrogen gas was passed through the machine in order to get a good response, especially in the shorter wavelength region. Even though the solvent itself absorbed to some extent at shorter wavelengths, this absorption was not strong enough to make the response inaccurate (Bayliss & Brackenbridge, 1955). This was proved by showing that the sample spectrum obtained with the salt solution as a reference fitted very well to that obtained with pure water after subtracting the absorption of the salt solution.

(c) *Polarimeter*

Rudolph's spectropolarimeter Model 80*S* was accessible for us through the courtesy of Dr. Kato of the Government's Industrial Research Institute of Tokyo. A Xenon lamp was used as a light source, which enabled us to measure the rotatory dispersion from 7500 Å down to 2800 Å.

3. Results

In Fig. 1 the ultraviolet spectra of poly-L-glutamic acid at pH 4·0 and 7·25 are shown. It is apparent that the shape and position of the peaks of the absorption curves are similar for both pH's. The molar extinction coefficients are quite different, however. In the acid region, where poly-L-glutamic acid is in the helical form, ϵ at

1900 Å is about 4000, while in the higher pH region, where poly-L-glutamic acid was forced to be in the random coil form, ϵ_{1900} increases to 7000. These results are quite in agreement with what is expected from previous work (Goldfarb & Saidel, 1951).

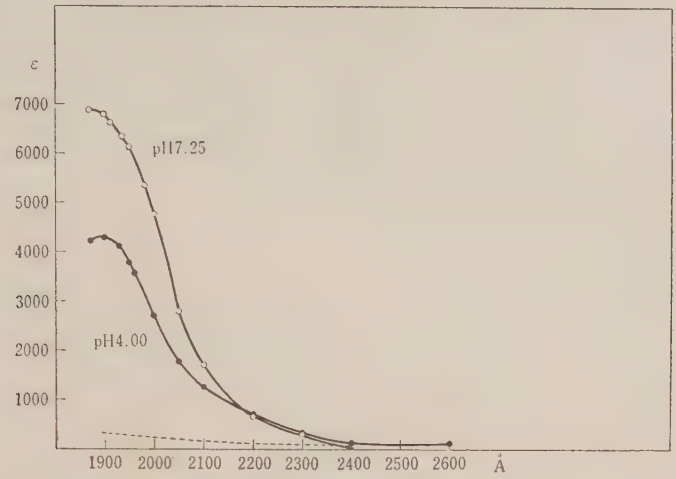

FIG. 1. U.v. absorption spectra of poly-L-glutamic acid. The broken line shows the scattering of the lower pH solution.

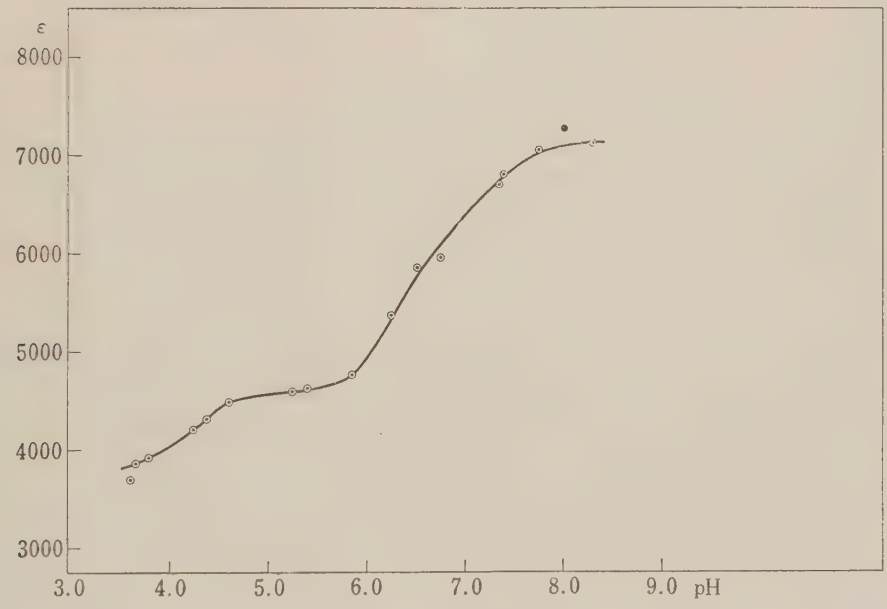

FIG. 2. pH dependence of absorption coefficient of poly-L-glutamic acid solution at 1900 Å.

However, the effect of ionization must be considered. As it is generally known that the extinction coefficient of the carboxyl group increases when it is ionized, it is possible that the higher optical density obtained for poly-L-glutamic acid in alkaline solution is due to the ionization of side chain carboxyl groups. We have examined the extinction coefficient of acetic acid in both the unionized and ionized form and

have found that the difference in ϵ for the two forms was less than 1000.† But, since the difference in ϵ for the two forms of poly-L-glutamic acid was over 3000, it is obvious that two-thirds of the observed increase in ϵ is the net change accompanying the transformation from helix into random coil.

Next, we examined how the extinction coefficient would change as the pH of the solution was raised. The results are shown in Fig. 2, where ϵ_{1900} increases gradually as the pH is raised from 3·8 to 4·7. In the range of 4·7 to 5·9 ϵ_{1900} remains almost constant. Above 5·9 it starts to increase again, reaching its maximum value at pH 7·8. This gradual change in extinction coefficient indicates that it accompanies the change in conformation of the poly-L-glutamic acid molecule.

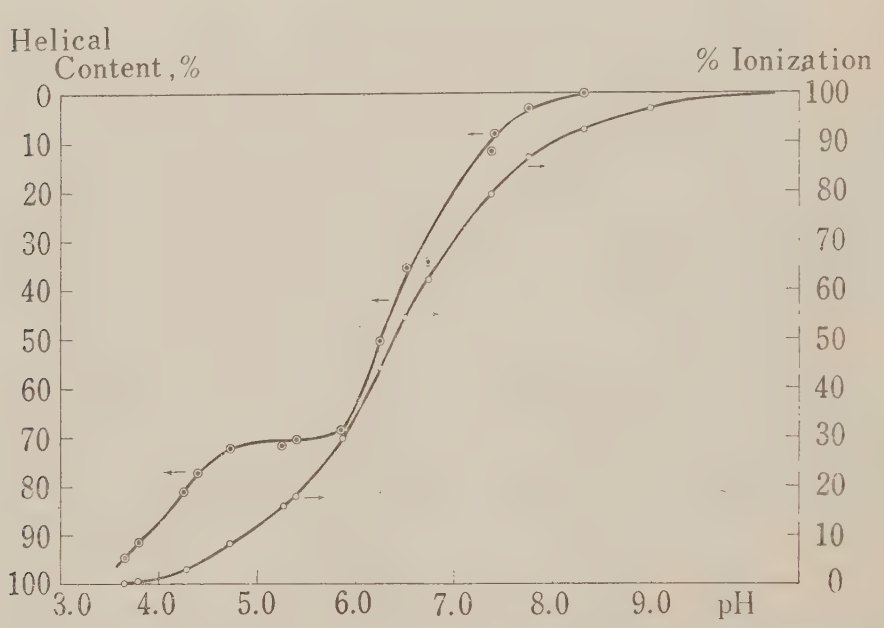

FIG. 3. Helical content and degree of ionization of poly-L-glutamic acid at various pH's.

Assuming ϵ_{1900} of the peptide chromophore in the random coil to be 6190 and that of the helix to be 3660, and taking scattering and ionization effects into consideration, we get the helix-coil transition curve indicated in Fig. 3. The titration curve is also shown. This transition curve is in fairly good agreement with those obtained from optical rotation and viscosity measurements by Doty *et al.* (1957). To check this result, we examined the rotatory dispersion of poly-L-glutamic acid at pH 5·3 and 8·0. The dispersion was measured in the wavelength region of 7500 to 2800 Å. The results are shown in Fig. 4, plotted according to Moffitt. The dispersion at pH 5·3 gives the following data: $[\alpha]_D = -14{\cdot}8$, $b_0 = -410$ and $a^H{}_0 = +482$ (Doty, Imahori & Klemperer, 1958). The b_0 value and a^H_0 value correspond to 70·5 and 71·0% helical content respectively, which are in perfect agreement with the value obtained in Fig. 4. The values $[\alpha]_D = -80$ and $b_0 = 0$ at pH 8·0 indicate that the helical configuration is completely broken at this pH.

† The molecular extinction coefficient at 1900 Å for the carboxyl anion was found to be 1000 at 17°C and that of the unionized carboxyl group at 2000 Å was 40.

Though our rotatory dispersion data do not cover the whole range of pH, it is obvious that helical contents obtained from those two methods are in fairly good agreement. This result proves that the u.v. absorption method furnishes another good way to get the helical content of polypeptides or proteins.

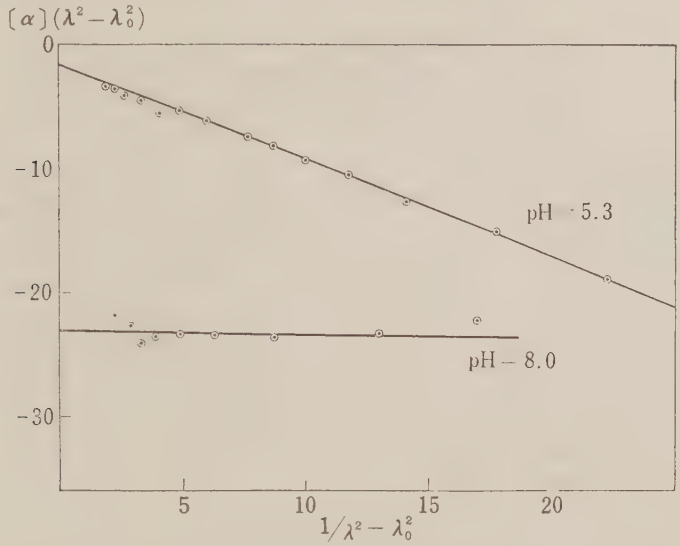

FIG. 4. Moffitt plot of rotatory dispersion of poly-L-glutamic acid.

4. Discussion

It was already found by Goldfarb & Saidel (1951) that the optical density of a protein solution at 2100 Å increased as the protein molecule was denatured. But since their measurement was carried out at a longer wavelength region than that of the characteristic absorption band of the peptide bond, and since their sample was protein itself which contains so many chromophoric groups absorbing near this region, it was not certain that this increase of the optical density was merely due to the change of the secondary structure of the protein molecule. There remained some possibility that the electronic states of these chromophoric groups were changed in such a way as to cause this change in optical density.

As we have chosen a sample which has no chromophoric group other than the peptide bond and the carboxyl group, there remains no more ambiguity about this increase of the optical density, which must be due to the unfolding of the molecule. But the application of this method for obtaining the helical content of a protein molecule is still restricted. We have to take the u.v. absorptions of such groups as tyrosine, phenylalanine, cysteine and histidine residues into consideration before we dare use it.

Our method would probably be superior to those of optical rotation and viscosity, especially in the acid region. Since our method needs only very low concentrations (lower than 0·01%) we can go down as low as pH 3·6 without getting any precipitation in the solution. Our results indicate that 30% of the helical form breaks up as the pH is raised from 3·6 to 4·7, but the structure containing 70% of helix seems to be rather stable until more than one-third of the carboxyl groups of the side chains are ionized. This confirms the conclusion of Doty *et al.* (1957) that side chain carboxyl

groups play a very important role in the stability of the helical structure of poly-L-glutamic acid, and that the helical configuration does not begin to break up until about 40% of the carboxyl groups are ionized. Of course, in comparing our results with those of Doty's group we have to keep in mind that our solvent is somewhat different from theirs. Nevertheless, our results are quite in accordance with those of Doty.

We were unable to detect any band splitting as predicted by Moffitt. According to Moffitt's theory, if the absorption band split into bands parallel and vertical to the screw axis of the helix, the parallel band should appear about 2800 wave numbers to the longer wavelength side of the vertical band. Using the polarization results of amide spectra of Peterson & Simpson, and taking the atomic coordinates of the α-helix presented by Pauling & Corey, the intensity ratio of parallel and vertical bands is estimated to be 1 : 2·17 on the basis of an oriented gas model. But, as is apparent from Fig. 1, we can see no splitting of the band and find only a marked decrease in absorption of the helix. The lowering of absorption intensities and the failure of predictions of calculated excitation splitting with molecular crystals were recently reviewed by Tanaka (1959). We will not discuss this point any further because it is not the purpose of our present paper; there remain to be investigated many subtle points about the mechanism of this process.

As to the band theory proposed by Evans & Gergely, our optical method cannot give any information about the structure of bands (Tanaka, 1959), because the optical transitions are allowed only for the case where the propagation vector **K** of the excitation equals $\mathbf{K}_0$, that of the incident radiation. Although the above-mentioned spectral features will be intimately related to the structure of the band, we are not in a position to make any conclusive criticism of their concept from our present results.

The authors wish to express their hearty thanks to Professor Doty for his kindness in reading thoroughly and giving comments on our paper before its publication. Viscosity measurements were made by Miss Yoko Kudo to whom our thanks are due.

REFERENCES

Bayliss, N. S. & Brackenbridge, C. J. (1955). *Chem and Ind.* **477**.
Doty, P., Imahori, K. & Klemperer, E. (1958). *Proc. Nat. Acad. Sci., Wash.* **44**, 424.
Doty, P., Wada, A., Yang, J. T. & Blout, E. R. (1957). *J. Polymer Sci.* **23**, 851.
Doty, P. & Yang, J. T. (1956). *J. Amer. Chem. Soc.* **78**, 498.
Evans, M. G. & Gergely, J. (1949). *Biochim. biophys. Acta*, **3**, 188.
Goldfarb, A. R. & Saidel, L. J. (1951). *Science*, **114**, 177.
Ham, J. G. & Platt, J. R. (1952). *J. Chem. Phys.* **20**, 335.
Hunt, J. D. & Simpson, W. T. (1953). *J. Amer. Chem. Soc.* **75**, 4540.
Moffitt, W. (1956*a*). *Proc. Nat. Acad. Sci., Wash.* **42**, 736.
Moffitt, W. (1956*b*). *J. Chem. Phys.* **25**, 467.
Peterson, D. L. & Simpson, W. T. (1956). *J. Amer. Chem. Soc.* **78**, 2375.
Preiss, J. W. & Setlow, R. (1956). *J. Chem. Phys.* **25**, 138.
Tanaka, J. (1957). *J. Chem. Soc. Japan*, **78**, 1636.
Tanaka, J. (1959). Supplement of *Progress of Theoretical Physics* (*Kyoto*), in press.

J. Mol. Biol. (1959) **1**, 365-374

Some Properties of Soluble Ribonucleic Acid from *Escherichia coli*

A. Tissières

Biological Laboratories, Harvard University, Cambridge, Mass., U.S.A.

(*Received 7 September 1959*)

1. Soluble ribonucleic acid has been prepared from *E. coli* by the phenol method.
2. The hypochromicity and the reactivity with formaldehyde suggest that the molecule has intramolecular hydrogen bonds.
3. Its sedimentation coefficient is 4 S, and there is little concentration dependence in salt solutions.
4. In water the molecule extends and the concentration dependence of the sedimentation coefficient is increased.
5. The molecular weight, calculated from sedimentation, diffusion, and partial specific volume, is 25,500 $\pm$ 10%.
6. Evidence is presented suggesting that S-RNA is free, i.e. not bound to any large molecule, in cell-free extracts.

1. Introduction

Besides the high molecular weight ribonucleic acid (RNA) of ribonucleoprotein particles (Hall & Doty, 1958) the cytoplasm contains low molecular weight or soluble RNA (S-RNA), *cf.* Smellie (1955). Experiments carried out with animal cells (Hoagland, Zamecnik & Stephenson, 1957; Hoagland, Stephenson, Scott, Hecht & Zamecnik, 1958) and with micro-organisms (Berg & Ofengand, 1958), indicate that this S-RNA binds amino acids in the presence of activating enzymes (Hoagland, 1955), adenosine triphosphate (ATP), and magnesium ions. It has been shown with preparations from animal cells that, under suitable conditions, amino acids are transferred from S-RNA to ribonucleoprotein particles (Hoagland *et al.*, 1957; 1958) where they are believed to be incorporated into peptide chains. These experiments suggest that S-RNA plays an essential role in the synthesis of proteins.

In the work presented here, S-RNA was prepared from *Escherichia coli* by a modification of the phenol method of Kirby (1956). Its hypochromicity, which had given valuable information about the secondary structure of ribonucleoprotein particle and tobacco mosaic virus RNA's (Hall & Doty, 1958; Doty, Boedtker, Fresco, Haselkorn & Litt, 1959), has been studied, and its sedimentation and diffusion coefficients, as well as its partial specific volume and intrinsic viscosity, have been determined. An average molecular weight, based on these values, has been calculated. Evidence is presented suggesting that in cell-free extracts S-RNA is not bound to proteins or to any other large molecule.

2. Material and Methods

E. coli, strain B, was grown, harvested, and the crude cell free extract made in 0·005 M-tris buffer pH 7·3 and 0·01 M-magnesium acetate, as described previously (Tissières, Watson, Schlessinger & Hollingworth, 1959). The extract was centrifuged at 78,000 *g* for 180 min to sediment the ribonucleoprotein particles. Two-thirds of the supernatant fluid was then carefully pipetted off, giving a solution free of particulate RNA. This solution was kept frozen unless used immediately.

From this, S-RNA was isolated by treatment with phenol (Kirby, 1956). Liquid phenol was purified on a column of aluminum oxide "Woelm" (non-alkaline, activity grade 1) from M-Woelm, Eschwege, Germany. 1 vol of solution was shaken vigorously for 2 to 3 min at room temperature with 1 vol aqueous phenol, in a separatory funnel. On standing, the phenol separated from the water, and a thin layer of denatured proteins formed at the interphase. Phenol and the denatured proteins were removed and the water phase was treated twice more, first with 1/2 vol, then with 1/4 vol phenol. The water extract was finally separated by centrifugation (700 *g*) from small amounts of phenol and denatured proteins. NaCl was added to a concentration of 0·1% (wt/vol), and S-RNA was precipitated by addition of 2 vols 95% ethanol. It was centrifuged down and redissolved in 0·1% NaCl. At this stage the preparation contained a small amount of insoluble material, which was discarded by 15 min centrifugation at 10,000 *g*. S-RNA was then precipitated three times from 0·5% NaCl solutions with 2 vols 95% ethanol. It was washed once with 60% and twice with 95% ethanol, once with peroxide-free ether, dried at 37°C, and kept in a desiccator, at room temperature, over P_2O_5. The white powder thus obtained consisted of about 80% S-RNA by weight, 10 to 15% water, probably a small amount of polysaccharides, and less than 2·5% protein (see below). In some cases, after washing in ethanol, S-RNA was dissolved in 0·1 M-NaCl, dialyzed free of ethanol, and kept frozen in solution.

Polysaccharides were removable by treatment with 2-methoxyethanol in presence of potassium phosphate according to Kirby (1956). S-RNA was stable at room temperature with respect to the properties described below. 750 ml. of supernatant, obtained from 300 g (wet wt) cells, yielded about 300 mg S-RNA.

A Model L Spinco ultracentrifuge was used for the preparation of the soluble fraction, free of ribonucleoprotein particles. The centrifugal forces given here represent *g* average, as calculated from the middle of the centrifuge tube. Analytical ultracentrifugation was done with a Model E Spinco centrifuge, with either schlieren or ultra-violet optics. The films taken with the latter were analyzed for their optical density with a Spinco Analytrol densitometer. The centrifuge cell had a light path of 12 mm. The sedimentation constants were corrected to 20°C in water and to zero concentration. They are expressed in Svedberg units, s ($= S^0_{20,w} \times 10^{13}$ sec).

Electrophoresis and diffusion measurements were performed with a Spinco Model H apparatus, in an 11 ml. Tiselius cell at 1°C.

Absorption spectra and optical densities were measured with a Beckman D.U. spectrophotometer.

Partial specific volume was measured in a 25 ml. pycnometer, and viscosity with an Ostwald-Fenske type viscometer with a solvent running time of 556 sec at 25 ± 0·02°C.

Phosphorus was estimated by the method of Fiske & Subbarow (1925) as described by Umbreit, Burris & Stauffer (1957). After digestion of the samples in the presence of H_2SO_4 and H_2O_2 at 150°C, a small amount of urea was added to decompose any excess H_2O_2 (Dryer, Tammes & Routh, 1957).

Protein was estimated by the biuret method of Gornall, Bardawill & David (1949) and by the Folin phenol reagent (Lowry, Rosebrough, Farr & Randall, 1951).

Deoxyribonuclease and pancreatic ribonuclease were obtained from Worthington Biochemical Corp., Freehold, New Jersey.

Tris(hydroxymethyl)aminomethane was Sigma 7–9 biochemical buffer from Sigma Chemical Company, St. Louis, Missouri. The pH of tris solution was adjusted by addition of 0·1 N-HCl. ATP was also obtained from Sigma Chemical Company.

3. Results

(a) *Phosphorus and protein content, and specific extinction coefficient of S-RNA*

The results of estimations of phosphorus and protein, together with the specific extinction coefficient in 0·1 M-NaCl at 258 mμ and the weight of S-RNA kept over P_2O_5, are shown in Table 1. The amount of protein found with the biuret method was equal to or lower than 1%, while with the Folin phenol reagent values up to 2·5% protein were obtained.

The specific extinction coefficient of preparation 3, which had been treated with 2-methoxyethanol, was about 20% higher than that of preparations 1 and 2. The phosphorus content of preparations 1 and 2 is higher than would be expected on the basis of the extinction coefficient, which suggests that a phosphorus-containing component was present. This component was removed by treatment with 2-methoxyethanol; it is therefore likely that it was polysaccharide in nature. The phosphorus

TABLE 1

Dry weight, phosphorus and protein content of S-RNA

S-RNA preparations	mg/ml. S-RNA (dried over P_2O_5)	phosphorus mg/ml.	mg/ml. RNA (based on 9·6% phosphorus)	protein content		Specific extinction coefficient at 258 mμ, $E^{1\%}_{1cm}$, based on P content of 9·6%
				biuret method	Lowry method	
1	2·52	0·236	2·460	1	2·5	204·0
2	2·26	0·206	2·141	<1	1·8	215·0
3	1·00	0·081	0·825	<1	1·9	249·0

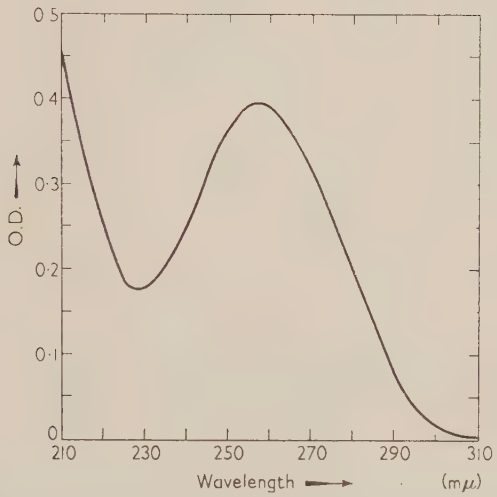

FIG. 1. Ultraviolet absorption spectrum of S-RNA (15·6 μg/ml. in 0·01 M-phosphate buffer pH 6·7, light path = 1 cm). The maximum of the absorption peak lies at 258 mμ.

value obtained with preparation 3 suggests that S-RNA, at constant weight over P_2O_5, still contained about 12 to 15% water.

(b) *Absorption spectrum*

The absorption spectrum of S-RNA in the ultra-violet region is given in Fig. 1. The ratios of the optical densities at 258 mμ and 230 mμ varied in 5 preparations between 2·20 and 2·35; at 258 mμ and 280 mμ they varied from 2·06 to 2·14. The highest ratios were observed after treating S-RNA with 2-methoxyethanol.

The optical density of a solution of S-RNA in 0·1 M-NaCl at 258 mμ increased 32% in presence of pancreatic ribonuclease (2 μg/ml.) and 45% on alkaline hydrolysis (0·3 N-KOH for 18 hr at 37°C).

(c) *Reaction with formaldehyde*

Formaldehyde reacts with the amino groups of purines and pyrimidines (Fraenkel-Conrat, 1954). Consequently the optical density in the 260 mμ region rises and the absorption maximum shifts slightly towards the longer wavelengths. S-RNA reacted very slowly with formaldehyde (2% wt/vol at 25°C): the optical density at 260 mμ increased by only 2% in 24 hr; at 45°C however, there was a 20% increase in 24 hr, and the reaction was completed in 48 hr with a 22% increase.

(d) *Hypochromicity of S-RNA*

The changes of optical density of S-RNA at 258 mμ were studied as a function of temperature and salt concentration.

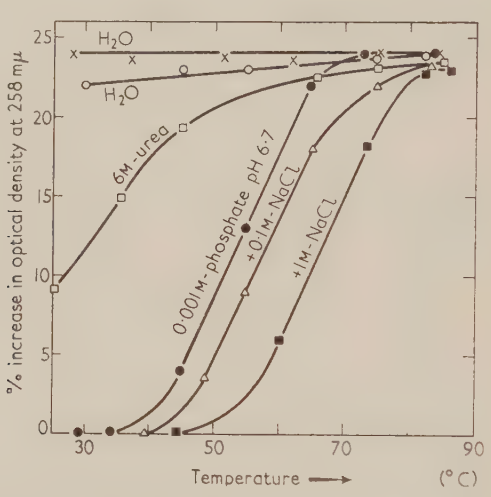

Fig. 2. Changes in optical density of S-RNA, in different solvents, as a function of temperature. Readings were taken after the sample had remained at a given temperature for 10 min.

The results, illustrated in Fig. 2, show that (a) the optical density of S-RNA in salt solutions increased as a function of temperature until the increase had reached 23 to 24% of the initial value; (b) in higher salt concentrations, this effect occurred at somewhat higher temperature, but the general aspect of the curve was the same: it was merely shifted to higher temperature; (c) in 6 M-urea, the optical density had already increased by 9% at 25°C, and the curve was shifted to lower temperatures; (d) the optical density increased by 22 to 24% when S-RNA was dissolved in distilled water at 25°C, and raising the temperature did not produce any change. The changes observed on heating were reversed 95 to 100% on cooling.

These results indicate that the molecules of S-RNA extend in distilled water, in 6 M-urea, and upon heating in salt solutions at 60° to 80°C. They suggest, together with the slow rate of reaction with formaldehyde at room temperature, as compared to 45°C, that there is substantial hydrogen bonding when the molecule is dissolved in salt solutions.

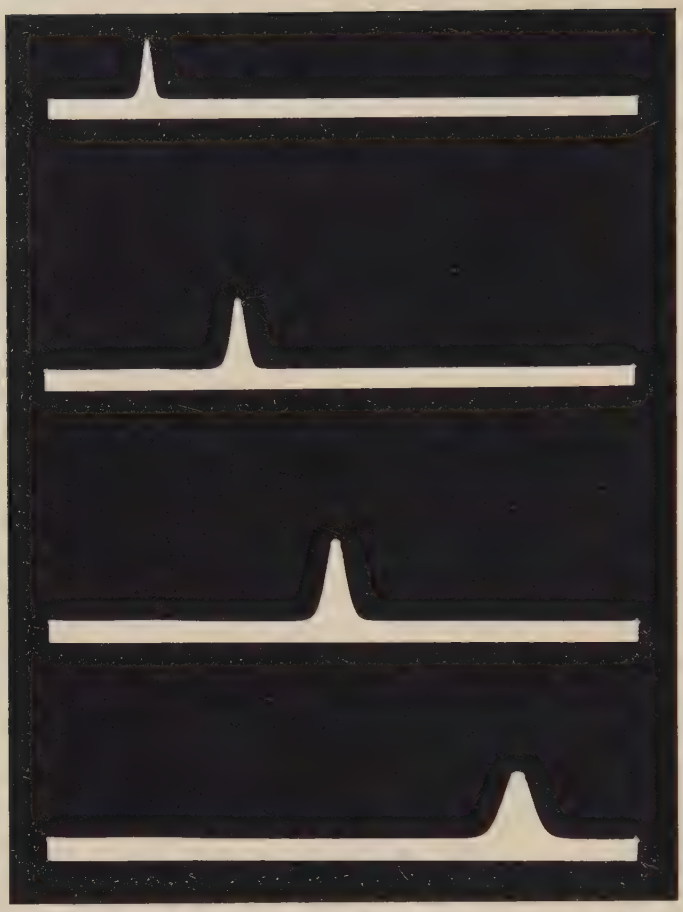

PLATE I. Schlieren pattern of free electrophoresis of 0·05% (wt/vol) S-RNA in 0·1 M-acetate buffer pH 4·6, at 159 v. Pictures (left channel) taken at 0, 30, 60 and 120 min.

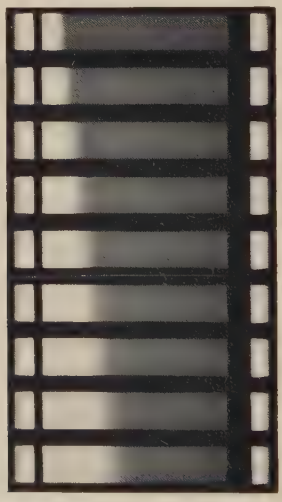

PLATE II. Sedimentation diagrams of S-RNA (about 40 μg/ml. in 0·05 M-phosphate buffer pH 6·2) with the ultraviolet optics. The pictures were taken at 8 min intervals. Speed: 59,780 rev/min. Sedimentation coefficient: 3·95 S.

[*To face page* 369

(e) *Optical rotation as a function of temperature*

The specific rotation, measured at a wavelength of 589 mμ with 0·45% S-RNA in 0·1 M-NaCl, was + 160° at 27°C. It decreased progressively as the temperature rose to reach a plateau at about 85°C, with a specific rotation of 19·6. Thus over this temperature range there was an eight-fold decrease. The curve obtained by plotting in ordinate the decrease in specific rotation and in abscissa the temperature, was similar to that of the hypochromic effect in the same salt solution.

(f) *Electrophoresis*

S-RNA (specific extinction coefficient 204) was found to move as a single symmetrical peak (Plate I) on electrophoresis in 0·1 M-acetate buffer, pH 4·6.

(g) *Sedimentation*

Plate II shows the sedimentation diagrams obtained with the ultra-violet optics, and Fig. 3(a) and (b), shows the tracings made with the analytrol densitometer of the ultra-violet sedimentation diagrams. The sedimentation constants were measured at concentrations of about 40 μg/ml. (ultraviolet optics) and 1 to 10 mg/ml. (schlieren optics), under a variety of conditions. The results, given in Table 2, show that (a) the

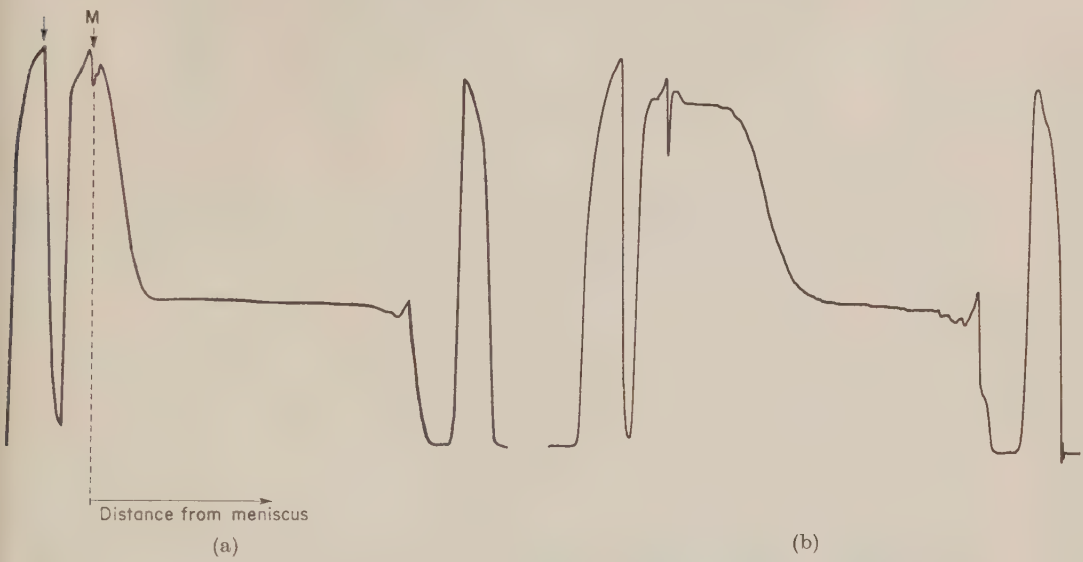

FIG. 3, (a) and (b). Analytical tracings of the sedimentation diagrams of Plate II, after 24 and 73 min respectively, at 59,780 rev/min.

values do not vary appreciably in phosphate or NaCl solutions of widely different ionic strengths; (b) in distilled water, in citrate buffer, in 6 M-urea (after corrections for viscosity and density) and in ethylene diamine tetra-acetate (EDTA), the values seem somewhat lower; (c) they were higher in presence of 0·01 M-magnesium acetate. The results of the study of concentration dependence are shown in Fig. 4. The concentration effect, which was small with an ionic strength of 0·1, was definitely larger when S-RNA was dissolved in distilled water. A value of 4 s was used for the calculation of the molecular weight.

TABLE 2

Sedimentation coefficients of S-RNA

Preparation	Solvent	Concentration	s
	Ultraviolet optics	%	
1	0·01 M-tris pH 7·4	0·004	4·05
1	same sample, left 24 hr at 25°C	0·004	4·00
1	0·05 M-phosphate pH 6·2	0·004	3·95
1	same sample, left 96 hr at 4°C	0·004	3·93
2	0·05 M-phosphate pH 6·2	0·004	4·04
2	0·001 M-phosphate pH 5·9	0·004	4·10
2	0·01 M-phosphate pH 6·2	0·004	3·94
3	0·001 M-tris pH 7·3	0·004	3·85
3	0·1 M-NaCl + 0·001 M-tris pH 7·3	0·004	4·16
3	0·2 M-NaCl + 0·001 M-tris pH 7·3	0·004	3·91
3	1·0 M-NaCl + 0·001 M-tris pH 7·3	0·004	4·00
3	distilled water	0·004	3·90
4	distilled water	0·004	3·80
3	0·01 M-magnesium acetate + 0·01 M-tris pH 7·3	0·004	4·65
3	0·1 M-magnesium acetate + 0·01 M-tris pH 7·3	0·004	4·12
4	0·01 M-magnesium acetate + 0·01 M-tris pH 7·3	0·004	4·65
4	0·1 M-magnesium acetate + 0·01 M-tris pH 7·3	0·004	4·24
4	2·0 M-urea	0·004	4·04
4	6·0 M-urea	0·004	3·90
5	0·02 M-citrate buffer pH 6·0	0·004	3·51
	Schlieren optics		
3	0·001 M-tris pH 7·3	0·1	4·02
3	0·1 M-NaCl + 0·001 M-tris pH 7·3	0·1	4·13
4	0·1 M-EDTA (neutral) + 0·01 M-tris pH 7·3	0·1	3·54
4	0·01 M-EDTA (neutral) + 0·01 M-tris pH 7·3	0·1	3·66
4	0·1 M-NaCl + 0·01 M-tris pH 7·3	0·5	3·80
5	distilled water	1·0	3·24
5	0·1 M-NaCl + 0·01 M-tris pH 7·3	1·0	3·74

(h) *Diffusion coefficients*

Free diffusion was measured on four different preparations for about 18 hr. The first preparation contained 0·15% (wt/vol) S-RNA in 0·05 M-phosphate buffer (1 part Na_2HPO_4 and 3 parts KH_2PO_4 solutions) pH 6·2. The second, third and fourth measurements were done with 0·18, 0·34 and 0·08% S-RNA, in 0·08 M-NaCl and 0·01 M-phosphate buffer pH 7·1. The values obtained were 7·26, 7·66, 8·38 and $8·06 \times 10^{-7}$ cm²/sec respectively, corrected for 20°C, in water. The reason for these variations is not clear. The first two values were given for similar concentrations of S-RNA, though in different buffers. It is possible that at low and high concentrations (preparations 4 and 5) the diffusion coefficient is equal or higher than 8×10^{-7} while at intermediary concentrations it is lower. If this were true, the coefficient at zero concentration would be about $8·2 \times 10^{-7}$. However, varying amounts of impurities may also explain the results.

An average value of $7·84 \times 10^{-7}$ cm²/sec $\pm$ 7% was used for the calculation of the molecular weight.

(i) *Partial specific volume*

The value obtained was 0·51 ± 3% at concentrations varying from 0·24 to 0·96%.

(j) *Viscosity*

Measurements were made at concentrations of 0·72, 0·48 and 0·24%, in 0·1 M-NaCl. The intrinsic viscosity (η) was found to be 0·075 (25°C). The error in this value was probably as great as 10%.

(k) *Molecular weight*

The molecular weight calculated by the Svedberg equation (Svedberg & Pedersen, 1940), from sedimentation, diffusion and partial specific volume data given above, was 25,500 ± 10%. It was 26,400 ± 15% when calculated from viscosity, sedimentation and partial specific volume data (Scheraga & Mandelkorn, 1953), using for β a value of $2{\cdot}35 \times 10^6$ (Hall & Doty, 1959).

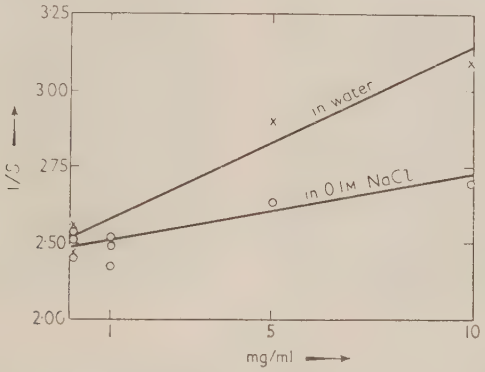

FIG. 4. Concentration dependence of sedimentation. The circles represent the values obtained when S-RNA was dissolved in 0·1 M-NaCl, and the crosses the values for S-RNA in distilled water.

(l) *Homogeneity*

The apparent diffusion coefficient was calculated from the area under the schlieren curve and from the maximum ordinate of the gradient curve (see Schachman, 1957). The values obtained did not increase with time, suggesting that the preparation was homogeneous. This method, however, is not sufficiently sensitive to detect a small amount of heterogeneity.

It was found that the sharpness of the boundary on pictures taken with the ultraviolet optics, or the angle of the slope on the analytrol tracing, varied slightly from one preparation to another, thus indicating a small and variable heterogeneity.

(m) *Evidence for the presence of free S-RNA in cell-free extracts*

If S-RNA is free, i.e. not bound to proteins or any large molecule in cell free extracts, as it is after treatment with phenol, its sedimentation coefficient should equal that of isolated S-RNA. If, however, it is bound to proteins, its sedimentation rate would probably be higher. The following experiments were designed to measure the sedimentation coefficient of S-RNA in cell-free extracts.

3 g washed cells were ground with 9 g alumina powder and extracted with 30 ml. 0·005 M-tris buffer pH 7·3, containing 0·005 M-Mg^{2+}. No deoxyribonuclease was added.

The mixture was centrifuged at 10,000 *g* for 15 min and the crude extract was centrifuged at 100,000 *g* for 120 min. Two-thirds of the supernatant was pipetted off, free of ribonucleoprotein particles. It was dialyzed at 2°C with stirring for 3 to 5 hr against 50 vols of the above tris-magnesium mixture to remove small molecules absorbing in the ultraviolet region. It was then diluted with the same buffer to give an optical density of 1 at 260 mμ, and divided into two samples. The first one was examined as such in the analytical centrifuge with the ultraviolet optics; the second one was examined after addition of 0·5 μg/ml. of pancreatic ribonuclease. The sedimentation pictures obtained are shown in Plate III(a) and (b). A slowly moving boundary is clearly seen in Plate III(a). Its sedimentation coefficient was 4·02. In Plate III(b) this boundary is not visible. A similar experiment was repeated starting from a different batch of cells; only in the absence of added ribonuclease was there a boundary, moving at a rate of 4·0 s. The substance responsible for this boundary was identified with S-RNA because: it absorbs in the ultraviolet region with a maximum at 258 mμ, it sediments at the same rate as S-RNA, and it is no longer present on addition of ribonuclease.

The S-RNA boundary was still visible in the dialyzed supernatant from cell-free extracts after standing at 4°C for 36 hr. Thus it appears that there is no active ribonuclease in the supernatant, after centrifuging the crude cell-free extracts at 100,000 *g* for 120 min.

(n) *Biochemical activity*

The ability of S-RNA to bind amino acids was investigated as follows. S-RNA was incubated with ^{14}C-labelled alanine, leucine and valine in the presence of

Table 3

Combination of S-RNA with amino acids. The complete reaction mixture consisted of 0·8 mg ATP, 0·1 mg $MgCl_2$, 0·05 mg [^{14}C]-L-alanine, [^{14}C]-L-leucine and [^{14}C]-L-valine, 0·1 ml. bacterial extract containing 0·5 mg protein, 0·05 ml. 0·1 M-tris buffer pH 7·3 and S-RNA in a total volume of 0·6 ml. The mixture was incubated at 37°C for 30 min. S-RNA was then precipitated by addition of perchloric acid (final concentration 0·4 M) and washed three times with 5·0 ml. 0·4 M-perchloric acid. The radioactivity of the acid-insoluble material was determined.

	Counts per min in acid-insoluble fraction	Amount of amino acid bound to 1 mg S-RNA
1. Complete reaction mixture + 0·74 mg S-RNA	1052	
2. No ATP + 0·74 mg S-RNA	5	
3. No Mg^{2+} + 0·74 mg S-RNA	21	
4. No extract + 0·74 mg S-RNA	0	
5. No [^{14}C]leucine, no [^{14}C]valine + 0·74 mg S-RNA	398	0·97 μg alanine
6. No [^{14}C]alanine, no [^{14}C]valine + 0·74 mg S-RNA	46	0·26 μg leucine
7. No [^{14}C]alanine, no [^{14}C]leucine + 0·74 mg S-RNA	483	0·52 μg valine
8. No S-RNA	15	
9. Complete reaction mixture + 0·37 mg S-RNA	541	

ATP, Mg^{2+} and a small amount of *E. coli* extract (dialyzed supernatant after centrifuging a crude extract at 100,000 *g* for 120 min), according to Berg & Ofengand (1958). The results of these experiments, given in Table 3, show that (a) in the system

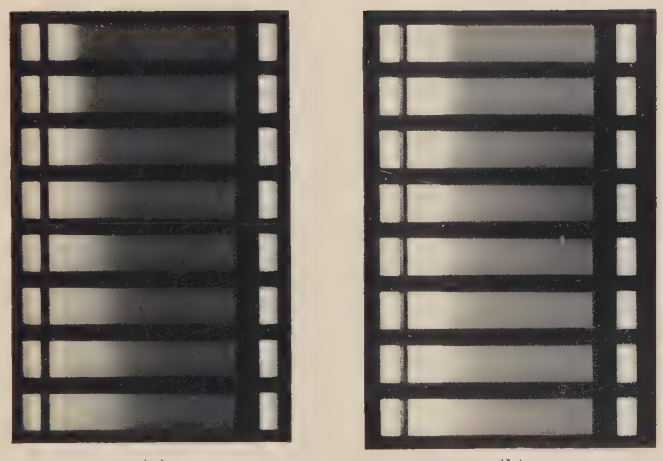

(a) (b)

PLATE III, (a) and (b). Evidence for the presence of free S-RNA in cell-free extracts. PLATE III(a) shows the sedimentation diagram taken with the ultraviolet optics at 8 min intervals, of a dialyzed cell-free extract of *E. coli*. Speed: 59,780 rev/min. The ultraviolet absorbing material sedimented at the rate of 4·02 s.

PLATE III(b): same after addition of 0·5 μg/ml. pancreatic ribonuclease.

[*To face page* 372

used, alanine, leucine and valine became bound to the acid-insoluble fraction; (b) ATP, Mg^{2+}, S-RNA and the extract were all required for this reaction; (c) in the absence of S-RNA the amount of label bound to the acid-insoluble fraction was negligible; (d) the incorporation of any one of the three amino acids occurred independently of that of the others; (e) the amount of amino acids incorporated into the acid-insoluble fraction was proportional to the amount of added S-RNA.

It was found that the amino acids are released from the acid-insoluble fraction on incubation at 37°C, in either 0·01 M-tris pH 8·4 for 30 min, or in 0·01 M-NaOH for 15 min, or in the presence of 0·5 μg/ml. of ribonuclease for 5 min.

These results are similar to those obtained by Berg & Ofengand (1958) with S-RNA from *E. coli*.

4. Discussion

The hypochromicity of S-RNA is similar to that studied by Hall & Doty (1958) and Doty *et al.* (1959) for tobacco mosaic virus and ribonucleoprotein particle RNA. The increase in optical density at 80 to 85°C is the same with S-RNA (22 to 24% increase) as with particulate RNA (Doty *et al.*, 1959), the reactivity with formaldehyde follows the same pattern, and the same changes in optical density are observed in 6 M-urea. Thus the extent of hydrogen bonding in the molecules in salt solutions appears to be similar for the two kinds of RNAs. Doty *et al.* (1959) concluded from the hypochromic effect and simultaneous changes in optical rotation, with tobacco mosaic virus and particulate RNA's as well as with polynucleotides, that in RNA a substantial part of the molecule consists of hydrogen-bonded bases, organized in helical regions. The same conclusion also applies to S-RNA. It is of interest to note that the nucleotide composition of particulate RNA (Spahr & Tissières, 1959) is quite different from that of S-RNA, (Spahr, P. F., 1959, personal communication) and that the latter contains a larger proportion of unusual bases (Dunn, D. B. & Smith, J. D., 1959, personal communication).

The concentration dependence of the sedimentation coefficient is very small when salt is present. A marked increase is obtained when S-RNA is dissolved in distilled water. This, together with the increase in optical density under these conditions, indicated that the molecule, tightly coiled in the presence of salts, extends in water.

It is likely that the secondary structure of S-RNA in the cells is identical to that observed with the isolated substance in salt solution, as S-RNA exists free, i.e. not bound to proteins, in cell-free extracts. Whether this secondary structure confers on the molecule some specificity for the attachment of amino acids, and for the transfer of the latter to ribonucleoprotein particles, remains to be known.

I wish to thank Drs. P. Doty, J. T. Edsall and J. D. Watson for their interest and for helpful discussions, Miss B. R. Hollingworth for diffusion measurements, and Miss C. Launont and Mrs. A. Nevins for technical assistance. This work was supported by a grant from the National Science Foundation.

REFERENCES

Berg, P. & Ofengand, E. J. (1958). *Proc. Nat. Acad. Sci., Wash.* **44**, 78.
Doty, P., Boedtker, H., Fresco, J. R., Haselkorn, R. & Litt, M. (1959). *Proc. Nat. Acad. Sci., Wash.* **45**, 482.
Dryer, R. L., Tammes, A. R. & Routh, J. I. (1957). *J. Biol. Chem.* **225**, 177.

Fiske, C. H. & Subbarow, Y. (1925). *J. Biol. Chem.* **66**, 375.
Fraenkel-Conrat, H. (1954). *Biochim. biophys. Acta*, **15**, 307.
Gornall, A. G., Bardawill, C. T. & David, M. M. (1949). *J. Biol. Chem.* **177**, 751.
Hall, B. D. & Doty, P. (1958). *Microsomal Particles and Protein Synthesis*, p. 27. New York: Pergamon Press.
Hall, B. D. & Doty, P. (1959). *J. Mol. Biol.* **1**, 111.
Hoagland, M. B. (1955). *Biochim. biophys. Acta*, **16**, 288.
Hoagland, M. B., Zamecnik, P. C. & Stephenson, M. L. (1957). *Biochim. biophys. Acta*, **24**, 215.
Hoagland, M. B., Stephenson, M. L., Scott, J. F., Hecht, L. I. & Zamecnik, P. C. (1958). *J. Biol. Chem.* **231**, 241.
Kirby, K. S. (1956). *Biochem. J.* **64**, 405.
Lowry, O. H., Rosebrough, N. J., Farr, A. L. & Randall, R. J. (1951). *J. Biol. Chem.* **193**, 265.
Schachman, H. K. (1957). *Methods in Enzymology*, vol. IV, p. 59. New York: Academic Press.
Scheraga, H. A. & Mandelkorn, L. (1953). *J. Amer. Chem. Soc.* **75**, 179.
Smellie, R. M. S. (1955). *The Nucleic Acids*, vol II, p. 411. New York: Academic Press.
Spahr, P. F. & Tissières, A. (1959). *J. Mol. Biol.* **1**, 237.
Svedberg, T. & Pedersen, K. O. (1940). *The Ultracentrifuge*, p. 5. Oxford: Clarendon Press.
Tissières, A., Watson, J. D., Schlessinger, D. & Hollingworth, B. R. (1959). *J. Mol. Biol.* **1**, 221.
Umbreit, W. W., Burris, R. H. & Stauffer, J. F. (1957). *Manometric Techniques*, p. 273. Minneapolis: Burgess Publishing Co.

J. Mol. Biol. (1959) **1**, 375-378

The Unit Cell and Space Group of Cubic Glucagon

MURRAY VERNON KING†

The Protein Structure Project,‡ Polytechnic Institute of Brooklyn, N.Y., U.S.A.

(*Received 23 September 1959*)

The hyperglycemic pancreatic hormone, glucagon, may be crystallized in cubic crystals showing the form {110}, and having the space group $P2_13$, with $a = 47{\cdot}94$ Å. There are 12 molecules of molecular weight 3,482 in the unit cell. A weight loss of $41 \pm 2{\cdot}5\%$ on drying shows a degree of hydration typical of protein crystals. The crystals could be grown from phosphate buffers, as well as from glycine buffers, as has been reported in the literature.

The space group requires that the molecules be grouped in triads about the three-fold axes. With this principle, and with the assumption that the molecules form unbroken α-helices under the conditions existing in the crystal (as permitted by the amino-acid sequence), a speculative structural model is developed.

1. Introduction

The study of the crystallography of glucagon was undertaken to determine whether this hyperglycemic polypeptide hormone is suitable for detailed crystal structure analysis. The peptide sequence of glucagon is completely known (Bromer, Sinn, Staub, & Behrens, 1956), and indicates a molecular weight of 3,482, comprising 29 amino acid residues in a single chain. This molecular weight is considerably smaller than that of any other protein which has hitherto been studied crystallographically, but is probably sufficiently high for this substance to show structural features characteristic of proteins. Thus, crystalline glucagon may be a uniquely simple type of protein crystal. Further, since the peptide sequence contains neither proline nor cystine, the possibility must be considered that the molecule may form a continuous segment of an α-helix under suitable physico-chemical conditions.

Glucagon was crystallized by Staub, Sinn, & Behrens (1955) from glycine buffers at pH 8·5 to 8·6. The material used in the present study was provided by the courtesy of the Lilly Research Laboratories in the form of a suspension of glucagon crystals of mixed porcine and ovine origin §. Some of this material was subsequently recrystallized from phosphate buffer by a method described below to give the same crystalline form as that occurring in the original suspension. A later batch, of porcine origin, has also been crystallized by this method.

2. Method of Recrystallization

Glucagon crystals were washed several times with distilled water, with the result that they broke down to form a gelatinous mass. This was isolated by centrifugation and lyophilized. From the dried material a 1% solution (w/v) was prepared in 0·2 M-K_3PO_4. The solution was then brought to a composition $[HPO_4^{2-}] : [PO_4^{3-}] = 2 : 1$, by either of two methods:

(1) 40 μl. 1M-KH_2PO_4 was added with stirring to 400 μl. of the glucagon solution.

(2) 80 μl. 2M-K_2HPO_4 was added with stirring to 400 μl. of the glucagon solution.

† *Present address: Orthopedic Research Laboratories, Massachusetts General Hospital, Boston 14, Mass., U.S.A.*

‡ Contribution No. 20.

§ The hormones from these sources have been shown to be chemically identical (Private communication).

In either case, a drop of toluene was added, and the sample was stored in the refrigerator until crystallization occurred.

The results depended sharply on which method was used for adjustment of the pH, even though the final compositions of the solutions were almost identical and the same crystal form was obtained. With method (1), crystallization occurred within a few days, with production of many small crystals (mostly $<0{\cdot}1$ mm in diameter, but with a few larger crystals). With method (2), crystallization was delayed for some weeks or months, but larger crystals were produced. After some repetitions of method (2), more prompt crystallization was observed, probably because of contamination of the laboratory with crystal nuclei. Apparently, the prompt crystallization obtained by method (1) is due to formation of nuclei in the region of local acid excess surrounding each drop of KH_2PO_4 solution. Indeed, microscopic crystals are obtained if the sample is not stirred promptly to destroy the local excess of acid.

3. X-Ray Diffraction Data

The crystals, which show dodecahedral morphology as noted by Staub *et al.* (1955), were mounted wet, in capillaries, by the method described by the author (King, 1954). The mounting was conducted in the cold because of the solubility of the crystals at room temperature, although the crystals were stable at room temperature after mounting. X-ray diffraction data were obtained on the Geiger counter spectrometer by the method of Furnas & Harker (1955) and on the Buerger precession camera. Crystals from the original sample showed a cubic cell with $a = 47{\cdot}94$ Å. The spectrometer data indicated space group $P2_13$, which was verified by precession photographs taken both of crystals from the original sample and of those grown from phosphate buffers. The photographs showed absence of the odd orders along all three cubic axes, and showed the appropriate symmetries about the [100], [110] and [111] axes.

Since the space group $P2_13$ requires 12 asymmetric units per unit cell, 12 or 24 molecules of glucagon could be contained within the cell of volume 110,200 Å^3 with reasonable values for the density. However, measurements of the weight loss of glucagon crystals on drying in air showed an average loss of 41 $\pm$ 2·5%. This indicates that the crystals are highly hydrated, as protein crystals are in general, and that the number of molecules in the unit cell must be 12.

A comparison of the glucagon crystals with other proteins and simple peptides also shows the porous nature of the glucagon crystals. In the absence of accurate data on the water content, the volume per molecular weight unit of protein or peptide (V/mwu) may serve as a parameter indicating the looseness of packing of such crystals. This parameter is primarily sensitive to the volume of liquid included within the crystal, although it is also sensitive to the partial specific volume of the protein or peptide. For cubic glucagon, $V/mwu = 2{\cdot}64$ Å^3, while for modification II of bovine pancreatic ribonuclease the value of V/mwu is 2·18 Å^3†, and for human serum albumin, $V/mwu = 3{\cdot}06$ Å^3‡. On the other hand, for a simple peptide with a low degree of hydration, L-leucyl-L-prolylglycine, $V/mwu = 1{\cdot}325$ Å^3§.

X-ray diffraction spectra were observed with spacings as low as 2·5 Å. This degree of resolution does not permit the finding of atomic positions from the diffraction data, but should permit the search for features on a larger scale, such as helical chain configurations.

†Calculated from the data of King, Magdoff, Adelman & Harker (1956).
‡Calculated from the data of Low (1952).
§Calculated from the data of Leung & Marsh (1958).

4. A Speculative Structural Model

The space group $P2_13$ is based essentially on the arrangement of triads of objects about the threefold axes in a packing based on the sub-group $P2_12_12_1$. This packing need not imply that the triads are chemical trimers. In each triad of glucagon molecules, like residues are found at the same level normal to the triad axis. Hence, it is unlikely that the triads consist of three elongated molecules parallel to the axis, for then side chains of like charge would always be juxtaposed, with the result of maximum electrostatic repulsion. However, triads of rod-like molecules in skew orientations are quite possible. In glucagon, many of the charged side chains of both charges are concentrated in a portion near the middle of the chain, as indicated by parentheses in the sequence:

His^{++}. Ser. Glu(NH_2). Gly. Thr. Phe. Thr. Ser. (Asp$^-$. Tyr. Ser. Lys$^+$. Tyr. Leu. Asp$^-$. Ser. Arg$^+$. Arg$^+$. Ala. Glu(NH_2). Asp$^-$.) Phe. Val. Glu(NH_2). Try. Leu. Met. Asp(NH_2). Thr$^-$.

This suggests that, if the molecules are rod-like (e.g., α-helices), a packing that would concentrate both plus and minus charges within a small region of space would be

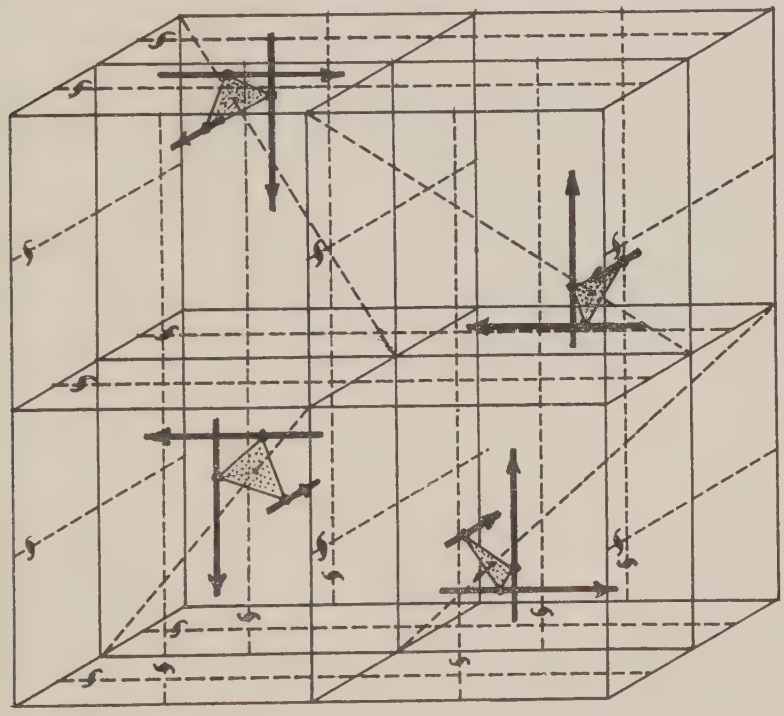

FIG. 1. Symmetry elements and possible arrangement of molecules in space group $P2_13$.

realized if each of the triads consisted of three skew rods in contact near their midpoints in the manner of a three-legged campstool. A diagram showing such an arrangement in relation to the symmetry elements of the space group $P2_13$ is given in Fig. 1, where the rods are arbitrarily taken at right angles to one another. If the molecules are assumed to be α-helices, their lengths would be about 43 Å, or slightly less than the unit cell edge. Reference to Fig. 1 shows that such a packing of helices is feasible, although nothing can be said of the angle of tilt of the rods, or of the positions of

the triads along the axes, while the general model is yet unproven. A structure of this type still requires the close approach of some of the like charges. However, it also permits the close approach of unlike charges, such as to stabilize the structure.

The question remains whether glucagon actually exists in a helical configuration in the crystal. Kay & Marsh (1959) have shown by optical studies that glucagon in glycine buffer, pH 10·4, is largely in a random-coil configuration. At this pH, the molecule has an excess of 1 to 2 negative charges. Optical study of whether the molecule goes over into the helical form in the isoelectric range (7·5 to 8·5, according to Staub *et al.* (1955)) is precluded by the low isoelectric solubility. However, further study of the crystal structure may throw light on this point.

The author wishes to thank Mr. Herbert Kwasnik and Mr. Edward J. Mordia for valuable assistance, the Lilly Research Laboratories for giving the glucagon on which the work was done, and the following organizations for their financial support of the Protein Structure Project which made this contribution possible: The Dean Langmuir Foundation, The Rockefeller Foundation, The Damon Runyon Memorial Fund, The New York Foundation, The International Business Machines Corporation, The Polytechnic Institute of Brooklyn.

REFERENCES

Bromer, W. W., Sinn, L. G., Staub, A. & Behrens, O. K. (1956). *J. Amer. Chem. Soc.* **78**, 3858. (See also *ibid.* **79**, 2794, 2798, 2801, 2805, 2807 (1957).)
Furnas, T. C., Jr. & Harker, D. (1955). *Rev. Sci. Instrum.* **26**, 449.
Kay, C. M. & Marsh, M. M. (1959). *Biochim. biophys. Acta*, **33**, 251.
King, M. V. (1954). *Acta Cryst.* **7**, 601.
King, M. V., Magdoff, B. S., Adelman, M. B. & Harker, D. (1956). *Acta Cryst.* **9**, 460.
Leung, Y. C. & Marsh, R. E. (1958). *Acta Cryst.* **11**, 17.
Low, B. W. (1952). *J. Amer. Chem. Soc.* **74**, 4830.
Staub, A., Sinn, L. & Behrens, O. K. (1955). *J. Biol. Chem.* **214**, 619.

J. Mol. Biol. (1959), **1**, 379-386.

Density Alterations Associated with Transducing Ability in the Bacteriophage Lambda†

J. Weigle and Matthew Meselson

Division of Biology, Norman W. Church Laboratory for Chemical Biology and Gates and Crellin‡ Laboratories of Chemistry, California Institute of Technology, Pasadena, Cal., U.S.A.

and

Kenneth Paigen

Roswell Park Memorial Institute, Buffalo, N.Y., U.S.A.

(*Received 2 October 1959*)

The transducing variant of the bacteriophage λ is thought to arise by a double crossover in which a section of the normal chromosome is exchanged for a region of the bacterial chromosome containing galactose fermentation markers. If the exchange were unequal, the resulting transducing phages should have an altered DNA content which might be detected as a modification of the density of the phage particle. An examination of ten independently arising populations of transducing phages showed that each had a different but essentially uniform density. In contrast, the non transducing phage contained in these lysates possessed a constant density. The density of a transducing phage was stable to a cycle of lysogenization, prophage replication and multiplication following induction, as well as to genetic interactions with normal λ and with the bacterial chromosome.

Assuming the observed density changes to be due to changes in DNA content, it was calculated that the maximum change corresponded to 10^7 mol wt units, or $1{\cdot}5 \times 10^4$ nucleotide pairs, and the smallest to 800 nucleotide pairs.

It is proposed that the unequal exchanges giving rise to the density alterations are the result of poor homology and incomplete pairing between the *Gal* region of the bacterial chromosome and the region of λ which is deleted.

1. Introduction

The bacterial strain *E. coli* K12, lysogenic for the bacteriophage λ, liberates upon either induced or spontaneous lysis a population of phages which contain one exceptional phage among approximately 10^4 "ordinary" λ. The exceptional quality of this phage is its transducing ability: it carries genes for galactose fermentation (*Gal*) from the original host bacterium into the bacterium it subsequently lysogenizes. Only *Gal* markers, which are closely linked to the prophage attachment site of λ, are known to be transduced by λ. Lysates from cells lysogenic for ordinary λ and containing this low proportion of transducing particles are called LFT (low frequency transducing). (Morse, Lederberg & Lederberg, 1956.)

Transducing λ is defective in the sense that it cannot multiply in the absence of ordinary λ and it is thus called λ*dg* (λ defective, galactose) (see Arber, Kellenberger & Weigle, 1957; Campbell, 1957; Arber, 1958). It can, however, establish itself as a prophage and be replicated as such when the bacterium multiplies. If ordinary λ is

†Aided by grants from the National Foundation and the National Institutes of Health.
‡Contribution No. 2463.

present in a cell together with *λdg*, as in the case of cells lysogenic for both *λ* and *λdg*, induction yields a lysate containing an equal proportion of both phages. Such lysates are called HFT (high frequency transducing).

The original event which gives rise to *λdg* may be thought of as a double crossover in which a piece of the *λ* chromosome has been exchanged for a section of the bacterial chromosome containing the *Gal* genes. In accord with this view the transducing phage is known from genetic experiments (Arber, 1958) not only to carry the *Gal* genes of the bacterium, but also to lack approximately one-fourth of the mapped length of the ordinary *λ* chromosome.

One might ask whether this exchange is exactly reciprocal, and thus whether *λdg* contains the same amount of genetic material as *λ*. A change in the quantity of genetic material might result in an altered ratio of DNA to protein and might thereby alter the density of the phage. To study this question we have investigated the density of phages from HFT lysates, assuming them to be the same as those from the LFT from which they were derived. The method of equilibrium density-gradient centrifugation (Meselson, Stahl & Vinograd, 1957) was used in these studies. It was found that the density of ordinary *λ* is constant whereas, *mirabile dictu*, the density of the *λdg* of each independent HFT has a characteristic and unique value different from that of *λ*. These densities are genetically stable. It is possible to explain the density changes as a consequence of the original event giving rise to *λdg*.

2. Material and Methods

(a) *Bacterial strains*

The bacterial strains were lysogenic 112–12 (Wollman, 1953) and a series of strains derived from Lederberg's 3110 (*F*$^-$, *Gal*$^+$, prototroph) either by lysogenization or by transduction of the *Gal* markers 1 and 2 (Morse *et al.*, 1956). The latter strains were used for most of the experiments described and are designated by their galactose markers and any prophage they carry. For example, *Gal* 1$^+$ 2$^+$ (*λ*) is the original strain 3110 lysogenic for *λ*, while *Gal* 1$^-$ 2$^-$ (*λ*) (*λdg Gal* 1$^+$ 2$^+$) is a strain having the 1$^-$ and 2$^-$ *Gal* markers, and is lysogenic for *λ* and for *λdg* carrying the *Gal* markers 1$^+$ and 2$^+$.

(b) *Bacteriophage*

Phage *λref* is the reference type of Kaiser (1955). Phage *λh* was derived from *λref* and has extended host range. Phage *λvir* is the virulent mutant described by Lederberg & Lederberg (1953). Phage *λvir h* was obtained from a cross of *λh* by *λvir*.

The techniques for assaying plaque-forming particles have been described by Adams (1950) and those for the assay of transducing phages and for u.v. induction have been given by Arber (1958).

(c) *Mèdia*

Growth medium was either tryptone broth (10 g Difco tryptone, 5 g NaCl, 1 l. H_2O) or K medium (100 ml. of double strength M9, 100 ml. of 3% casamino acids treated with decolorizing charcoal to remove u.v. absorbing material, 0·1 g NaCl, 0·06 g $MgSO_4$ and 0·4 g glucose). Suspension medium contained 6 ml. M-tris (2-amino-2-hydroxymethyl-propane-1:3-diol) at pH 7·5, 0·12 g $MgSO_4$, 4 g NaCl, 0·05 g gelatin, and 1 l. H_2O. To distinguish *Gal*$^+$ from *Gal*$^-$ colonies, tetrazolium triphenyl chloride was used as a fermentation indicator in a plating medium of the following composition: 15 g agar, 10 g tryptone, 5 g NaCl, 0·5 g tetrazolium triphenyl chloride, 4 g galactose, and 1 l. H_2O.

Cesium chloride obtained from the American Potash Company was recrystallized from water and treated in solution with decolorizing charcoal to remove u.v. absorbing material.

(d) *Preparation of purified phage*

Lysogenic bacteria were grown in K medium to a titer of about 4×10^8 per ml. The cultures were induced in samples 2 mm deep and were allowed to lyse at 37°C with aeration. Several drops of chloroform were added and the suspensions were centrifuged at low speed before being filtered through a No. 9 candle. The filtrates contained 2 to 4×10^{10} plaque-forming particles per ml. They were centrifuged for 90 min at 30,000 rev/min in a No. 30 Spinco preparative ultracentrifuge rotor and the pellet was resuspended by standing overnight in suspension medium. Another low speed centrifugation brought down debris which had passed the filter.

(e) *Analytical density-gradient centrifugation*

A portion of purified phage was added to a 57% (w/w) stock solution of CsCl buffered at pH 8·0 with 0·015 M-tris buffer to give a final concentration of 1 to 2×10^{10} plaque-forming particles per ml. after the density of the sample had been adjusted to 1·50 ± 0·01 g cm^{-3} by the addition of water. The density at 20°C was calculated according to the relation

$$\sigma^{20} = 10{\cdot}860\ n_D^{25} - 13{\cdot}500$$

where n_D^{25} is the index of refraction of the solution for sodium light at 25°C determined in an Abbé refractometer. A 0·70 ml. portion of the adjusted phage suspension was then placed in a cell equipped with a plastic (Kel-F) centerpiece and was centrifuged in a Spinco model E analytical ultracentrifuge at 27,690 rev/min at 20°C.

The various phages move through the CsCl concentration and density gradient, which forms during the first few hours of centrifugation, to the region at which their buoyant density equals that of the solution, thereby forming bands. Equilibrium is closely approached in 10 hr, whereupon ultraviolet absorption photographs are taken.

The determination of the relative buoyant densities of banded phage was greatly facilitated by the addition to each sample of a density reference material. This was a dense λ variant obtained from cells of the lysogenized K12 strain 112–12 whose density was increased by growth in a medium containing ^{15}N. This phage has a buoyant density in CsCl solution of 1·525 g cm^{-3}, considerably greater than that of any other λ phage we have studied.

(f) *Preparative density-gradient centrifugation*

To recover the phages from each band separately, CsCl phage suspensions prepared as described above were centrifuged in "lusteroid" tubes in a Spinco SW39 swinging bucket rotor at 22,000 rev/min. After 16 hr, equilibrium is closely approached and the rotor was allowed to come to rest without braking. The plastic tube was withdrawn and its bottom was pierced with a fine needle. Successive emergent drops were collected for subsequent examination. A 3 ml. sample yielded approximately 120 drops, each drop comprising a successive density layer in the gradient. This technique permits even a single virus particle to be isolated and characterized biologically.

3. Results

(a) *Centrifugation of ordinary lambda*

The phage λ formed a single sharp band at equilibrium in a CsCl density gradient as shown in Plate I. The buoyant density of λ in CsCl solution at 20°C calculated from the position of the band, the value of the density gradient and the initial density of the suspension is 1·508 g cm^{-3}. This value is close to the average of the buoyant density of DNA (1·7 g cm^{-3}) and of protein (1·3 g cm^{-3}), suggesting that the virus contains approximately equal volumes of each.

With one exception, the densities of mutants of non-transducing λ were indistinguishable even when the viruses were grown under widely different conditions.

The various preparations of phages examined were obtained:

1. by the induction of different strains of K12 lysogenic for *λref*.
2. by the induction of *Gal*⁻ doubly lysogenic for *λref* and *λh*.
3. by infection of *Gal*⁺ with *λvir h*.
4. by infection of strain C, showing host controlled variation, with *λvir h*.
5. by induction of lysogenic bacteria such as *Gal* 1⁻ 2⁺ (λ) (*λdg Gal* 1⁺ 2⁻) or *Gal* 1⁻ 2⁻ (λ) (*λdg Gal* 1⁺ 2⁺).
6. by induction of the defective lysogenic *Gal* 1 · 2⁺ (*λdg Gal* 1⁻ 2⁺) and superinfection with *λref*.
7. by infection of *Gal*⁺ with four independent spontaneous clear mutants of *λref*.

The exceptional phages were obtained by induction of the lysogenic strain 112–12. These phages have a uniform density greater than that of any other λ. Grown in ^{15}N

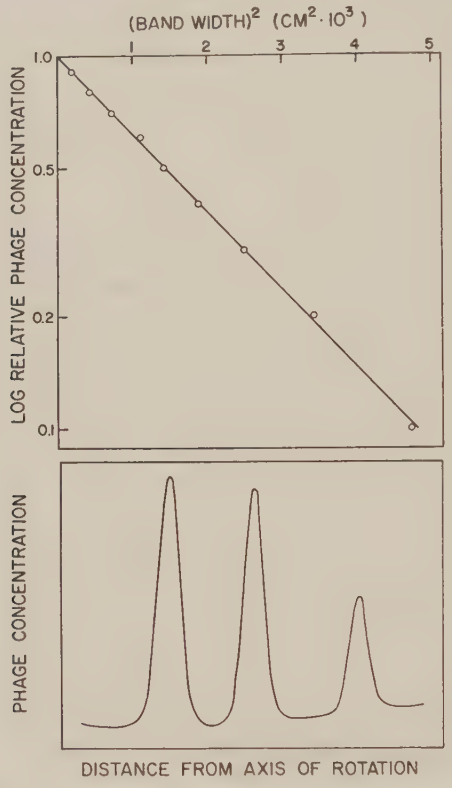

FIG. 1. Photometer tracing of Plate I. The Gaussian character of the center band is shown in the upper portion in which the logarithm of the concentration is plotted as ordinate against the square of the band width for ordinary λ.

medium to increase their density, they have been used, as mentioned above, as density reference material.†

The concentration distribution of λ and *λdg* in a band is Gaussian within experimental error as may be seen in Fig. 1. If all the phages had the same density the width of the band, due to thermal motion, would indicate a value of $3{\cdot}8 \times 10^7$ for their molecular weight. This value is in disagreement with the approximate value of $1{\cdot}4 \times 10^8$ which may be calculated from the inactivation cross section or phosphorus content per

†Subsequent experiments done in collaboration with Mrs. G. Kellenberger and Mrs. M. Zichichi have shown that the λ mutants *c mi*, *c m6*, *m5 co* of Kaiser (1955) are much less dense than *λref*.

PLATE I. Photograph by u.v. absorption of the centrifuge cell after sedimentation equilibrium has been closely approached (21,740 rev/min at 20°C for 48 hr). The initial density of the suspension was 1·522 g cm^{-3} and it contained ordinary λ (left band), λdg (center band) and λ dense grown in ^{15}N (right band).

[*To face page* 382

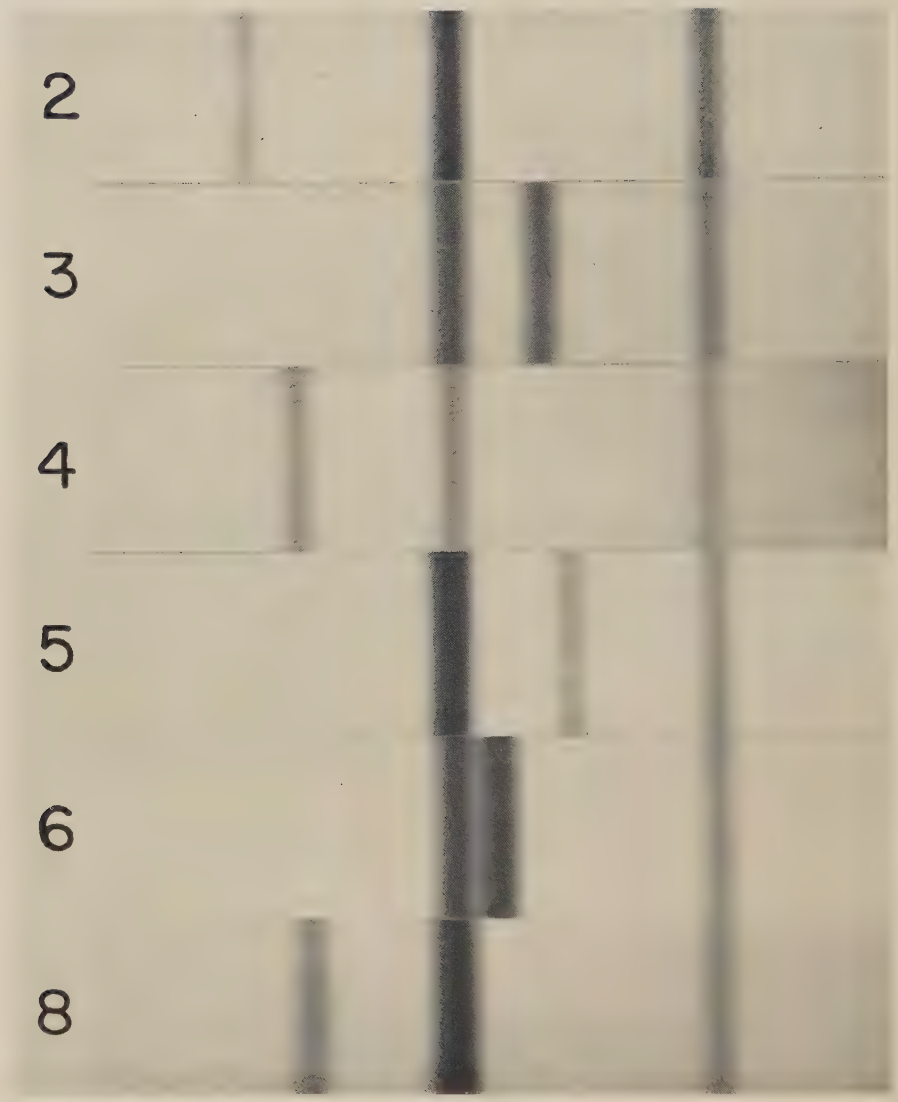

PLATE II. Photographs by u.v. absorption of the centrifuge cell after the phage distribution has reached approximate equilibrium (27,690 rev/min at 20°C for 12 hr). The cell contained different independent HFT lysates and some λ dense *vir h* grown in ^{15}N. The photographs have been aligned using this phage as density marker; it forms the band on the extreme right in each photograph. It can be seen that each independent HFT lysate contains two bands. One of these bands has the density of ordinary λ and the other band (the transducing phage) has a density which is either greater or less than that of ordinary λ. The numbers appearing on the left of each photograph refer to the HFT's listed in Fig. 2.

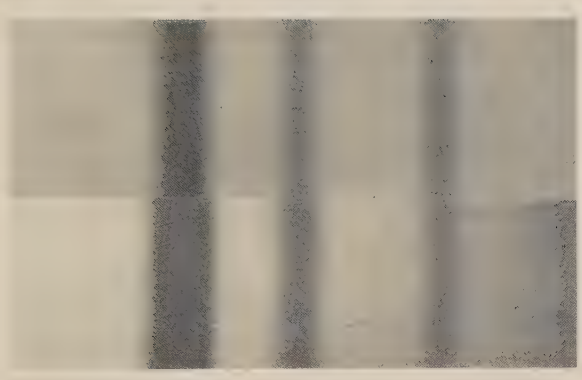

PLATE III. Photographs by u.v. absorption of the density-gradient distribution of the HFT lysate No. 5 and of the HFT lysate of an induced strain transduced by the *λdg* of lysate No. 5. It is seen that the density of *λdg* has not been altered. Upper photograph: original lysate No. 5. lower photograph: lysate of strain transduced by *λdg* of No. 5.

plaque-forming unit (Stent & Fuerst, 1955) when taken together with the percentage of DNA in the phage. It would thus appear that λ phages are not uniform with respect to density in cesium chloride solution. A population of particles uniform with respect to molecular weight but heterogeneous with respect to density forms a Gaussian band if the density distribution is itself Gaussian (Baldwin, 1959). One may calculate that a standard deviation of only 0·0003 g cm^{-3}, that is 0·02% of the density of λ, would account for the low apparent molecular weight obtained from the observed band width.

(b) *Centrifugation of transducing λdg*

To insure that each HFT lysate studied was the product of an independent genetic event the following procedure was employed:

A culture of *Gal* 1^{+}2^{+}(λ) derived from a single cell was streaked out; ten single colonies were picked and grown into ten cultures. Each culture was induced and the resulting LFT lysate was used to infect sensitive *Gal* 1^{-}2^{-} bacteria at a multiplicity of approximately three phages per bacterium. Each of the ten infected suspensions was plated on indicator plates and from each plate a single colony of transduced cells was selected. These *Gal* 1^{-}2^{-}(λ) (λ*dg Gal* 1^{+}2^{+}) colonies were purified twice by streaking and then were grown to yield ten separate cultures. Upon induction each gave an HFT lysate. The phages of these HFT lysates were purified and examined by density-gradient centrifugation.

The results of some of the ten independent density determinations are presented in Plate II. The density differences between ordinary λ and the ten independent λ*dg*'s are shown in Fig. 2. The separation of the bands of λ and λ*dg* from another HFT

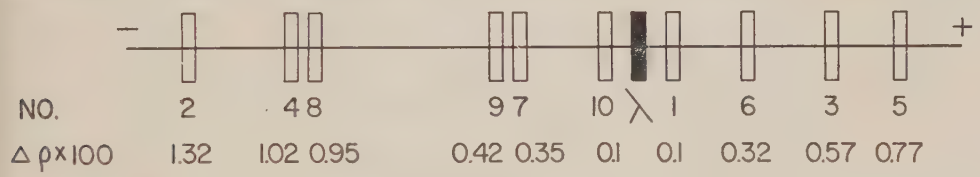

Fig. 2. Densities of ten independent λ*dg*'s. The number given identifies each of the ten independent isolates of λ*dg*. For each of them the difference in density from that of ordinary λ is shown multiplied by 10^2.

lysate was carried out by centrifuging a suspension of phage in CsCl solution in the swinging bucket rotor as described in the section on methods. Fig. 3 shows the titer of plaque-forming and transducing phages as a function of distance along the centrifuge tube as expressed by the drop number. The difference in density between λ and λ*dg* obtained in this experiment was 0·0052 g cm^{-3}, equal, within the experimental error, to that found from centrifugation in the analytical machine (0·0060 g cm^{-3}).

Similar separations of the bands of λ and λ*dg* were performed for a fairly large number HFT lysates.

(c) *The association of altered density with transducing ability*

From Fig. 3 it may be seen that no λ*dg* with normal density was found in an HFT lysate. It thus appears that the characteristics of density and transducing ability have not reassorted during multiplication of λ*dg* in the presence of ordinary λ, even though genetic interactions have been shown to occur (Arber, 1958).

To test the stability of the density of *λdg* upon relysogenization followed by prophage replication and then induction with subsequent phage multiplication, the following experiment was performed. The HFT number 5 was used to infect a sensitive *Gal* 1⁻2⁻ culture at multiplicity of 4 plaque-forming phages per bacterium. At this multiplicity all the transduced cells carry both *λ* and *λdg* prophages. A single colony of transduced cells was selected and from this a pure clone of *Gal*⁺ cells was obtained. A culture of these cells was grown, induced, allowed to lyse, and the phage was purified and examined in a CsCl density gradient. Plate III shows the density gradient photograph obtained during centrifugation of this lysate together with the photograph of the banded phage of the parent number 5 lysate. It can be seen that the density of the phages in the new lysate is the same as in the original HFT No. 5.

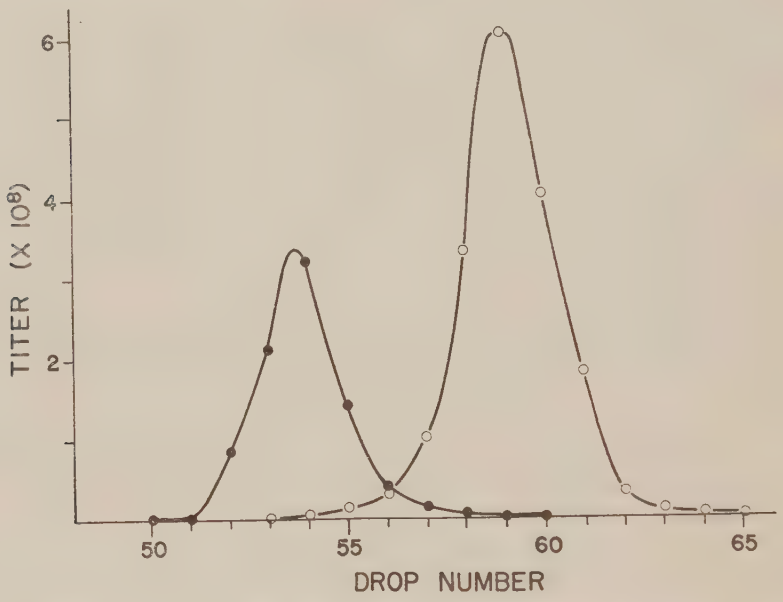

FIG. 3. An HFT lysate was centrifuged in the swinging bucket rotor as described under Methods, and the droplets were collected in separate tubes containing 1 ml. of suspension medium. Each tube was assayed for plaque-forming phages and for transducing phages. Increasing tube number represents decreasing density. Filled circles: transducing phages; empty circles: plaque-forming phages.

The density of *λdg* appears also to remain unchanged after genetic recombination with the bacterial chromosome in the *Gal* region, as shown by the following experiment. Sensitive *Gal* 1⁻2⁺ bacteria were infected with an HFT containing *λdg Gal* 1⁻2⁺ phages of known density. A colony from a cell *Gal* 1⁻2⁺(*λ*) (*λdg Gal* 1⁺2⁻) was picked, purified and grown into a culture. From this culture a strain *Gal* 1⁻2⁺(*λ*) (*λdg Gal* 1⁻2⁺) was selected (Morse *et al.*, 1956). Density-gradient centrifugation of the HFT lysate of this strain showed that its *λdg* had a density not detectably different from that of the *λdg Gal* 1⁺2⁺ which had been used for the original transduction.

4. Discussion

Let us summarize the main features of the alterations in density of transducing *λ*. Induction of a bacterial culture doubly lysogenic for normal *λ* and any one of ten

transducing λ of independent origin yields a population of phage particles which are genetically of two types, plaque-forming and transducing λ; and physically of two types, those having the density of normal λ and those having a new characteristic density. Plaque-forming λ is identified with the particles of normal density, and transducing λ with those particles showing the new density. No reassortment of density and transducing ability is observed. Each of ten independent *λdg* has its own characteristic density which is genetically stable and is not altered by a cycle of growth involving transduction and multiplication. Finally, an exchange of galactose markers between a transducing phage and its host cell had no apparent effect on the characteristic density of the transducing phage.

These facts may be accounted for simply by the following model in which no distinction is made between the structure of the original transducing phage from an LFT and that of the *λdg* in the HFT derived from it. The prophage λ has a region, extending on both sides of the *h* marker, which is sufficiently similar to the region of the bacterial chromosome surrounding the *Gal* markers to permit occasional pairing between the two chromosomes. Upon rare occasions a double crossover occurs and the *Gal* markers are integrated into the prophage chromosome where they replace that part of the prophage genome surrounding the *h* region.

This event renders the prophage defective through its loss of genes essential for independent multiplication, but able to transduce through its acquisition of the *Gal* markers. Because the transducing phage chromosome carries a segment strictly homologous to a part of the bacterial chromosome, genetic exchange at normal crossover frequencies is now possible in the *Gal* region between transducing phage and bacterium, and outside the *Gal* region between transducing and normal phages.

The region transferred from the bacterial chromosome includes genetic determinants for the density of *λdg*. The altered density of transducing λ could result from changes in the intrinsic densities or relative amounts of DNA, protein, or other possible viral constituents or from changes in packing or solvation. None of these possibilities is exclusive of the others and direct experimentation alone can ultimately decide among them.

A simple and appealing hypothesis is that the genetic determinant of density and the physical factor responsible for the determination of density are in fact identical, namely the quantity of DNA per phage. This assumption fits the proposed model if the chromosomal segments lost by the phage and acquired from the bacterium are of unequal size. The *λdg* chromosome would then differ in size from the original λ chromosome, and if replicated as such would give rise to a genetically stable population of phages of a new density. Since the genetic exchange in which *λdg* arises might involve a bacterial segment either greater or smaller than that deleted from the phage, the transducing phage may be either more or less dense than ordinary λ.

The absence of a double occurrence of a given density among the various independently arisen transducing phages implies that the possible number of unique exchanges between phage and bacterium must be much larger than the number of cases studied.

As this model suggests, the determinants of altered density are not affected when the transducing prophage exchanges homologous *Gal* markers by normal recombination with the bacterium nor are they ever a part of a plaque-forming non-transducing phage.

It is unlikely that changes in elements physically unlinked to DNA are responsible for the density changes since no phenotypic mixing was observed between the genetic

determinants of density and the density itself. Thus, no transducing phages of normal density or active phages of a typical density were found.

To estimate the increment in density corresponding to a change in DNA content by a fraction α from that present in ordinary λ, we assume first that the volume and mass of phage material is increased or decreased by the volume and mass of the DNA added or subtracted, and, second, that the partial specific volume of phage DNA in cesium chloride solution is independent of the particular phage from which it might be isolated. It follows that the change $\Delta\rho$ in density of the phage is given by

$$\Delta\rho = \rho_0 \alpha \frac{F_m - F_v}{1 + \alpha F_v} \tag{1}$$

where F_m and F_v are respectively the mass and volume fraction of DNA in ordinary λ with buoyant density ρ_0. The measured value for ρ_0 is 1·51 g cm^{-3}; for λ DNA the density is 1·71 g cm^{-3}, and we take the value 1·30 g cm^{-3} for protein. Then F_m and F_v are found to be 0·57 and 0·50 respectively and equation (1) becomes

$$\Delta\rho = \frac{0{\cdot}21\,\alpha}{2 + \alpha} \cong 0{\cdot}10\,\alpha \tag{2}$$

Accordingly, the least dense λdg has 14% less DNA than λ and the most dense contains 8% more. If we take the total DNA content of the virus to be 7×10^7 molecular weight units (MWU) (Stent & Fuerst, 1955), then the greatest alteration entails a loss of about 10^7 MWU. The smallest density differences observed between pairs of λdg correspond to a DNA increment of 5×10^7 MWU, about 800 nucleotide pairs. If the amounts of DNA which are gained or lost in the formation of λdg possess a common denominator, this elementary unit cannot be larger than 5×10^5 MWU.

Unequal genetic exchanges of the type described here seem to take place only during the original event leading to the formation of transducing phages. Thus genetic exchanges within the *Gal* region between transducing phage and bacterial chromosome, between normal and transducing phage outside the *Gal* region, and among ordinary λ during multiplication in induced cultures of doubly lysogenic cells, all had no demonstrable effect on the density of the participating phages. It is possible that the occurrence of unequal genetic exchange is a consequence of incomplete pairing between partially homologous chromosomes.

One must remember that the model described above has not been demonstrated to be correct. The possibilities that the density differences between different lambda phages are due to changes in their protein coat, or to changes in both the DNA and the protein components of the particles, are being tested.

REFERENCES

Adams, M. H. (1950). *Methods of study of bacterial viruses*, in *Methods in Medical Research*, Vol. 2, pp. 1–73. Chicago.
Arber, W., Kellenberger, G. & Weigle, J. (1957). *Schweiz. Z. Allg. Path.* **20**, 659.
Arber, W. (1958). *Arch. Sci. Phys. Nat.* **11**, 259.
Baldwin, R. L. (1959). *Proc. Nat. Acad. Sci., Wash.* **45**, 939.
Campbell, A. (1958). *Virology*, **4**, 366.
Kaiser, A. D. (1955). *Virology*, **1**, 424.
Lederberg, E. M. & Lederberg, J. (1953). *Genetics*, **38**, 51.
Meselson, M., Stahl, F. & Vinograd, J. (1957). *Proc. Nat. Acad. Sci., Wash.* **43**, 581.
Morse, M. L., Lederberg, J. & Lederberg, E. M. (1956). *Genetics*, **41**, 142.
Stent, G. S. & Fuerst, C. R. (1955). *J. Gen. Physiol.* **38**, 441.
Wollman, E. L. (1953). *Ann. Inst. Pasteur*, **84**, 281.

J. Mol. Biol. (1959) **1**, 387-397

Molecular Organisation in Feather Keratin

R. D. B. Fraser and T. P. MacRae

Division of Protein Chemistry, Wool Research Laboratories, C.S.I.R.O., Parkville N.2 (Melbourne), Victoria, Australia.

(*Received 8 June 1959, and in revised form 6 October 1959*)

The molecular organisation in the fibrous protein feather keratin has been investigated by studying the effect of reaction with heavy atoms and various swelling agents on the X-ray diffraction pattern. Considerable variations in the intensities of the low angle reflections were observed after the deposition of silver, mercury and osmium in the structure, and their implication is discussed in relation to the organisation of the polypeptide chains into sheets. In addition X-ray diagrams have been obtained from films cast from aqueous dispersions of reduced or oxidised feather keratin, which show spontaneous orientation and retain many of the diffraction properties of the original material. A heuristic model based on an orthogonal unit cell of dimensions $34 \times 95 \times 4{\cdot}7$ Å which contains one particle of molecular weight $\sim$ 10,000 is proposed to account for the main features of the low-angle diffraction pattern.

1. Introduction

It is immediately apparent from the X-ray diffraction diagram yielded by feather rachis that the structure is one of considerable complexity and it is doubtful whether the large scale features of the structure can be deduced by trial and error methods using scale models of the polypeptide chain. On the other hand a direct analysis of the intensities of the X-ray reflections using the methods developed for crystals appears equally unpromising. However, as in the case of α-keratin, there are certain broad features of the diffraction pattern which may be attributed to the groups of polypeptide chains which constitute the fibrous element of the structure and others which are associated with the mode of packing of these elements.

It has been found that these features of the diffraction pattern can be modified by combining heavy atoms with the structure, or by treatment with swelling agents, and an analysis of these modifications is given in the present communication.

2. Experimental

A Hilger micro-focus X-ray unit producing Cu Kα radiation was used in conjunction with a micro-camera capable of resolving spacings up to 50 Å. In order to observe the effects of the heavy-atom treatments at higher resolution, certain of the diffraction photographs were repeated using a camera capable of resolving 200 Å.

Diffraction diagrams of feather rachis in water, *o*-chlorophenol, glacial acetic acid, and 98% formic acid were obtained with the specimen completely immersed in a sealed thin-walled Pyrex capillary. All other specimens were mounted in a continuous stream of hydrogen at about 2% r.h.

Films were cast from dispersions of feather rachis prepared by the method described by O'Donnell & Thompson (1959) for the performic oxidation of wool. Other films were prepared from dispersions obtained by reducing feather rachis at pH 11 for 18 hr in 0·1 M-sodium thioglycollate at 4°C, filtering and substituting the filtrate with iodoacetate at pH 8·5. The solution was dialysed for 2 days and concentrated down in the dialysis bag before casting the film.

Other treatments of feather rachis in solutions containing heavy atoms are summarised in Table 1. Optical transforms of trial structures were obtained in the manner described

Table 1

Treatment	Concentration	Time (days)	Remarks
Mercuric acetate	1% in 1% acetic acid	1	
Silver nitrate	1%	4	Treatment carried out in the dark.
Osmium tetroxide	2%	4	Further specimen reduced in 0·1 M–sodium thioglycollate for 2 days prior to treatment.
Uranyl acetate	1%	1	Little effect on diagram except alteration in profile and intensity of 24 Å meridional reflection.
Cupric acetate	1% in 1% acetic acid	1	
Lead acetate	1%	1	
Iodine	0·1 N in KI and sodium borate	1	Method of Richards & Speakman (1955).

by Elliott & Malcolm (1958), to whom the authors are indebted for making the diffractometer available for the present investigation.

3. The Diffraction Pattern of Feather Rachis

A fairly complete description of the diffraction pattern yielded by feather rachis has been given by Bear (1944) and Bear & Rugo (1951) and some points made by

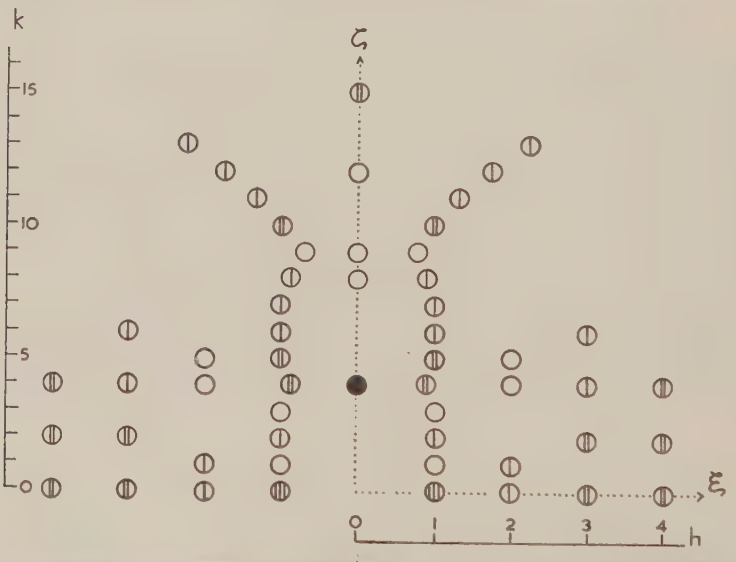

Fig. 1. X-ray diffraction diagram of dry feather rachis plotted in terms of the reciprocal space co-ordinates ζ and ξ (Å $^{-1}$). The layer lines (k) are indexed on a 95 Å repeat of structure parallel to the fibre axis, and the row lines (h) are indexed on a 34 Å repeat of structure perpendicular to this direction. Relative intensities are indicated by ● v. strong, ◍ strong, ◍ medium, ⓘ weak, ○ v. weak.

these authors are, of necessity, reiterated in the present discussion. When plotted in reciprocal space coordinates ζ and ξ most of the reflections lie on a set of equispaced planes perpendicular to b^*. These reflections are depicted diagrammatically in Fig. 1 and the planes are assigned an index k appropriate to a 95 Å repeat of structure in the direction of the b or fibre axis.

(a) *Meridional reflections*

The first three orders of the 95 Å repeat are absent on the meridian but the fourth is extremely intense, so that in axial projection the structure must have a prominent periodicity of about 24 Å in the distribution of electron density. In the present series of experiments which included deposition of heavy metals, treatment with swelling agents, reduction and oxidation, the 24 Å meridional reflection continued to dominate the entire diffraction pattern and is therefore a feature of fundamental importance to the whole understanding of the structure. This is supported by the fact that this reflection is also observed in films cast from soluble derivatives of feather rachis prepared either by oxidation or reduction.

Apart from weak reflections with $k = 9$ and possibly 11, a selection rule $k = 4n$ applies on the meridional row line for values of k up to 12, where k is the layer line index and n is an integer, but at higher angles meridional reflections with odd indices are common. In particular a strong reflection occurs with $k = 15$, corresponding to a periodicity of 6·3 Å. Now it is generally true that the low angle transform is determined primarily by the large scale distribution of electron density, usually the "shape" of the fibrous element, whilst the high angle transform is determined by the organisation of the constituent atoms into polypeptide chains within the element. It would appear therefore, that although the repeat of structure is 95 Å long, the shape, in axial projection, has a pseudoperiod of 24 Å whilst the chain structure has various pseudoperiods of small spacing which are submultiples of 95 Å but not of 24 Å.

A similar situation is encountered in α-keratin (McArthur, 1943), where the axial repeat of structure is 198 Å but meridional reflections with $k = 1$ and 2 are absent, so that in axial projection the shape of the fibrous element has a pseudoperiod of 66 Å. Again, at higher angles, meridional reflections are observed on layer lines of indices other than those given by $k = 3n$.

(b) *Non-meridional reflections*

In the diffraction diagram of native feather rachis the non-meridional reflections with $k < 8$ lie on well developed row lines, which shows at once that the fibrous elements are packed together side by side in an orderly manner in at least one dimension perpendicular to the fibre axis. The equatorial reflection on the first row line ($h = 1$) corresponds to a Bragg spacing of about 34 Å and further row lines with $h = 2$, 3 and 4 are observed. Near-equatorial reflections on the 3rd and 4th row lines only occur on even layer lines, indicating that when the structure is projected on to near-equatorial planes there is a marked pseudoperiod of 48 Å.

It is possible to give several explanations of the non-appearance of row lines at low angles associated with a second index, l, and mixed hl. Both Bear & Rugo (1951) and Hosemann (1957) have pointed out that the observed system of row lines could be due to a two-dimensional array or net of equivalent diffraction centres, whilst Sasisekharan & Ramachandran (1957) suggested that a cylindrical or spiral lattice would have the appropriate diffraction properties. An alternative possibility is that the structure is truly three-dimensional, but that the repeat of structure in the third dimension is of small spacing. In this case the row lines $l = 1$, 2, etc., and all row lines with mixed indices would occur at high angles of diffraction and would not be readily recognisable.

No certain choice between these suggestions can be made at present, but it is important to note that all imply sheet structures of one form or another. In the case of

the two-dimensional diffractor the 34 Å periodicity must exist in the plane of the sheet and the sheet must be of sufficient thickness to prevent appreciable streaking of the reflections along the layer lines. In the three-dimensional type of structure the combination of a lateral repeat of long spacing with a second repeat of short spacing at right angles again leads to a sheet structure, except that the 34 Å periodicity is now an *intersheet* spacing. This is also true of the cylindrical lattice as it is the spacing between adjacent cylindrical layers which gives rise to the sharp diffraction series.

4. Modified Diffraction Patterns

(a) *Treatment with osmium tetroxide*

When feather rachis is treated with solutions of osmium tetroxide, considerable deposition of osmium occurs within the structure as evidenced by the dark coloration produced and the high absorption coefficient for X-radiation. Despite this, the wide angle diffraction pattern is unaffected and it may be concluded that as in α-keratin deposition of osmium occurs mainly between, rather than within, the fibrous elements of the structure. At low angles the principal effect is a dramatic intensification of the (10) equatorial reflection, indicating periodic fluctuations in density of osmium of large amplitude in directions perpendicular to the axis but little variation parallel to the axis. This again is consistent with a deposit concentrated between fibrous elements elongated in the axial direction.

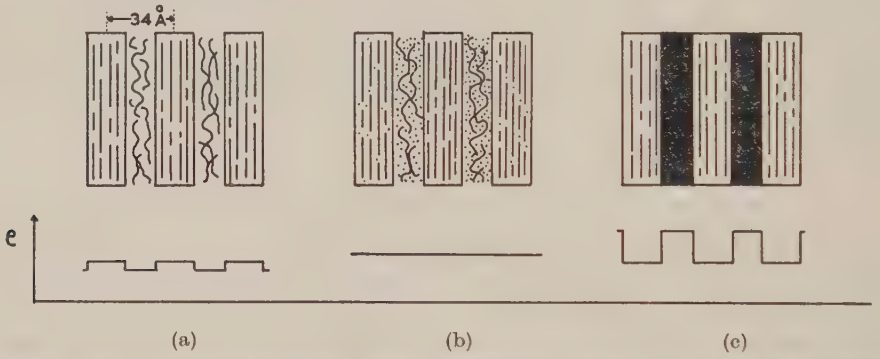

Fig. 2. A possible explanation of the observed intensities of the equatorial low angle reflection in (a) dry, (b) hydrated and (c) osmium treated feather rachis. In (a) the average electron density, ρ, in the fibrous element is slightly greater than in the intervening amorphous material; in (b) the sorbed water reduces this difference, and in (c) the contrast is greatly increased by the preferential deposition of osmium in the spaces between the fibrous elements.

In native feather the (10) reflection is strong in dry specimens and very weak in hydrated specimens, and in the light of the result obtained with osmium it is suggested that the distribution of water in a hydrated specimen and of osmium in a treated specimen are similar. As shown schematically in Fig. 2 the contrast between the fibrous elements and the regions between them is reduced compared with dry feather when water intervenes, and increased when osmium intervenes, thus leading to the observed diffraction effects. This view is supported by the observation that hydration of specimens containing osmium has little effect on the innermost low-angle equatorial reflection. Attempts to produce condition (b) in Fig. 2 by light staining with osmium were inconclusive, as the solutions tend to react to completion in the outer regions of the specimen before penetrating the inner regions.

It is difficult to decide whether the intense 24 Å meridional reflection is affected either by hydration or by treatment with osmium tetroxide, but in both cases the intensity of the near-meridional reflection on this layer line is modified. Thus the osmium deposit is not entirely featureless in the axial direction.

The fact that the (20) equatorial reflection is very weak in osmium-treated specimens enables some general conclusions to be drawn about the lateral dimensions of the fibrous elements. An investigation was made of the equatorial scattering from some plausible model distributions of osmium, in which it was assumed that the fibrous element was either a rod, an ellipsoid of revolution about the fibre axis, or a parallel-sided layer. In each case the deposit of osmium was supposed uniform, external to the element, and values ~ 19 to 24 Å for the rod diameter and ~ 15 to 19 Å for the layer thickness were deduced. With ellipsoids of revolution the scattering is much more rapidly damped with increasing ξ and diameters from ~ 22 to 34 Å would give satisfactory agreement with the observed diffraction.

(b) *Reduction and treatment with osmium tetroxide*

If feather rachis is reduced with thioglycollate prior to treatment with osmium tetroxide, the resulting diffraction pattern is similar to that obtained with osmium alone, except that an even greater intensification of the (10) reflection is obtained. Again it may be inferred that the deposit of osmium is external to the fibrous elements, but several explanations of the increased extent of reaction are possible. It may be that the cystine residues are concentrated on the surface of the fibrous elements and that the SH groups, exposed by reduction, provide additional sites for reaction. Additionally, there is the possibility that the entry of osmium tetroxide in untreated feather is restricted by disulphide linkages between the fibrous elements and that reduction also increases the accessibility of the intervening regions.

If, as appears to be the case in α-keratin, the space between the fibrous elements is occupied by a matrix of amorphous protein (Fraser & MacRae, 1958), it could be argued that the electron density in the matrix is likely to be lower than that in the fibrous elements in dry feather. In hydrated feather rachis the amorphous protein would absorb more water than the fibrous elements, thus reducing the contrast, and in osmium treated rachis the residues in the matrix would be more accessible to the reagent. If in addition the matrix were rich in cystine as in α-keratin the accessibility and reactivity would be increased by reduction. It does not appear possible at present to decide whether there is such a matrix in feather keratin and a decision must await the results of physico-chemical investigations now in progress.

(c) *Treatment with swelling agents*

Bear & Rugo have commented previously on the effect of water and alcohol sorption on the diffraction pattern of feather rachis. In both cases the (10) equatorial reflection was reduced in intensity and a similar effect was obtained with formic and acetic acids and *o*-chlorophenol in the present investigations. In the case of formic acid and *o*-chlorophenol, however, the entire diffraction pattern disappeared apart from the strong meridional reflection with $k = 4$. It may be concluded that in contrast to water, alcohol and acetic acid, these swelling agents enter and disrupt the internal organisation of the fibrous element of the structure. The absence of diffraction on row lines other than the meridian suggest that in the swollen state the fibrous element behaves as a diffractor with one-dimensional fluctuations of electron density of period 24 Å parallel to the *b* axis.

The only other diffraction observed in specimens swollen in formic acid or *o*-chlorophenol was a pair of diffuse haloes centred at about 10 and 4·7 Å and a diffuse streak on the fourth layer line in the vicinity of the reciprocal lattice point with $h = 1$. The diffuse haloes probably have the same origin as those observed in denatured proteins and the diffuse streak may be due to the limited lateral extent of the one-dimensional diffractor. It is probably significant that the diffraction in this region in native rachis is appreciably displaced from the first row line and is sorption-sensitive as regards intensity. If the pattern of native rachis is in fact that of a two-dimensional diffractor, as suggested by Bear & Rugo, this sorption-sensitive reflection and the diffuse streak in swollen rachis may both be related to the shape and thickness of the diffractor in the third dimension.

(d) *Treatment with silver nitrate*

After treatment with silver nitrate the diffraction pattern of feather rachis shows intense general low-angle scatter which cuts off sharply at a spacing of about 17 Å in the meridional direction and at a somewhat greater spacing equatorially. From the theoretical treatment of such scatter, given by Guinier & Fournet (1955), the linear dimensions of the silver deposits, or the spaces delineated by them, must be of the order of 20 Å axially and somewhat greater laterally.

In addition to the appearance of general scatter the low-angle reflections with $k = 0$ and 2 on the first row line and $k = 2$ on the second row line are greatly intensified. The intensification of the equatorial reflection may, as in the case of osmium, be attributed to a preponderance of silver on the surface of the fibrous elements and in the regions between them, whilst the intensification of the reflections on the second layer line again emphasises the axial pseudoperiod of 48 Å within the structure.

(e) *Treatment with mercuric acetate and iodine*

The diffraction pattern obtained after treatment with mercuric acetate is quite remarkable for the general increase in clarity of the low and intermediate angle pattern as well as the number of reflections in which the intensity is modified. Previously Rudall (1947) had noted the intensification of the 34 Å equatorial reflection, which was confirmed in the present work, and once again this may be ascribed to a delineation of the fibrous elements by mercury atoms. A complete tabulation of the changes in intensity will be reserved for a further publication, but preliminary estimates indicate a general increase in the intensity on the first row line up to values of $k = 3$ and minor intensification of the meridional reflections with $k = 4$ and 8. In addition, a weak meridional reflection with $k = 1$ appears and a streak is observed on the 3rd layer line between the meridian and the first row line. A detailed interpretation of these effects must await more precise intensity measurement but it is noteworthy that the mercury is deposited in such a way as to emphasise the full axial period of 95 Å. In contrast, treatment with iodine only intensifies reflections with even k on the first row line, thus emphasising the axial pseudoperiod of 48 Å.

5. A Diffraction Model for Feather Keratin

Although a detailed model for feather keratin has recently been proposed by Krimm & Schor (1956), we have not been able to interpret the diffraction data described earlier in terms of this structure. Some progress has been possible, however,

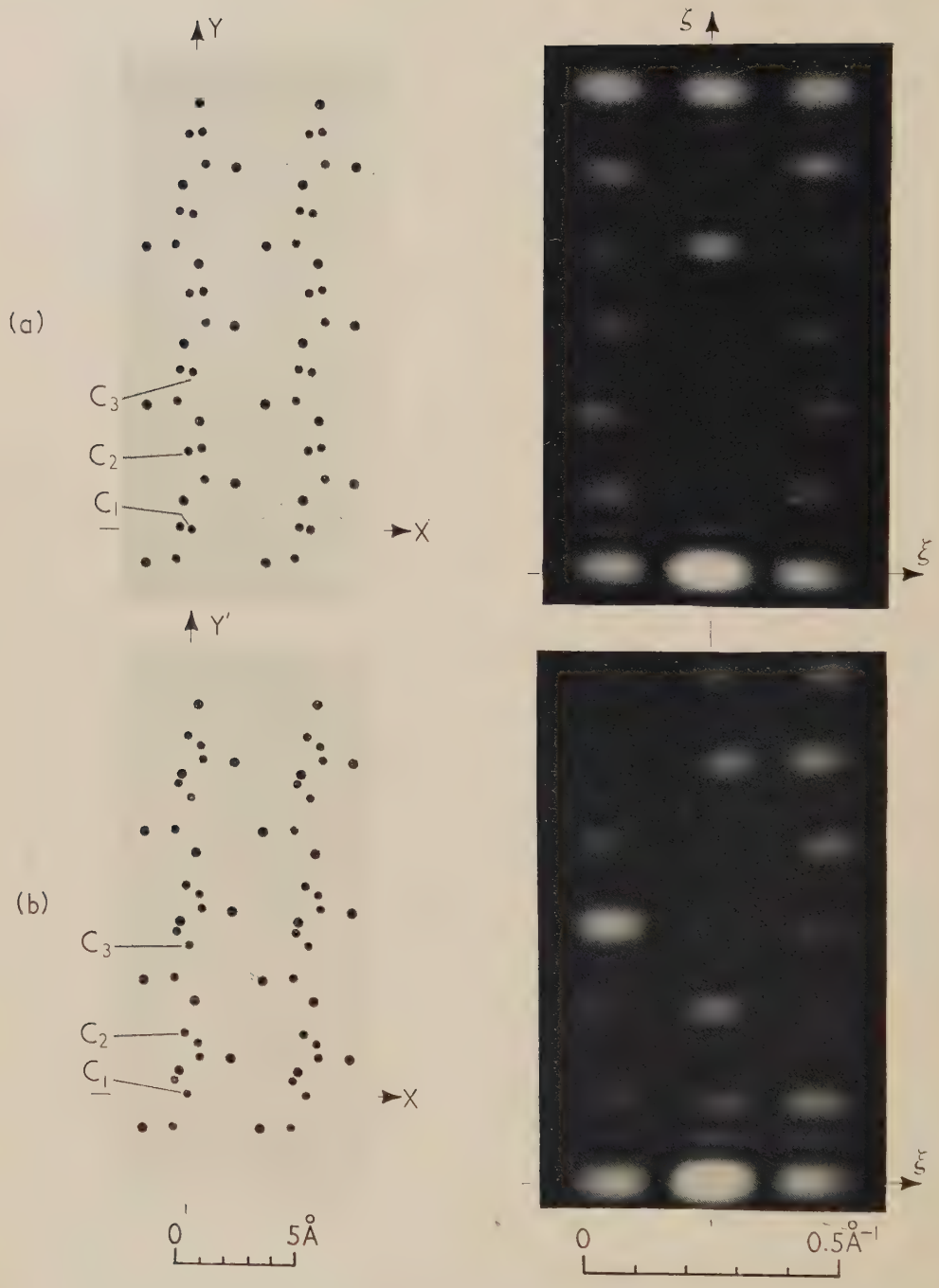

Plate I(a). Mask (left) and optical transform (right) of an xy projection of the parallel pleated sheet configuration described by Pauling & Corey (1953). The repeat of pattern in the y direction is 6·5 Å.

Plate I(b). Mask (left) and transform (right) of an xy' projection where y' is a direction in the yz plane inclined at 18° to the y axis. The repeat of pattern in the y' direction is 6·16 Å.

[*To face page* 393

by modifying and elaborating the scheme proposed by Bear & Rugo (1951). The structure so derived is concerned primarily with the mode of molecular organisation and does not require a detailed description of chain configuration or residue distribution. Other modes of organisation involving helical structures have also been investigated and it appears possible to account, in a general way, for some features of the low angle diffraction pattern. Thus the present model must be regarded as heuristic and a full discussion of alternative helical modes of organisation will be reserved for a later publication. The derivation of the present model is as follows.

(a) *Chain configuration*

The high-angle meridional diffraction pattern of feather keratin differs from that of other β-structures in three important details: (a) the axial pseudoperiod of 3·08 Å is considerably less than that of β-keratin (3·3 Å) or silk (3·5 Å), (b) a meridional reflection corresponding to about twice this spacing is observed (6·3 Å), (c) so far no meridional spacing in the 1 Å region has been observed. Astbury & Marwick (1932) suggested that the short pseudoperiod indicated a somewhat contracted β-configuration and Pauling & Corey (1951) devised a model structure of similar axial repeat (3·07 Å), termed the polar pleated sheet. Successive (C—NH—CO) units are related by a glide plane of symmetry, and so the only contribution to the 6·14 Å meridional reflection is from the β-carbon atoms. Examination of optical transforms of the polar pleated sheet revealed that this contribution is in any case very small.

The considerable intensity of the 6·3 Å reflection in feather keratin suggests rather that the foreshortening of the polypeptide chain from the fully extended configuration occurs in such a way that the projected lengths of alternate residues are unequal, so that the fibre axis is no longer a two-fold screw axis or contained in a glide plane of symmetry. The simplest means of achieving this is to suppose that the polypeptide chains are not parallel to the axis but tilted through a small angle. In order to test this suggestion, optical transforms of the parallel-chain pleated sheet structure described by Pauling & Corey (1953) were obtained for various projections. Transforms of projections on to the xy plane (nomenclature of Pauling & Corey) and on to a plane xy' containing the x axis and inclined at 18° to the y axis, are reproduced in Plates I(a) and I(b) respectively. In (a) the 3·25 Å meridional reflection is weak, the 6·5 Å reflection is absent and the 1·08 Å reflection very strong whilst in (b) the situation is more nearly that obtaining in feather keratin, in that appreciable diffraction occurs at spacings of both 3·08 and 6·16 Å, and the 1·03 Å reflection is considerably weaker than its counterpart in (a). Further progress in exploring this notion would require some knowledge of side chain contribution, but it does appear that simple tilting could account for the unusual features of the high-angle meridional diffraction in feather keratin and no further elaboration is required in the present model.

(b) *Chain packing*

Diffraction patterns obtained from feather keratin under conditions of low instrumental resolution closely resemble those of β-proteins as regards the equatorial distribution of intensity, exhibiting pronounced maxima at 4·7 and 10 Å. These are the spacings normally associated with the distance between chains in the hydrogen-bonded layers and the distance between adjacent layers, respectively. With higher resolution the 10 Å maximum is resolved, as shown in Fig. 1, into two components on row lines with $h = 3$ and 4. So it follows, as pointed out by Bear & Rugo (1951), that the 34 Å interplanar periodicity must be perpendicular to the hydrogen-bonded

layers. Each period would therefore contain three layers, and it is significant that the observed breadth of the 10 Å equatorial maximum is of appropriate width, as shown in Fig. 3. The apparently two-dimensional nature of the low-angle diffraction pattern, discussed earlier, could thus be explained by supposing that the hydrogen-bonded layers exist in groups of 3 giving a unit cell with base $34 \times 4{\cdot}7$ Å. Thus all low angle reflections would be of the ($hk0$) type.

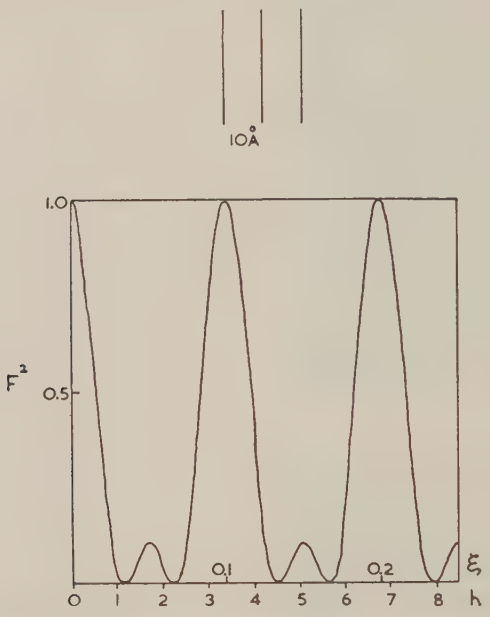

Fig. 3. Equatorial intensity transform of 3 planes spaced 10 Å apart, the normal to the planes being perpendicular to the fibre axis.

$$F^2 = \left(\frac{\sin 30\pi\xi}{\sin 10\pi\xi}\right)^2$$

(c) *Chemical evidence*

Although certain features of the diffraction pattern can be accounted for by assuming the presence of hydrogen-bonded layers of polypeptide chains inclined to the fibre axis, the intense meridional reflection of spacing 24 Å indicates some major structural discontinuity at this interval, and it is natural to suppose that this discontinuity is associated with chemical constitution.

In α-keratin, which is closely related to feather keratin both in function and composition, there is good evidence that the fibrous elements or microfibrils are embedded in an amorphous matrix of distinctly different chemical composition (Fraser, MacRae & Rogers, 1959). If the same is true in feather keratin, arguments about the nature of the fibrous elements based on chemical analyses or on measurements of the molecular weights of soluble derivatives are of limited value unless they relate to the fibrous element alone. Nevertheless, in the absence of evidence for a matrix in feather keratin it is worth pursuing the implications of the overall chemical composition and the particle weight of soluble derivatives.

When the disulphide linkages of feather keratin are reduced, a high proportion of the structure may be dispersed into particles of molecular weight about 10,000 (Woodin, 1954), and as the mean residue weight is close to 100 each particle must

[To face page 395

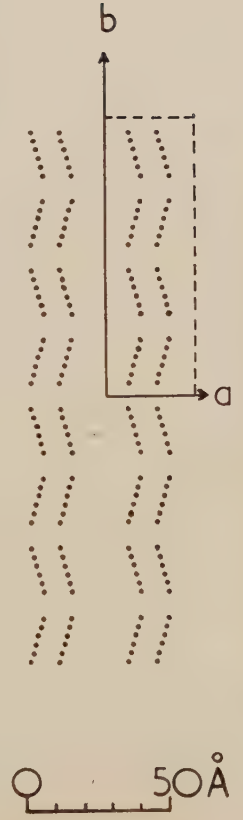

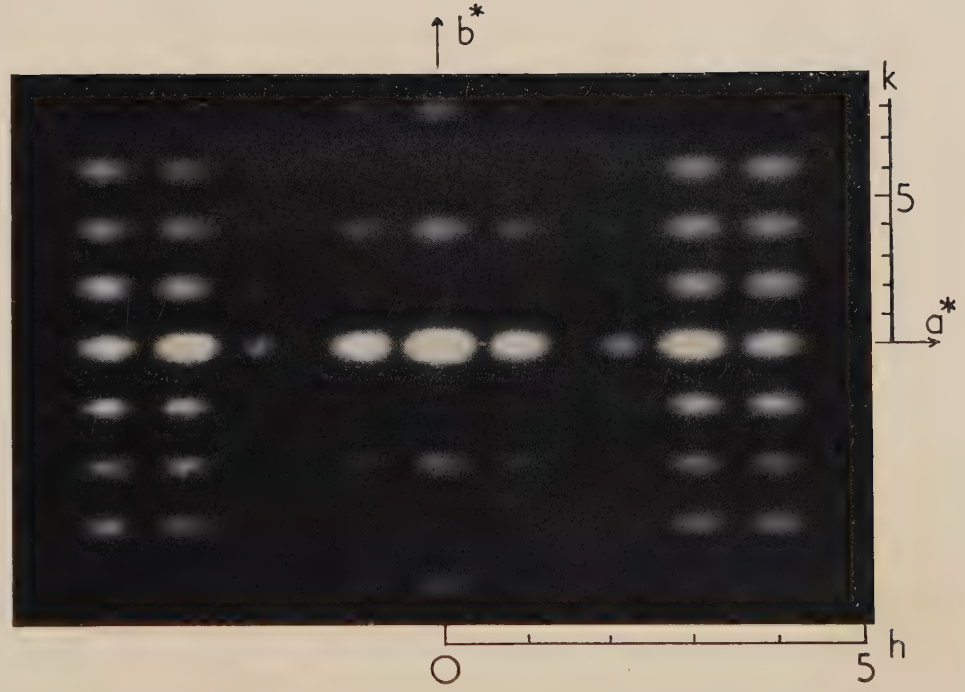

PLATE II(a). Mask representing a possible disposition of β-crystallites in feather keratin, each crystallite being represented for the purpose of low-angle diffraction by two rows of 6 holes spaced 10 Å apart.

PLATE II(b). Optical transform of mask shown in (a), indexed on a 34×95 Å unit of structure.

contain about 100 residues. If the composition is similar to that determined by Schroeder & Kay (1955) for the complete structure, each particle contains about 6 half-cystine residues and 40 amino acids with small side chains (glycine, serine and alanine). It is significant that the amino acids glycine, alanine and serine, which constitute the crystalline regions of silk fibroin, form such a high proportion of the total residues in feather which also contains extended polypeptide chains. However, as Schroeder & Kay comment, the high proportion of proline would interfere with the formation of a silk-like structure if these residues were randomly dispersed along the length of the chain.

Provided the proline residues are not confined to an amorphous matrix, the chemical evidence therefore suggests that the polypeptide chains are of the order of 300 Å long but bend or loop at frequent intervals. The fact that insufficient end groups are detectable to account for the measured molecular weight (Woodin, 1956) may indicate that the chains are cyclic, although this observation might also be explained by masking. Perhaps the simplest explanation of the strong persistent 24 Å meridional reflection is that it originates from an alternation of regions with well-developed β-structure, with regions of irregular packing associated with folds or loops. Two examples of the way in which this notion may be reconciled with a pseudo cell of base $34 \times 4{\cdot}7$ Å. are shown in Fig. 4.

In case (a) the full axial period of 95 Å is accounted for in a very simple way by the length of the particle, but this type of folding would not be consistent with a cyclic structure. In case (b) cyclic particles could be accommodated. Evidence from physicochemical studies (Woodin, 1954) suggests that in solution the particle is rod-like, and if this form is retained on drying then a configuration of the type shown in Fig. 4(a) is more probable, as many of the features of the X-ray diagram are present in the regenerated material (Woodin, 1956). In the present work the meridional or near-meridional reflections with $k = 4$, 15 and 19 and equatorial maxima at spacings of 34, 10 and 4·7 Å were particularly noticeable.

As regards the distribution of amino acids, it might be supposed that in both cases proline would be associated with the bends and the smaller residues concentrated in the interior of the particle, thus permitting the formation of β-crystallites of limited dimensions parallel to a and b but of considerable extent parallel to c. These dispositions would entail a preponderance of charged groups on the lateral surfaces of the particle and account for the deposition of osmium between the particles in layers parallel to the bc plane.

(d) *The optical transform*

The anticipation that the low-angle transform of β-structures can be closely approximated by representing each residue by a single point was confirmed by experiment, and thus the denser regions of the structures shown in Fig. 4 could be represented by small grids of points as in Plate II. The fact that all the intense observed X-ray reflections for values of h or k up to 4 occur on layer lines of even index, and that the (02) reflection is absent, suggests that the dense regions are related by a pseudo two-fold screw axis parallel to b. The combination of this feature with the chain-tilting discussed earlier leads to a consideration of the type of organisation shown in Plate II(a). Comparison of the optical transform obtained from this mask, reproduced in Plate II(b), with the observed X-ray diffraction pattern shows a considerable measure of agreement. Further masks, in which the introduction of additional scattering material between the particle rows was simulated by inserting

columns of randomly-spaced holes parallel to *b*, showed that the intensity of the (10) reflection could be reduced or increased by choosing a suitable concentration of holes, without significant influence on the remainder of the transform. Thus the present model is capable of accounting for the observed effects of hydration and osmium deposition through the mechanism outlined in Fig. 2. An intensification of the (10) reflection may also be produced by superposing columns of randomly spaced holes on

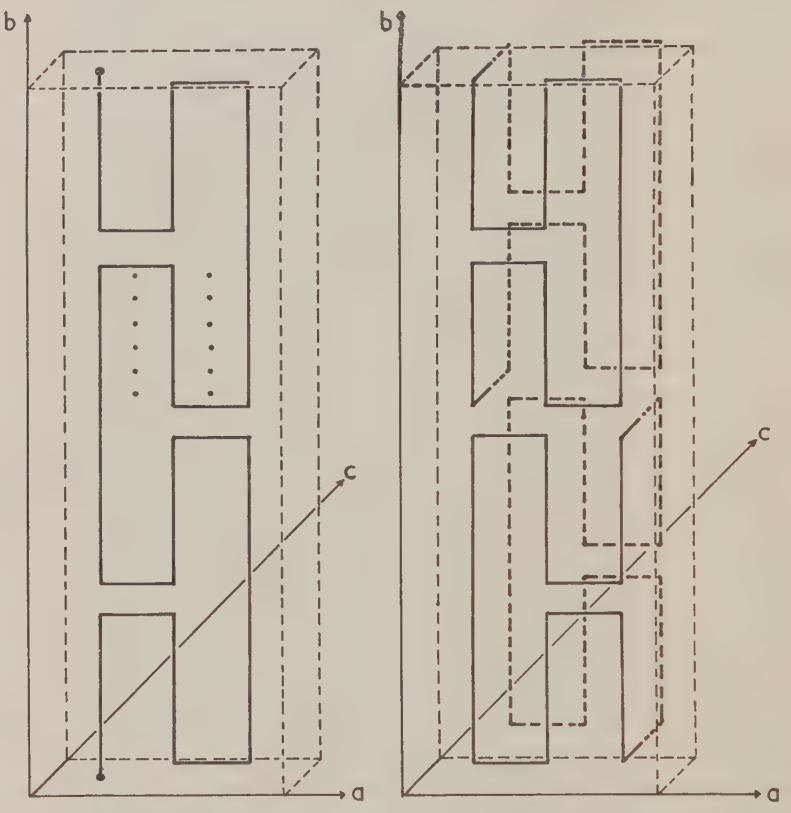

FIG. 4. (a) An example of the way in which a polypeptide chain of molecular weight $\sim$ 10,000 and length $\sim$ 300 Å could be accommodated in an orthogonal unit cell of dimensions 34 × 95 × 4·7 Å. The grid of dots shows how the small regions of regular β-structure are represented in the mask of Plate II(a).

(b) An alternative scheme by which cyclic particles could be accommodated in a pseudo cell of the same dimensions as in (a).

In both cases the side chains are supposed extended in the direction of the *a* axis in the β-crystallites and hydrogen bonds formed in the *c* direction.

the fibrous elements themselves, and so the observed intensification of this reflection in the X-ray diagram after silver or mercury deposition could also be explained as a staining of the fibrous element.

The model proposed here for the molecular organisation in feather keratin fails to account for the strong (15) reflection, and also the weak reflections at low angles on layer lines with odd *k*. These features require that alternate unit cells of the simple 48 × 34 Å unit used in the masks differ slightly to give a true unit of 95 × 34 Å. This difference may well be chemical, for example reflecting differences in amino acid distribution or the presence of a chain terminus as in Fig. 4(a).

The density computed from the unit cell and particle weight given above is about 1·09 gm cm^{-3} which is very much less than the measured value of 1·27 gm cm^{-3} (Fraser & MacRae, 1957) for dry rachis. However, the unit cell size for dry keratin is somewhat less than that used in the present model (Bear & Rugo, 1951), and if this were combined with a particle of molecular weight 11,200 the density would be satisfactory. The value of 11,200 for particle weight is well within the range of values obtained by Woodin (1954) using physicochemical methods.

(e) *Possible relation to cross-β structures*

During revision of the present contribution a description of models for the cross-β configuration of supercontracted proteins was published by Astbury, Beighton & Parker (1959). The regular folding and distance between folds in this model are so similar to those envisaged in Fig. 4 as to prompt the suggestion that the cross-β and feather keratin structures in fibrous proteins may be very closely related, apart from the fact that in the first case the polypeptide chains are approximately perpendicular to the fibre axis and parallel in the latter case.

REFERENCES

Astbury, W. T., Beighton, E. & Parker, K. D. (1959). *Biochim. biophys. Acta*, **35**, 17.
Astbury, W. T. & Marwick, T. C. (1932). *Nature*, **130**, 309.
Bear, R. S. (1944). *J. Amer. Chem. Soc.* **66**, 2043.
Bear, R. S. & Rugo, H. J. (1951). *Ann. N.Y. Acad. Sci.* **53**, 627.
Elliott, A. & Malcolm, B. R. (1958). *Proc. Roy. Soc. A*, **249**, 30.
Fraser, R. D. B. & MacRae, T. P. (1957). *Text. Res. (J.)* **27**, 384.
Fraser, R. D. B. & MacRae, T. P. (1958). *Biochim. biophys. Acta*, **29**, 229.
Fraser, R. D. B., MacRae, T. P. & Rogers, G. E. (1959). *Nature*, **183**, 592.
Guinier, A. & Fournet, G. (1955). *Small-angle scattering of X-rays*. London: Chapman & Hall.
Hosemann, R. (1957). *Elektrochemie*, **61**, 1008.
Krimm, S. & Schor, R. (1956). *J. Chem. Phys.* **24**, 922.
McArthur, I. (1943). *Nature*, **152**, 38.
O'Donnell, I. J. & Thompson, E. O. P. (1959). *Aust. J. Biol. Sci.*, in press.
Pauling, L. & Corey, R. B. (1951). *Proc. Nat. Acad. Sci., Wash.* **37**, 251.
Pauling, L. & Corey, R. B. (1953). *Proc. Nat. Acad. Sci., Wash.* **39**, 253.
Richards, H. R. & Speakman, J. B. (1955). *J. Soc. Dy. Col.* **11**, 551.
Rudall, K. M. (1947). *Biochim. biophys. Acta*, **1**, 549.
Sasisekharan, J. & Ramachandran, G. N. (1957). *Proc. Indian Acad. Sci.* **45**, 363.
Schroeder, W. A. & Kay, L. M. (1955). *J. Amer. Chem. Soc.* **77**, 3901.
Woodin, A. M. (1954). *Biochem. J.* **57**, 99.
Woodin, A. M. (1956). *Biochem. J.* **63**, 576.

J. Mol. Biol. (1959) **1**, 398-401

LETTERS TO THE EDITOR

Large Axial Spacings in Striated Muscle

Striated muscle is known to contain principally two proteins, myosin and actin. The wide angle X-ray diffraction pattern of muscle is the usual α-pattern which is identical to that of myosin. X-ray patterns of reconstituted actin fibres (Astbury & Spark, 1947; Cohen & Hanson, 1956) indicate that the actin component does not contribute to the wide angle pattern of muscle, but gives a well known series of meridional or close meridional reflections of weak intensity at moderate angles of diffraction. Reconstituted myosin fibres only give wide angle diffraction, and the actin component has been thought to be responsible for the low angle X-ray diffraction of striated muscle (Astbury & Spark, 1947; Huxley, 1953). However, the present observations suggest that at least one series of low angle reflections is due to the myosin component in striated muscle.

The low angle X-ray diffraction camera used in this work is a modification of the original camera of Franks (1955). Two movements have been added which effectively bring the camera axis into alignment with the point focus on the X-ray tube, namely a vertical adjustment on the front support and a horizontal vernier adjustment on the base plate. The camera permits extended exposures to be taken with greater simplicity of alignment. X-ray patterns are obtained in two dimensions with resolution up to 500 Å in the principal direction.

TABLE 1

Actin		Paramyosin		Striated muscle
layer line spacing	index	meridional spacing	index	meridional spacing
Å		Å		Å
58·8 ± 0·15	1	145	5	145 ± 1·0
27·40 ± 0·07	k	72·5	10	72·5 ± 0·7
18·71 ± 0·04	$k + 1$	48·3	15	
13·69 ± 0·03	$2k$	36·3	20	
11·11 ± 0·03	$2k + 1$	29·0	25	
9·16 ± 0·02	$3k$	24·2	30	

The actin pattern is known to occur in all types of muscle, striated or smooth. In the present studies the best patterns have been obtained from certain smooth muscles in the dry state. To register the pattern in detail with the above equipment requires an exposure time of about 3 weeks. The actin reflections from smooth muscle occur together with the detailed paramyosin pattern (Bear & Selby, 1956). Air-dried paramyosin has an axial period of 725 Å with meridional reflections occurring at diffraction orders which are multiples of 5. These reflections have been used solely for calibration purposes and are listed in Table 1. X-ray measurements have been made on actin patterns from striated and smooth muscles and the spacings are practically identical. Actin layer line spacings from an air-dried smooth muscle of the

pharynx retractor of *Helix pomatia* are given in Table 1. Only the first six spacings are included although higher orders and other off-meridional reflections are observed. The reflections with indices k, $2k$, $3k$ are meridional, whereas the reflections with layer line indices 1, $k + 1$, $2k + 1$ are off-meridional. The actin reflections can be correlated with a helical structure which has a residue repeat of 27·4 Å and a pitch of 58·8 Å. Selby & Bear (1956) have given two alternatives, either 15 residues in 7 turns or 13 residues in 6 turns. The ratio 7:15 = 0·467 and 6:13 = 0·462, while the observed ratio of layer line indices 1 : k = 0·467. This favours 15 residues in

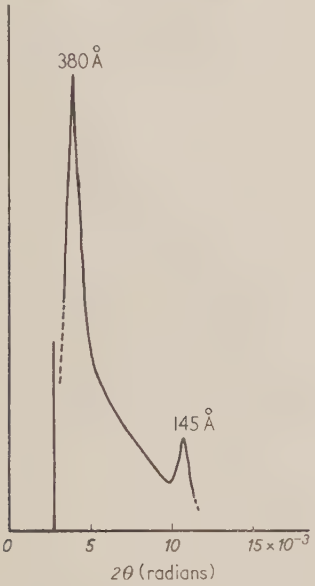

FIG. 1. Densitometer trace of low angle pattern of air-dried formaldehyde-fixed rabbit psoas muscle.

7 turns and the layer line repeat of actin is 15 × 27·4 = 410 Å. It may be noted that there is no obvious relation between the paramyosin and actin periods in smooth muscles.

Low angle X-ray observations have been made on striated muscle, frog sartorius, rabbit psoas or the indirect flight muscle of a blowfly, untreated or extracted in glycerol. Specimens have been examined in both the wet and dry state. In all cases there is a strong 145 Å reflection on the meridian, and sometimes its second order at 72·5 Å is just visible. Huxley (1953) has obtained low angle reflections from living muscle using slit collimation, which provides resolution in one dimension, and which showed the first six or seven orders of an axial repeat of 415 Å. The 145 Å reflection described here, whose spacing has been measured accurately, would correspond to the third order of a 435 Å axial period, slightly larger than the previous estimate. The experimental observations relating to these reflections can be summarised as follows:

(1) Precise measurements on the actin pattern do not fit the 145 Å reflection. The estimated errors in the actin spacings are given in Table 1 and are less than 0·5% whereas the striated muscle reflections are known to an accuracy of 1%.

(2) X-ray patterns with resolution in two dimensions permit a study of line shapes. The actin reflections clearly arise from thin filaments whereas the 145 Å reflection

is associated with filaments of larger diameter. The interdigitating model for striated muscle advocated by Huxley & Hanson (1954) consists of a primary array of myosin filaments and a secondary array of thinner actin filaments.

(3) If the muscle is treated with formaldehyde the actin reflections are removed but the 145 Å reflection is unaffected.

It is concluded that it is the myosin component and not the actin which gives rise to these reflections at small angles of diffraction. Thus, myosin in striated muscle behaves similarly to paramyosin in smooth muscle since both occur with actin, and both give rise to the observed small angle reflections which have been described. They show typical α-protein wide angle diffraction whereas actin does not. The striated muscle spacings given in Table 1 are identical to the first two meridional spacings from paramyosin. At present the X-ray data from striated muscle are insufficient to determine the packing unit of myosin but some similarity between paramyosin in smooth muscle and myosin in striated muscle is already indicated.

In addition to the above reflections in striated muscle there is a larger spacing on the meridian at about 400 Å. The magnitude of this spacing can vary from 360 Å to 410 Å depending on previous treatment. The experimental error is estimated at less than 2% and within this limit the 145 Å reflection remains unchanged. Glycerol-extracted rabbit psoas muscle equilibrated with 0·1 N-KCl at neutral pH and examined in the wet state gives a 410 Å spacing together with the 145 Å reflection and a 59 Å actin line. This 410 Å spacing has the same magnitude as the actin period as well as the non-net reflections observed by Selby and Bear (1956) in the translucent parts of the adductor muscle of the mollusc *Venus mercenaria*. However, when rabbit psoas muscle is immersed in 5% aqueous formalin at neutral pH for at least one day, the actin reflections vanish but the 145 Å reflection remains unchanged, while the large spacing is now at 380 Å. This 380 Å reflection is meridional and of strong intensity, and for clarity of presentation a densitometer trace taken along the meridian of the X-ray pattern is shown in Fig. 1. After the formaldehyde fixation the muscle was air dried although a similar pattern is obtained in the wet state. An exposure time of 15 hr was required with a specimen to film distance of 6·7 cm. If the specimen is further treated with phosphotungstic acid the spacing is reduced to 360 Å.

The above observations determine that an axial spacing or repeat distance exists in striated muscle at about 400 Å. This spacing has not been previously described in the literature and it is of interest that the magnitude of this spacing corresponds with the fine axial period seen in the electron microscope associated with both the A and I bands of striated muscle (Draper & Hodge, 1949). Further work is necessary to characterise this spacing and to find out whether this spacing changes in any way during muscle contraction.

I wish to thank Professor J. T. Randall for the provision of facilities, Mr. G. F. Elliott for the use of his camera in the early stages of this work and Dr. J. Hanson for provision of some striated muscle specimens. I am indebted to members of this laboratory, especially Dr. J. Hanson, Dr. J. Lowy and Mr. G. F. Elliott, for helpful discussions.

C. R. Worthington

Medical Research Council,
Biophysics Research Unit,
King's College,
London, England

Received 15 August 1959

REFERENCES

Astbury, W. T. & Spark, L. C. (1947). *Biochim. biophys. Acta*, **1**, 388.
Bear, R. S. & Selby, C. C. (1956). *J. Biophys. Biochem. Cytol.* **2**, 55.
Cohen, C. & Hanson, J. (1956). *Biochim. biophys. Acta*, **21**, 177.
Draper, M. H. & Hodge, A. J. (1949). *Aust. J. Exp. Biol. Med. Sci.* **27**, 465.
Franks, A. (1955). *Proc. Phys. Soc. Lond.* B, **68**, 1054.
Huxley, H. E. (1953). *Proc. Roy. Soc.* B, **141**, 59.
Huxley, H. E. & Hanson, J. (1954). *Nature*, **173**, 973.
Selby, C. C. & Bear, R. S. (1956). *J. Biophys. Biochem. Cytol.* **2**, 71.

J. Mol. Biol. (1959) **1**, 402–404

Chemical and Crystallographic Study of the two Fractions of Adult Horse Haemoglobin

Cabannes & Serain (1955) and Bangham & Lehmann (1958) have shown that adult horse haemoglobin consists of two electrophoretically distinct components which were present in roughly equal amounts in most of the horses they examined. The three-dimensional X-ray analysis of horse haemoglobin (Perutz, Rossmann, Cullis, Muirhead, Will & North, 1960) depends for its success on the homogeneity of the material. For instance, if horse haemoglobin consisted of mixed crystals of two widely different components, electron density maps would be confused and hard to interpret. For these reasons, and because of the intrinsic interest of the problem, we have investigated the chemical and crystallographic differences between the two components. Bangham & Lehmann achieved their separation by starch gel electrophoresis at pH 8·6. Since then the two components have also been separated by ion exchange chromatography on carboxymethyl cellulose (Huisman, Martis & Dozy, 1958 ; Gutter, Peterson & Sober, 1959), a method developed by Peterson & Sober (1956) and followed by us.

The column (25 × 1·8 cm) was first equilibrated with sodium phosphate buffer, pH 7·2, which was 0·01 M with respect to sodium. Haemoglobin was prepared from freshly drawn blood to which oxalate had been added to prevent coagulation (Ingram, 1955). Excess ferricyanide was added to convert it to methaemoglobin, and the protein solution was then dialysed against several changes of the same buffer with which the column had been equilibrated. The concentration of haemoglobin was determined spectrophotometrically, and an amount equal to 0·5 to 1 g of protein was applied to the column in the form of a 2% solution. Under these conditions approximately 50% of the protein moved slowly through the column (fast fraction). The remainder was adsorbed at the top of the column. This latter haemoglobin (slow fraction) was eluted by raising the sodium concentration to 0·4 M. After separation on the column each fraction was concentrated by pervaporation (Kober, 1917). Both fractions were tested for homogeneity by starch gel electrophoresis at pH 8·6 and were found to consist of the pure fast and slow components respectively. Each haemoglobin was crystallized from 2 M-ammonium sulphate for examination by X-rays. Their unit cell dimensions and the intensities of their X-ray reflexions were found to be indistinguishable from each other and from the mixture of the two components normally used for X-ray work. Absorption spectra of the two solutions in the ultraviolet and visible regions have also failed to show differences. These results would exclude any gross structural differences between the two components.

The separated fractions were each treated with HCl-acetone to precipitate free globin. Tryptic digestion of the globins followed by "fingerprinting" of the peptides soluble at pH 6·4 (Ingram, 1958) showed identical patterns with the exception of one peptide in each (Plate I and Fig. 1). The trypsin-resistant cores were digested with chymotrypsin, and "fingerprinting" of the additional peptides obtained showed no differences (Hunt & Ingram, 1958) (Plate II and Fig. 2).

[To face page 402

PLATE I(a)

PLATE I(b)

Comparison of fingerprints of tryptic digests of globins obtained from fast (a) and slow (b) fractions of adult horse haemoglobin.

PLATE II(a)

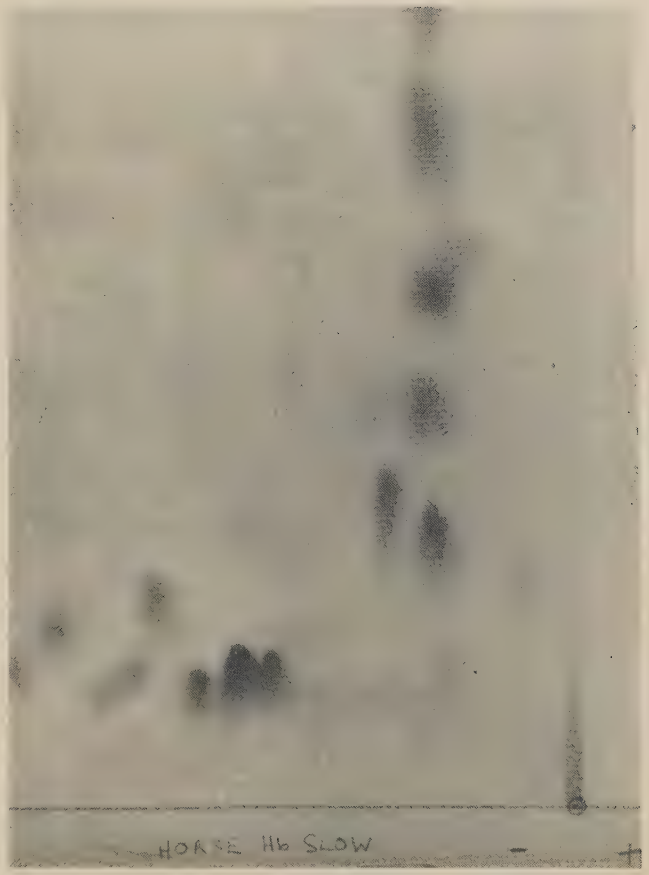

PLATE II(b)

Comparison of fingerprints of chymotryptic digests of trypsin-resistant cores of the globins of fast and slow fractions of adult horse haemoglobin. (a) Fast fraction. (b) Slow fraction.

The differences between the two fractions thus appear to reside in a single peptide in the half-molecule of haemoglobin and may well be found to consist in the replacement of a single amino-acid residue, as in the abnormal human haemoglobins studied

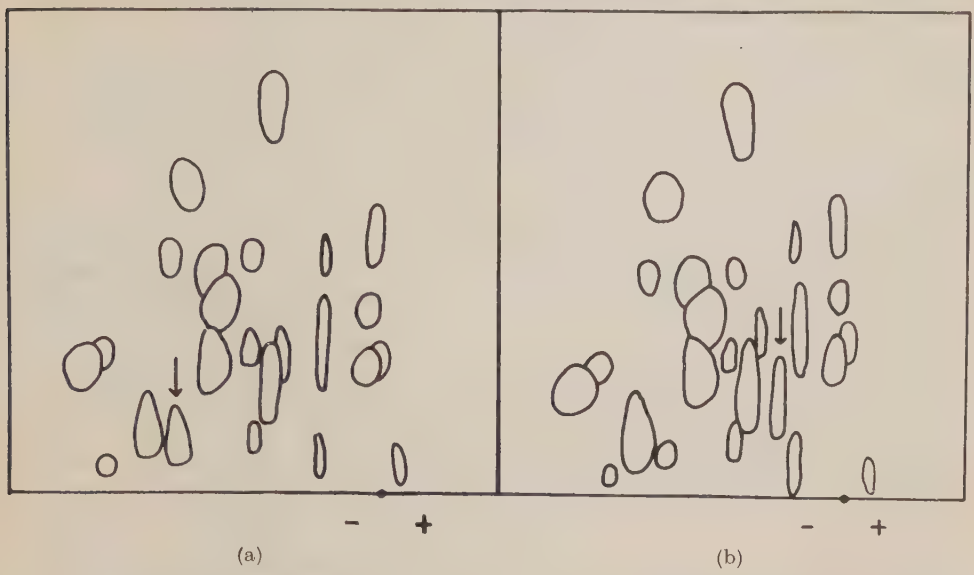

FIG. 1. Tracings of the fingerprints in Plate I. The peptides which are different in the two proteins are marked by arrows. (a) Fast fraction. (b) Slow fraction

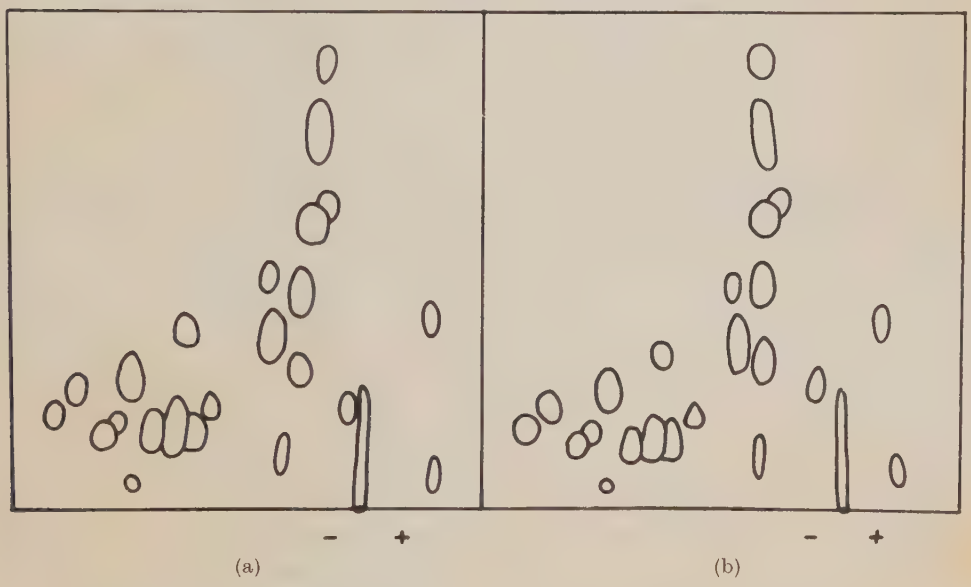

FIG. 2. Tracings of the fingerprints in Plate II. (a) Fast fraction. (b) Slow fraction

by Hunt & Ingram (1958). The electron density maps obtained from an X-ray analysis of the mixture should therefore be obscure in only a small local region and the results bearing on the general structure of the molecule should not be affected by the presence of two fractions.

Since examination of horse haemoglobin always reveals two components, these probably represent the product of two closely linked genes rather than the expression

of two allelomorphs at a single locus. It is not clear what biological advantage the presence of two fractions confers. Normal oxyhaemoglobin of horse is rather insoluble, yet its concentration in the red cell is over 30%. By the phase rule it is to be expected that a saturated solution of two fractions would contain more haemoglobin than a saturated solution of either one. Thus it is conceivable that their joint presence prevents crystallization of the haemoglobin in the red cell.

The authors are indebted to Miss Eileen Blincoe for her capable technical assistance.

Medical Research Council Unit for Molecular Biology,
Cavendish Laboratory, Cambridge, England — M. F. PERUTZ

Agricultural Research Council,
Institute of Animal Physiology,
Babraham, Cambridge, England — L. K. STEINRAUF †, ANNE STOCKELL ‡, A. D. BANGHAM

Received 11 October 1959

† U.S. Public Health Service Research Fellow of the National Heart Institute. Now at Dept. of Chemistry, University of Illinois, Urbana, Illinois, U.S.A.

‡ U.S. Public Health Service Research Fellow of the National Institute of Arthritis and Metabolic Diseases.

REFERENCES

Bangham, A. D. & Lehmann, H. (1958). *Nature*, **181**, 267.
Cabannes, R. & Serain, C. (1955). *C.R. Soc. Biol., Paris*, **149**, 1193.
Gutter, F. J., Peterson, E. A. & Sober, H. A. (1959). *Arch. Biochem. Biophys.* **80**, 353.
Huisman, T. H. J., Martis, E. A. & Dozy, A. (1958). *J. Lab. Clin. Med.* **52**, 312.
Hunt, J. A. & Ingram, V. M. (1958). *Biochim. biophys. Acta*, **28**, 546.
Ingram, V. M. (1955). *Biochem. J.* **59**, 653.
Ingram, V. M. (1958). *Biochim. biophys. Acta*, **28**, 539.
Kober, P. A. (1917). *J. Amer. Chem. Soc.* **39**, 944.
Perutz, M. F., Rossmann, M. G., Cullis, A. F., Muirhead, H., Will, G. & North, A. C. T. (1960), *Nature*, **185**, 416.
Peterson, E. A. & Sober, H. A. (1956). *J. Amer. Chem. Soc.* **78**, 751.

Index to Volume 1

Adenovirus, icosahedral form, 84
Amino acid-ribonucleic acid complexes in *Escherichia coli*, 301
Apoferritin (see ferritin), 69
Aschaffenburg, R. (see Green, D. W.), 54

Bacteria, gene replication and mutation induction, 81
Bacteriophage λ, density alterations associated with transducing ability, 379
Bacteriophage φX174, a single stranded deoxyribonucleic acid from, 43
— electron microscopy of structure, 192
— purification and properties, 37
Bacteriophage, structural components, 281
Bacteriophage T2: precursor protein synthesis in infected bacteria, 260
Bacteriophage T4, dispersal of parental nucleic acid among progeny, 134
— mutagenic effect of base analogues, 87
Balazs, E. A., Bothner-By, A. A. & Gergely, J. Proton magnetic resonance studies on water in the presence of various macromolecular substances, 147
Bangham, A. D. (see Perutz, M. F.), 402
Barnard, E. A. (see Stein, W. D.), 350
— & Stein, W. D. The histidine residue in the active centre of ribonuclease I. A specific reaction with bromoacetic acid, 339
Barnett, L. (see Brenner, S.), 281
Bassham, J. A. (see Moses, V.), 21
Beet yellows virus filaments, electron microscopy of structure, 234
Bendich, A. (see Borenfreund, E.), 195
Benzer, S. (see Brenner, S.), 281
Borenfreund, Ellen, Rosenkranz, H. S. & Bendich, A. Studies on deoxyribonucleic acid after exposure to tritium gas, 195
Bothner-By, A. A. (see Balazs, E. A.), 147
Brenner, S. (see Horne, R. W.), 84
— Streisinger, G., Horne, R. W., Champe, S. P., Barnett, L., Benzer, S. & Rees, M. W. Structural components of bacteriophage, 281
Bromoacetic acid reaction of histidine residue in ribonuclease, 339
Burge, R. E. & Hynes, R. D. The thermal denaturation of collagen in solution and its structural implications, 155
Byrne, R. (see Morgan, R. S.), 188

Calcification of collagen, 65
Calvin, M. (see Moses, V.), 21
Carboxyl group interactions in lysozyme, 293
Champe, S. P. (see Brenner, S.), 281
Chloromycetin-inhibited *Escherichia coli*, ribonucleoprotein particles, 204
Chromosomes, X-ray diffraction studies, 179
Code, two-symbol, for the nucleic acid message? 218
Coiled-coil, transition to straight configuration in the α-helix, 186
Collagen, calcification, 65
— thermal denaturation in solution, structural implications, 155

Davidson, N. (see Kon, H.), 190
Dawson, I. M. & Watson, D. H. An electron microscope study of the structure of crystalline ribonuclease, 30
Denaturation of collagen in solution, 155
Deoxyribonucleic acid, exposure to tritium gas, 195
— from bacteriophage φX174, 43
— low angle X-ray scattering from gels, 127

Deoxyribonucleoprotein particles containing single nucleic acid molecules, 1
Donovan, J. W., Laskowski, M., Jr. & Scheraga, H. A. Carboxyl group interactions in lysozyme, 293
Doty, P. (see Hall, B. D.), 111
— (see Zubay, G.), 1
Doudney, C. O. & Haas, F. L. Gene replication and mutation induction in bacteria, 81

Escherichia coli, amino acid-ribonucleic acid complexes, 301
— electron microscopy of ribonucleoprotein particles, 329
— "inducibility" in the synthesis of β-galactosidase, 165
— ribonucleoprotein particles, 221
— ribonucleoprotein particles under chloromycetin inhibition, 204
— soluble ribonucleic acid, 365

Feather keratin, molecular organization, 387
Ferrihemoglobin, nuclear magnetic relaxation, 190
Ferrimyoglobin, nuclear magnetic relaxation, 190
Ferritin structure, some X-ray data, 69
Fraser, R. D. B. & MacRae, T. P. Molecular organization in feather keratin, 387
Freese, E. The specific mutagenic effect of base analogues on phage T4, 87
Fresco, J. R. Polynucleotides II. The X-ray diffraction patterns of solutions of the randomly coiled and helical forms of polyriboadenylic acid, 106
Friesen, B. & Sinsheimer, R. L. Partition cell analysis of infective tobacco mosaic virus nucleic acid, 321

β-Galactosidase, "inducibility" in *Escherichia coli*, 165
Gene replication in bacteria, 81
Gergely, J. (see Balazs, E. A.), 147
Glucagon, unit cell and space group of cubic form, 375
Green, D. W. & Aschaffenburg, R. Twofold symmetry of the β-lactoglobulin molecule in crystals, 54
Gros, F. (see Lacks, S.), 301
Grunberg-Manago, Marianne. Phosphorolyse et configuration macromoléculaire des polyribonucléotides biosynthétiques et des acides ribonucléiques, 240

Haas, F. L. (see Doudney, C. O.), 81
Haemoglobin, chemical and crystallographic study of fractions in horse, 402
— (see ferrihemoglobin), 190
Hall, B. D. & Doty, P. The preparation and physical chemical properties of ribonucleic acid from microsomal particles, 111
Hall, C. E., Maclean, Elizabeth C. & Tessman, I. Structure and dimensions of bacteriophage φX174 from electron microscopy, 192
— & Slayter, H. S. Electron microscopy of ribonucleoprotein particles from *Escherichia coli*, 329
Harrison, Pauline M. The structures of ferritin and apoferritin: some preliminary X-ray data, 69
Hayes, T. L., Murchio, J. C., Lindgren, F. T. & Nichols, A. V. A determination of lipoprotein molecular weight by use of the electron microscope, 297
α-Helix, transition between straight and coiled-coil configurations, 186
Hershey, A. D. (see Koch, G.), 260
Hills, G. J. (see Smith, K. M.), 277
Histidine residue in ribonuclease. I. Reaction with bromoacetic acid, 339
— II. Position in primary protein chain, 350
Hollingworth, B. R. (see Tissières, A.), 221
Holm-Hansen, O. (see Moses, V.), 21
Horne, R. W. (see Brenner, S.), 281
— Brenner, S., Waterson, A. P. & Wildy, P. The icosahedral form of an adenovirus, 84
— & Nagington, J. Electron microscope studies of the development and structure of poliomyelitis virus, 333

Horne, R. W., Russell, G. E. & Trim, A. R. High resolution electron microscopy of beet yellows virus filaments, 234
Hynes, R. D. (see Burge, R. E.), 155

Icosahedral form of an adenovirus, 84
Imahori, K. & Tanaka, J. Ultraviolet absorption spectra of poly-L-glutamic acid, 359
"Inducibility" of β-galactosidase in *Escherichia coli*, 165

Jacob, F. (see Pardee, A. B.), 165
Jerne, N. K. (see Stent, G. S.), 134

Keratin (see feather), 387
King, M. V. The unit cell and space group of cubic glucagon, 375
Koch, G. & Hershey, A. D. Synthesis of phage-precursor protein in bacteria infected with T2, 260
Kon, H. & Davidson, N. Nuclear magnetic relaxation of water protons by ferrihemoglobin and ferrimyoglobin, 190

Lacks, S. & Gros, F. A metabolic study of the ribonucleic acid-amino acid complexes in *Escherichia coli*, 301
β-Lactoglobulin, twofold symmetry of crystals, 54
Laskowski, M., Jr. (see Donovan, J. W.), 293
Lindgren, F. T. (see Hayes, T. L.), 297
Lipoprotein, molecular weight by electron microscopy, 297
Low angle X-ray scattering from gels of deoxyribonucleic acid and nucleoproteins, 127
Luzzati, V. & Nicolaieff, A. Etude par diffusion des rayons X aux petits angles des gels d'acide désoxyribonucléique et de nucléoprotéines: (Note préliminaire), 127
Lysozyme, carboxyl group interactions, 293

Maclean, Elizabeth C. (see Hall, C. E.), 192
MacRae, T. P. (see Fraser, R. D. B.), 387
Macromolecular substances, proton magnetic resonance studies, 147
Meselson, M. (see Weigle, J.), 379
Metabolic pools of photosynthetic and respiratory intermediates, 21
Microsomal particles from ribonucleic acid, preparation and properties, 111
Monod, J. (see Pardee, A. B.), 165
Morgan, R. S. & Byrne, R. "Alkaline" polyadenylic acid, 188
Moses, V., Holm-Hansen, O., Bassham, J. A. & Calvin, M. The relationship between the metabolic pools of photosynthetic and respiratory intermediates, 21
Murchio, J. C. (see Hayes, T. L.), 297
Muscle, striated, large axial spacings, 398
Mutagenic effect of base analogues on bacteriophage T4, 87
Mutation induction in bacteria, 81
Myoglobin (see ferrimyoglobin), 190

Nagington, J. (see Horne, R. W.), 333
Nichols, A. V. (see Hayes, T. L.), 297
Nicolaieff, A. (see Luzzati, V.), 127
Nomura, M. & Watson, J. D. Ribonucleoprotein particles within chloromycetin-inhibited *Escherichia coli*, 204
Nuclear magnetic relaxation in ferrihemoglobin and ferrimyoglobin, 190
Nucleic acid message, a two-symbol code? 218
— molecules in deoxyribonucleoprotein particles, 1
— parental, dispersal in bacteriophage T4 progeny, 134
— tobacco mosaic virus, partition cell analysis, 321
Nucleohistone, X-ray diffraction studies, 179
Nucleoprotein, low angle X-ray scattering from gels, 127
Nucleotide composition of ribonucleic acid protein particles from *Escherichia coli*, 237

Paigen, K. (see Weigle, J.), 379
Pardee, A. B., Jacob, F. & Monod, J. The genetic control and cytoplasmic expression of "inducibility" in the synthesis of β-galactosidase by *Escherichia coli*, 165
Partition cell analysis of infective tobacco mosaic virus nucleic acid, 321
Perutz, M. F., Steinrauf, L. K., Stockell, Anne & Bangham, A. D. Chemical and crystallographic study of the two fractions of adult horse haemoglobin, 402
φX174 (see bacteriophage), 192
Phosphorolysis of biosynthetic polyribonucleotides and ribonucleic acids, 240
Photosynthetic and respiratory intermediates, relationship between metabolic pools, 21
Poliomyelitis virus, electron microscopy of structure, 333
Polyadenylic acid, "alkaline," 188
Poly-L-glutamic acid, ultraviolet absorption spectra, 359
Polyriboadenylic acid, X-ray diffraction patterns of solutions, 106
Polyribonucleotides, phosphorolysis and configuration, 240
Proton magnetic resonance studies on water, 147

Rees, M. W. (see Brenner, S.), 281
Respiratory and photosynthetic intermediates, relationship between metabolic pools, 21
Ribonuclease, histidine residue in the active centre. I. Reaction with bromoacetic acid, 339
— II. Position of histidine residue in the primary protein chain, 350
Ribonucleic acid-amino acid complexes in *Escherichia coli*, 301
Ribonucleic acid from microsomal particles, preparation and properties, 111
— soluble, from *Escherichia coli*, 365
Ribonucleic acids, phosphorolysis and configuration, 240
Ribonucleoprotein particles from *Escherichia coli*, 221
— electron microscopy of structure, 329
— nucleotide composition, 237
Rosenkranz, H. S. (see Borenfreund, Ellen), 195
Russell, G. E. (see Horne, R. W.), 234

Santanam, M. S. Calcification of collagen, 65
Sato, G. H. (see Stent, G. S.), 134
Scheraga, H. A. (see Donovan, J. W.), 293
Schlessinger, D. (see Tissières, A.), 221
Sinsheimer, R. L. A single-stranded deoxyribonucleic acid from bacteriophage φX174, 43
— Is the nucleic acid message in a two-symbol code? 218
— Purification and properties of bacteriophage φX174, 37
— (see Friesen, B.), 321
Slayter, H. S. (see Hall, C. E.), 329
Smith, K. M. & Hills, G. J. Further studies on the electron microscopy of the *Tipula* iridescent virus, 277
Spahr, P. F. & Tissières, A. Nucleotide composition of ribonucleoprotein particles from *Escherichia coli*, 237
Stein, W. D. (see Barnard, E. A.), 339
— & Barnard, E. A. The histidine residue in the active centre of ribonuclease II. The position of this residue in the primary protein chain, 350
Steinrauf, L. K. (see Perutz, M. F.), 402
Stent, G. S., Sato, G. H. & Jerne, N. K. Dispersal of the parental nucleic acid of bacteriophage T4 among its progeny, 134
Stockell, Anne. (see Perutz, M. F.), 402
Streisinger, G. (see Brenner, S.), 281

T2 (see bacteriophage), 260
T4 (see bacteriophage), 87
Tanaka, J. (see Imahori, K.), 359
Tessman, I. (see Hall, C. E.), 192
Tipula iridescent virus, electron microscopy of structure, 277
Tissières, A. Some properties of soluble ribonucleic acid from *Escherichia coli*, 365
— (see Spahr, P. F.), 237

Tissières A., Watson, J. D., Schlessinger, D. & Hollingworth, B. R. Ribonucleoprotein particles from *Escherichia coli*, 221
Tobacco mosaic virus nucleic acid, partition cell analysis, 321
Transducing ability in bacteriophage λ and density alterations, 379
Trim, A. R. (see Horne, R. W.), 234
Tritium gas, effect on deoxyribonucleic acid, 195

Ultraviolet absorption spectra of poly-L-glutamic acid, 359

Waterson, A. P. (see Horne, R. W.), 84
Watson, D. H. (see Dawson, I. M.), 30
Watson, J. D. (see Nomura, M.), 204
— (see Tissières, A.), 221
Weigle, J., Meselson, M. & Paigen, K. Density alterations with transducing ability in the bacteriophage lambda, 379
Wildy, P. (see Horne, R. W.), 84
Wilkins, M. H. F., Zubay, G. & Wilson H. R. X-ray diffraction studies of the molecular structure of nucleohistone and chromosomes, 179
Wilson, H. R. (see Wilkins, M. H. F.), 179
Worthington, C. R. Large axial spacings in striated muscle, 398

X-ray data on structure of ferritin and apoferritin, 69
— diffraction of coiled and helical forms of polyriboadenylic acid, 106
— diffraction of nucleohistone and chromosomes, 179

Zubay, G. The transition between straight and coiled-coil configurations of the α-helix, 186
— (see Wilkins, M. H. F.), 179
— & Doty, P. The isolation and properties of deoxyribonucleoprotein particles containing single nucleic acid molecules, 1

FILED IN STACKS

CONTENTS

LACKS, SANDFORD and GROS, FRANÇOIS, A Metabolic Study of the RNA-Amino Acid Complexes in *Escherichia coli* 301

FRIESEN, BENJAMIN S. and SINSHEIMER, ROBERT L., Partition Cell Analysis of Infective Tobacco Mosaic Virus Nucleic Acid . . . 321

HALL, C. E. and SLAYTER, H. S., Electron Microscopy of Ribonucleoprotein Particles from *E. Coli* 329

HORNE, R. W. and NAGINGTON, J., Electron Microscope Studies of the Development and Structure of Poliomyelitis Virus 333

BARNARD, E. A. and STEIN, W. D., The Histidine Residue in the Active Centre of Ribonuclease. I. A Specific Reaction with Bromoacetic Acid . 339

STEIN, W. D. and BARNARD, E. A., The Histidine Residue in the Active Centre of Ribonuclease. II. The Position of this Residue in the Primyar Protein Chain 350

IMAHORI, KAZUTOMO and TANAKA, JIRO, Ultraviolet Absorption Spectra of Poly-L-Glutamic Acid 359

TISSIÈRES, A., Some Properties of Soluble Ribonucleic Acid from *Escherichia coli* 365

KING, MURRAY VERNON, The Unit Cell and Space Group of Cubic Glucagon 375

WEIGLE, J., MESELSON, MATTHEW and PAIGEN, KENNETH, Density Alterations Associated with Transducing Ability in the Bacteriophage Lambda 379

FRASER, R. D. B. and MACRAE, T. P., Molecular Organisation in Feather Keratin 387

Letters to the Editor—

Large Axial Spacings in Striated Muscle, C. R. WORTHINGTON . . 398

Chemical and Crystallographic Study of the two Fractions of Adult Horse Haemoglobin, M. F. PERUTZ, L. K. STEINRAUF, ANNE STOCKELL, A. D. BANGHAM 402

Printed in Great Britain at the Aberdeen University Press